2009

Inositol phospholipid and tyrosine phosphorylation signaling in the biology of hematopoietic stem cells

Amy L. Hazen
University of South Florida

Inositol Phospholipid and Tyrosine Phosphorylation Signaling in the Biology of Hematopoietic Stem Cells

by

Amy L. Hazen

A dissertation submitted in partial fulfillment
of the requirements for the degree of
Doctor of Philosophy
Department of Cancer Biology
College of Graduate Studies
University of South Florida

Major Professor: William G. Kerr, Ph.D.
Alan F. List, M.D.
Gary W. Reuther, Ph.D.
Paul R. Sanberg, Ph.D.

Date of Approval:
February 19, 2009

Keywords: SHIP, PI3K, Niche, Extramedullary hematopoiesis, Kinome

Dedication

In loving memory of my mother Victoria, an amazing parent and friend who inspired me to be a strong intelligent woman, and my step-father Dony, a loving father and husband who lost his brave battle with cancer far too young.

‘The greatest fan of your life.’

Acknowledgements

First and foremost, I would like to express my deepest gratitude to my wonderful husband and best friend, Joshua, who has been my pillar of strength through tragedies and triumphs. I am very fortunate to have him by my side.

I would also like to thank my mentor, William G. Kerr, for his guidance and patience over the years. He has provided me with many opportunities and challenges to help me become a stronger scientist. I am appreciative for having a great committee and would like to thank Dr. Alan List, Dr. Gary Reuther and Dr. Paul Sanberg for all of their support and direction. I am also honored to have Dr. Christopher Klug of the University of Alabama at Birmingham as the outside chairperson for my dissertation committee.

Thank you to all the members of the Kerr lab, both past and present, who have contributed to my training and made my time at Moffitt a pleasure.
I would especially like to thank Kim Paraiso, Cheryl Meyerkord and Daniela Wood for always being there for me during the hard times and helping me keep things in perspective.

I would like to give a special thanks to two former graduate students, Joseph Wahle and Caroline Desponts, who contributed to my training and helped me to become a better scientist.

I would like to thank Michelle Smith for all her hard work and companionship this past year. Team HSC lives on with her.

Lastly, I am very grateful for my family and their never-ending support and encouragement. Without their love, I never would have made it this far.

Table of Contents

List of Figures

List of Tables

Inositol Phospholipid and Tyrosine Phosphorylation Signaling in the Biology of Hematopoietic Stem Cells

Amy L. Hazen

ABSTRACT

Blood cells are continuously produced throughout our lifetime by a rare pluripotent cell that primarily resides in the adult bone marrow. This hematopoietic stem cell (HSC) must maintain a careful balance between self-renewal, differentiation and apoptosis in order to support hematopoiesis for such a long duration. Understanding the mechanism of balance between these fates is crucial to our understanding and clinical application of these cells.

From previous studies, we know Src homology 2 domain containing 5' inositol phosphatase 1 (SHIP) plays an important role in HSC homeostasis and function. Most interestingly SHIP impacts HSC homing to the bone marrow niche. An ideal location and environment is essential for HSC to fulfill their physiological roles. Here we present evidence that SHIP is expressed by cells of the HSC niche. Furthermore, SHIP deficiency severely alters this environment and thus damages HSC function.

In addition to the extrinsic effects of a SHIP-deficient microenvironment on HSC, there is an intrinsic requirement for SHIP expression in confining HSC to the bone marrow niche. We previously demonstrated that lack of SHIP leads to an increase in peripheral HSC. Here we demonstrate that SHIP-deficient HSC from the spleen can provide radioprotection and sustained multi-lineage repopulation in lethally irradiated hosts. This indicates extramedullary HSC can function outside the traditional bone marrow niche in SHIP-deficient mice.

Combined, these studies indicate both extrinsic and intrinsic factors contribute to HSC homeostasis and function. In order to better understand the signaling pathways involved in self-renewal and differentiation, we applied an array-based technology to hematopoietic cells at various levels of differentiation. Comparing the phosphorylation signature, or ‘kinome’, of these cell types can help pinpoint signaling mechanisms important for HSC self-renewal and lineage commitment.

Introduction

SHIP

Discovery of SHIP

Src homology (SH) 2 domain containing 5' inositol phosphatase 1 (SHIP) was first cloned in 1996 by five independent groups based on its ability to bind the protein-tyrosine binding domain (PTB) of SH2-containing sequence protein (Shc)[1,2], the SH3 domain of growth factor receptor-bound protein 2 (Grb2)[1,3], the FcγRIIB receptor[4] and by gene trapping[5]. SHIP was initially observed as a 145kDa protein in human hematopoietic cell lines that became tyrosine phosphorylated and associated with Shc after stimulation with erythropoietin (Epo)[6]. Due to its broad expression in the hematopoietic compartment[1-3,7], it became important to determine SHIP's role in hematopoiesis. Since its identification in the mid-90's its role in the hematopoietic system has undergone extensive research.

Structure of SHIP

Structurally, SHIP contains an amino terminal SH2 domain, a 5' inositol phosphatase, two NPXY motifs and several polyproline rich domains (Figure 1). Its primary role is believed to be the hydrolysis of the 5' phosphate of phosphatidylinositol-3,4,5-phosphate (PI(3,4,5)P3) and inositol-1,3,4,5–

tetrakisphosphate (I(1,3,4,5)P4)[2,3,8]. The hydrolysis of the 5' phosphate of PI(3,4,5)P3 gives SHIP the ability to oppose phosphatidyl inositol 3' kinase (PI3K) activity, thereby regulating a variety of cellular signaling pathways important for proliferation, differentiation, apoptosis and migration.

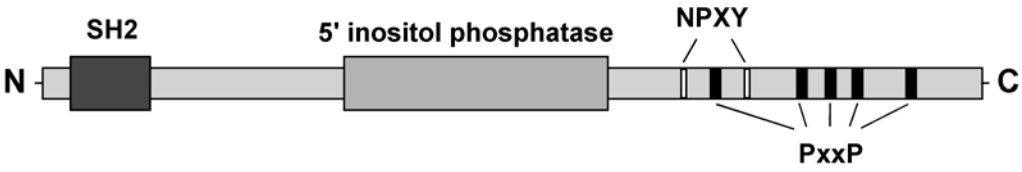

Figure 1: Structural diagram of SHIP.
Full-length SH2 domain containing 5' inositol phosphatase is a 145 kDa protein primarily expressed in the hematopoietic system.

SH2 Domain

SHIP can bind to phosphorylated immunoreceptor tyrosine based inhibition or activation motifs located in the tail of several receptors such as FcγRIIB on B cells, Ly49 receptors on natural killer cells, and FcεRI on mast cells [4,9-11] via its SH2 domain, which has the potential to bind phosphotyrosines[12,13]. The SH2 domain of SHIP also interacts with tyrosine phosphorylated Shp-2[14,15] and the Src kinase Lyn[16]. This latter interaction can stabilize SHIP near the membrane and enhance its function. The SH2 domain of SHIP competes with Grb2 for the phosphorylated tyrosine on Shc[7]. This competition for Shc inhibits its interaction with Grb2 which in turn prevents the recruitment of a complex of proteins that catalyze the activation of Ras and downstream mitogen-activated

protein kinase (MAPK) activation[7]. Thus SHIP can negatively regulate MAPK activation by preventing the formation of this complex.

5' Inositol Phosphatase

As evidenced by its ability to influence PI3K signaling in vivo[3], SHIP has an important role as an inositol phosphatase. The catalytic domain can hydrolyze the 5' phosphate from PI(3,4,5)P3 and I(1,3,4,5)P4 generating PI(3,4)P2 and I(1,3,4)P3, respectively[3,8,17]. In contrast, PI3K can add a 3' phosphate to PI(4,5)P2 thereby generating more PI(3,4,5)P3. This careful balance of enzymatic activity is needed to control the levels of PI(3,4,5)P3 in the cell, as it plays a key role in the recruitment of pleckstrin homology (PH) domain containing proteins such as Akt[18-21].

Upon generation of PI(3,4,5)P3 in the plasma membrane, Akt translocates to this site and becomes phosphorylated at Threonine 308 and Serine 473 resulting in its activation[22,23]. Phosphorylated Akt functions primarily to attenuate the activation of the intrinsic apoptosis pathway by phosphorylation and inactivation of pro-apoptotic proteins such as BAD[24]. In essence, by limiting PI(3,4,5)P3 levels, SHIP can prevent the recruitment of effector molecules such as Akt and negatively regulate downstream signaling of PI3K[18-21,25]. This inhibition of Akt recruitment and activation leads to decreased proliferation and survival signaling[26,27]. A recent study also described a C2 domain located at the carboxyl end of SHIP's phosphatase domain as an allosteric activation domain[28].

NPXY Motifs and PxxP Region

The carboxyl terminus of SHIP contains several NPXY motifs, where NPXY indicates arginine (N) followed by proline (P) then any amino acid (X) followed by a tyrosine (Y). Upon activation, these motifs are tyrosine phosphorylated and become a binding site for PTB domain containing proteins such as Shc[29-31]. These NPXY motifs can also directly bind the p85 subunit of PI3K, indicating another potential role for SHIP in limiting PI3K signaling[32-34]. Proline rich (PxxP) motifs are also found throughout the carboxyl terminus of SHIP and allow interaction with SH3 domain containing proteins[35]. Importantly, although SHIP can be phosphorylated, this does not appear to be required for its 5' inositol phosphatase activity. This suggests that the location of SHIP at the membrane, in proximity to target molecules, may play an equally important role to phosphorylation in SHIP's activation[36].

SHIP Isoforms and Homolog

Full length SHIP is a 145kDa protein primarily expressed in the hematopoietic compartment, however additional isoforms have been identified in both mice and humans. In mice, the lower molecular weight 110, 124 and 135kDa isoforms are generated from the alternative splicing or proteolytic cleavage at the carboxyl terminus of full-length SHIP[1,4,37-40]. Hematopoietic cell lines frequently have expression of both the full-length 145kDa protein and a 135kDa SHIP isoform[38], which results from the deletion of an internal PxxP motif within the carboxyl terminus.

An additional 110kDa isoform was isolated from both mice and humans. In lieu of a deletion in the carboxyl terminus, this isoform is missing the SH2 domain[2,41]. The human version lacks 214 amino acids at the amino terminus and is named SIP-110[2]. Similarly, the homologous murine version lacks 260 amino acids at the amino terminus resulting in the absence of the SH2 domain[41]. In mice, the 110kDa isoform is expressed in embryonic and hematopoietic stem cells from an internal promoter region within the intron between exons 5 and 6 of the SHIP gene[41,42]. Interestingly, unlike full-length SHIP, this isoform is not expressed in more differentiated hematopoietic cells and was therefore designated stem cell restricted SHIP or s-SHIP. Although this work does not examine the role of s-SHIP in the regulation of HSC, it should be noted that the specific expression pattern of this isoform makes it important to these studies and certainly warrants further investigation.

SH2 domain containing 5' inositol phosphatase 2 (SHIP2) belongs to the same class of inositol 5' phosphatase proteins as SHIP1 and is its closest relative[43]. It was first identified as inositol polyphosphate-like-protein 1 (INPPL-1)[44] but in 1997 was discovered by a separate group as a 150kDa protein with 38% amino acid homology to SHIP1 and was thereafter named SHIP2[45]. Although this sequence homology may not seem high, the majority of homology is located within the functional domains of the proteins. The SH2 domains share 54% homology and the 5' inositol phoshatase domains are 64% homologous[45]. Similar to SHIP1, SHIP2 contains a PxxP region and an NPXY motif allowing interactions with both SH3 and PTB domains. Despite their structural similarities

there are differences in expression and function, which at least partially segregates their roles in signaling. SHIP2, a 150kDa protein, is encoded by an entirely different gene. In fact, they are expressed from different chromosomes in both mouse and human[46], and although SHIP1 is primarily expressed in hematopoietic cells, SHIP2 has a ubiquitous expression pattern[45,47,48]. Both can dephosphorylate PI(3,4,5)P3, however SHIP2 can not hydrolyze I(3,4,5)P4. Furthermore, studies have shown that SHIP1, not SHIP2, plays the dominant role in controlling PI(3,4,5)P3 levels in response to activation in hematopoietic cells[49]. Accordingly, studies in SHIP2$^{-/-}$ mice have indicated no hematopoietic abnormalities. The dominant role of SHIP2 appears to be in modulating glucose homeostasis[50]. However, the presence of SHIP2 cannot compensate for the lack of SHIP1 in mice harboring a homozygous SHIP1 deletion. These SHIP1 deficient mice have severe hematological defects, making it safe to conclude that, despite the structural homology between these proteins, they are not functionally redundant.

PTEN

Phosphatase and tensin homolog deleted on chromosome ten (PTEN) is a ubiquitously expressed 54kDa inositol phosphatase that hydrolyzes the 3' phosphate of PI(3,4,5)P3 generating PI(4,5)P2[51]. Unlike SHIP, which needs growth factor stimulation for activation, PTEN constitutively reduces the level of PI(3,4,5)P3 in the cell and downregulates Akt activation[51]. When PTEN is mutated, causing loss of function or inactivation, cell growth and apoptosis

signals become unregulated frequently resulting in cancer[52]. In fact, PTEN is a potent tumor suppressor and one of the more commonly inactivated genes in cancer[53]. Because PTEN constitutively acts to reduce basal PI(3,4,5)P3 levels, its loss leads to such severe abnormalities that $PTEN^{-/-}$ mice are embryonic lethal[54].

SHIP Signaling

PI(3,4,5)P3 is a key second messenger in the PI3K pathway and plays a central role in regulating many cellular functions. Low basal levels of PI(3,4,5)P3 in the cell are rapidly increased by PI3K upon stimulation. PI(3,4,5)P3 attracts PH domain containing proteins to the membrane to mediate survival and/or proliferation signaling[55-57]. Several inositol phophatases such as PTEN and SHIP keep this activation in check. Ubiquitously expressed PTEN constitutively breaks down PI(3,4,5)P3 levels and generates PI(4,5)P2, whereas SHIP requires activation to reduce PI(3,4,5)P3 levels in hematopoietic cells[51,57,58].

As mentioned earlier, SHIP was initially observed as a protein that became tyrosine phosphorylated after stimulation of human hematopoietic cell lines with Epo[6]. In fact, the stimulation of several growth factor and immunological receptors leads to the recruitment of SHIP to the plasma membrane where tyrosine phosphorylation occurs. This triggers the association of SHIP with other signaling molecules, such as Grb2[14]. (Figure 2) Growth factors known to stimulate SHIP are granulocyte-macrophage-colony stimulating factor (GM-CSF), granulocyte-CSF(G-CSF), stem cell factor (SCF), thrombopoietin

(TPO), Fms-like tyrosine kinase 3 ligand (Flt3L), interleukin-3 (IL-3), IL-4 and importantly stromal cell derived factor-1 (SDF-1)[7,32,59-68]. Some immunological receptors that recruit SHIP are the B cell receptor, the T cell receptor and the Fc receptor[4,69-74].

Interestingly, it appears that the membrane proximal location, not its tyrosine phosphorylation, may be required for the primary inositol phosphatase activity of SHIP[3,75]. The method of this translocation to the plasma membrane is not completely understood and appears to have some variation dependent on the cell type[76]. Once located at the membrane, the inositol phosphatase domain of SHIP can reduce PI(3,4,5)P3 levels by generating PI(3,4)P2 and inhibit downstream Akt activation. Additionally, this decrease in PI(3,4,5)P3 can lead to a reduction in Btk membrane localization and activation. Inhibiting Btk activation results in a subsequent decrease in PLCγ levels and an arrest of extracellular calcium influx[77,78]. By dampening PI(3,4,5)P3 levels SHIP can also down regulate NFκB induced gene transcription in myeloid cells and inhibit the NFκB pathway[79]. At the membrane, the SH2 domain of SHIP preferentially binds to tyrosine phosphorylated forms of Shc, among other adaptor proteins[7]. SHIP competes for Shc interaction with Grb2 thereby inhibiting the formation of the multi-protein complex between Shc, Grb2 and son of sevenless (SOS). Prevention of the formation of this complex inhibits the activation of the MAPK pathway. Combined, the roles of SHIP can influence survival, proliferation, and differentiation signaling.

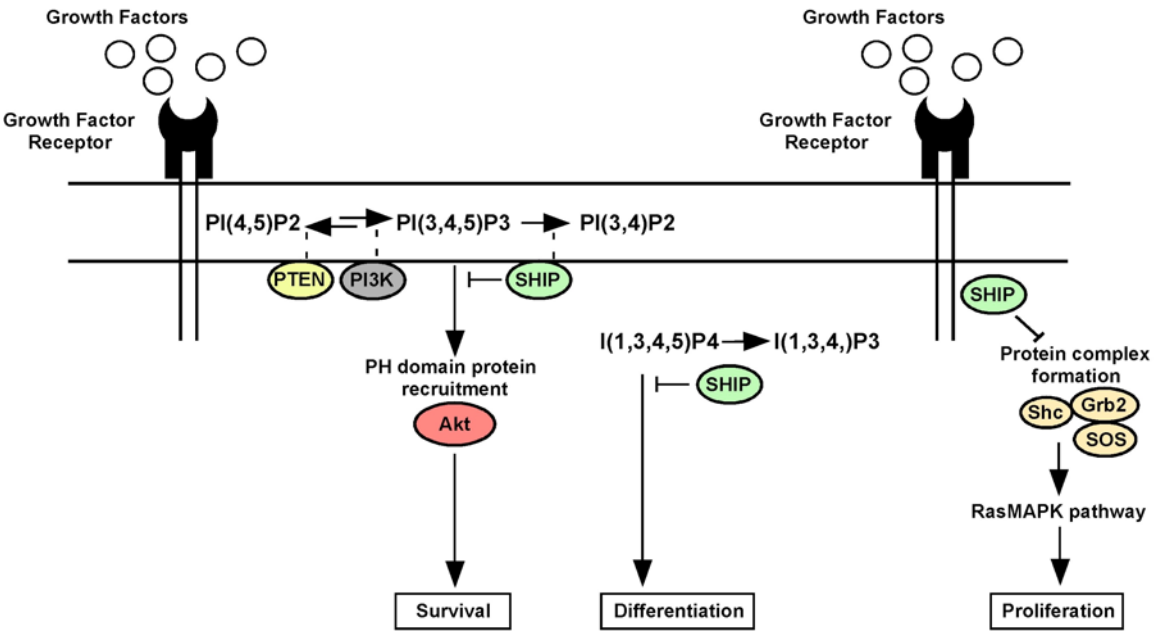

Figure 2: Simplified schematic of signaling pathways influenced by SHIP. Upon growth factor receptor engagement, SHIP is recruited to the membrane. Once there SHIP can influence multiple signaling pathways. SHIP can hydrolyze the 5' phosphate of PIP3, opposing PI3K signaling. This inhibits the recruitment of PH domain containing proteins such as Akt and inhibits downstream survival signaling. SHIP can also reduce IP4 levels and limit differentiation signaling. By binding Shc, SHIP inhibits the formation of a protein complex between Shc, Grb2 and Sos. This in turn inhibits downstream MAPK activation and proliferation signaling.

SHIP Knockout Mouse Models

To better understand the function of SHIP, various groups have created versions of the SHIP knockout (KO) mouse by deleting different portions of the protein[80-82]. The study of these mouse models has provided a wealth of insight into SHIP's role in the hematopoietic compartment. Although viable, the SHIP KO mice harbor profound abnormalities including: hyper-resorptive osteoclasts[83], reduced CD8 T cell numbers[81], a disrupted NK cell repertoire[11], hyperresponsive mast cell degranulation[84], increased myeloid cells in the bone marrow and periphery[60,81] and an increase in myeloid suppressor cells[85]. Interestingly, the increase in myeloid suppressor cells combined with a promiscuous NK cell repertoire mediates a significant decrease in graft-versus-host disease (GVHD) and BM rejection, respectively after allogeneic bone marrow transplant[11,85,86]. However, collectively the pathological effects of SHIP deficiency harbor detrimental effects. The myeloproliferative disorder, causing expansion of macrophages in the bone marrow and spleen, also results in infiltration and consolidation of the lungs. This ultimately leads to the mouse's death at 6 to 10 weeks of age[81]. Not surprisingly, $SHIP^{-/-}$ mice share phenotypic characteristics with $PTEN^{+/-}$ mice[87], suggesting that elevated levels of PI(3,4,5)P3 are the primary cause of these characteristics.

Studies contained here within were completed using two mouse models of SHIP deficiency. Both models were created by flanking the region to be deleted with Cre recombinase recognition sites or loxP sites[11]. The promoter and the first exon of the SHIP gene were floxed by homologous recombination in ES cells[88].

The SHIP$^{flox/flox}$ animal is then crossed with a Cre transgenic animal, resulting in the deletion of the targeted (or floxed) region. The Cre recombinase recognizes the loxP sites and deletes the intervening DNA. This model deletes SHIP in the entire animal generating mice with germline SHIP deficiency, indicated as SHIP$^{-/-}$ mice[11]. However, this strategy also allows SHIP to be targeted for deletion in a specific cell type or at a specific time depending on the promoter used to drive Cre expression. The other model used here permits the inducible deletion of SHIP at the time of our choice. Using our existing colony of SHIP$^{flox/flox}$ mice and MxCre transgenic mice purchased from The Jackson Laboratory, we generated MxCreSHIP$^{flox/flox}$ mice[86]. In these mice, the Cre recombinase is under control of the Mx1 promoter, which is generally silent in healthy mice. However, upon administering a series of polyinosinic-polycytidylic acid injections, interferon levels can be elevated causing the Mx1 promoter to drive the expression of Cre recombinase, which in turn results in the excision of the targeted SHIP sequence flanked by loxP sites. These mice are indicated as MxCreSHIP$^{flox/flox}$ or SHIP-deleted mice.

Hematopoietic Stem Cells

Discovery of HSC

Despite our growing knowledge about stem cells, there is still no universally acceptable definition for the term. Most attempts to define them are made by assigning certain attributes; stem cells have the capacity to self-renew as well as to produce a full range of differentiated progeny. Since we know an

adult vertebrate is made up of over 200 different cell types, the existence of stem cells in embryogenesis seems intuitive. However, whether stem cells still persist in the adult vertebrate is somewhat less obvious. Certainly, the male reproductive organs continue to produce a large number of cells throughout life. Yet, upon gross inspection, somatic tissues do not appear to be expanding during adulthood. The most obvious evidence for the persistence of adult stem cells is probably wound healing. Possibly the most crucial role for an adult stem cell is the daily production of blood cells. Some blood cells, such as neutrophils and platelets, may only survive for hours or days in the blood. Without the existence of a hematopoietic stem cell (HSC) it would be impossible to support sustained blood production throughout the vertebrate lifespan.

The first scientific evidence of a regenerative cell in the hematopoietic system was shown in the 1940's when shielding the spleen from radiation allowed the survival of lethally irradiated animals[89-91]. Two years later studies injecting bone marrow cells into irradiated animals yielded a similar result[92]. This lead to the identification of a transplantable cell in the bone marrow, which could prevent hematological failure after radiation[93]. We now know that cells obtained from the bone marrow and cytokine-mobilized blood of healthy donors are useful for transplantation. In the past ten years, HSC transplantation has evolved into a common clinical practice. In order to improve the clinical efficacy of these transplants, it is crucial to understand the biological functions necessary for HSC to both self-renew and provide differentiated cells of the lymphoid and myeloid lineages.

Development of the Hematopoietic System

The founding HSC originate during embryogenesis in a complex process that involves multiple successive anatomical sites. Just after gastrulation the hemangioblast gives rise to a subset of mesodermal precursors, which in turn commit to becoming blood cells and embryonic hematopoiesis begins[94]. The first precursors move to the yolk sac and begin to produce red blood cells. The yolk sac provides initial transport from mother to fetus and is essential to murine development[95]. Between E7.0 and 8.5 precursors in the yolk sac begin to develop primitive erythrocytes, followed by primitive myeloid cells[96]. However, the yolk sac microenvironment does not support full differentiation into definitive lineages. Therefore these primitive cells must leave the yolk sac and seed the fetal liver where they can complete terminal differentiation. Functional long-term repopulating HSC (LT-HSC), which can provide sustained long-term hematopoiesis, are not found until day E11.0 in the fetal liver. This indicates that despite extensive production of progenitors, the yolk sac cannot support HSC generation[97]. The primary hematopoietic organ during fetal development is the fetal liver. It is the main site of HSC expansion and differentiation[98]. The fetal liver microenvironment promotes self-renewing divisions of the HSC, rapidly expanding the pool to a maximum plateau at E15.5 to 16.5[99]. During this period, a portion of HSC are relocated to the spleen, which can remain a site for extramedullary hematopoiesis throughout adulthood. Skeletal development begins at day E12.5 and functional HSC can be found in the bone marrow from

E17.5 onwards[100]. However, HSC can be found in the circulation several days before seeding the bone marrow. Indicating, a delay in colonization while the bone marrow microenvironment forms[100]. Bone marrow stromal cells produce a gradient of SDF-1 which attracts HSC, yet this chemokine appears to play little role in the formation of the fetal liver HSC pool[101]. The switch from fetal liver to bone marrow hematopoiesis is yet to be fully understood.

In addition to these concrete hematopoietic niches, a very small percentage of HSC remain in circulation in both fetal and adult stages. In the adult mouse approximately 100 HSC are in circulation during steady state conditions[102]. The placenta also exhibits hematopoietic activity. In fact, HSC can be found in the placenta (E10.5) before the circulation or fetal liver. This suggests the placenta may be a source of *de novo* HSC. At day E12.5 there is a rapid expansion of HSC in the placenta, indicating a microenvironment that supports rapid self-renewal without differentiation[103]. The number of HSC in the placenta rapidly decreases after E13.5 as the fetal liver pool begins to expand. It remains to be shown whether the placenta supplies the major portion of HSC to the fetal liver, however we know the fetal liver is directly downstream of the placenta in circulation[103].

Adding to the complexity of hematopoietic development, investigators strongly argue a role for the aorta-gonad-mesonephros (AGM) region as a second site of pre-fetal liver hematopoiesis[104,105]. Interestingly, the generation of hematopoiesis in the yolk sac, placenta and AGM coincides with the development of endothelial cells, which are a key component in supportive

microenvironments[106]. In reality there are probably multiple independent origins of HSC during fetal development.

Hematopoietic Hierarchy

HSC develop into differentiated blood cells via several lineage-restricted pathways in distinct steps (Figure 3). Cells committed to lymphoid fates, such as B cells, natural killer (NK) cells, T cells and dendritic cells develop through a common lymphoid progenitor (CLP)[107]. This CLP is restricted to the production of cells within the lymphoid lineage. Erythrocytes, granulocytes, macrophages, and megakaryocytes are all derived from a common myeloid progenitor (CMP)[107], which similarly to the CLP is restricted to the formation of cells from the myeloid arm. These progenitors have the ability to self-renew and create differentiated blood cells, but because they are restricted to a single arm of hematopoiesis they are considered “progenitors”, not stem cells. Once cells are committed to myeloid differentiation, the CMP undergoes further commitment steps to restrict its lineage potential to either a megakaryocyte and erythrocyte progenitor (MEP) or a granulocyte and erythrocyte progenitor (GMP)[108]. This hierarchy is a simplification of the intermediates involved in the differentiation steps between HSC and mature blood cell.

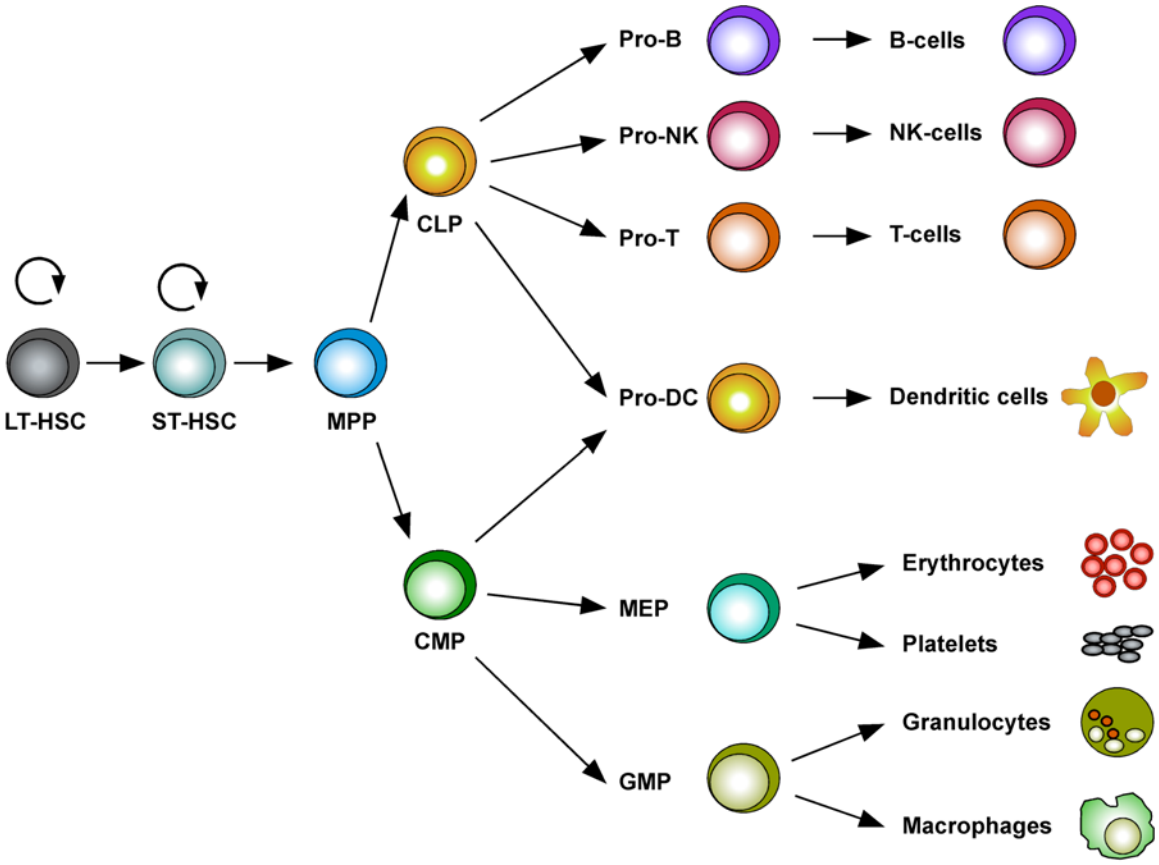

Figure 3: Schematic illustration of the hematopoietic hierarchy.
LT-HSC have near limitless self-renewal potential and can differentiate to produce all the lineages of the blood. ST-HSC have reduced self-renewal potential and can not sustain long-term multi-lineage hematopoiesis. Multi potent progenitors (MPP) have limited self-renewal capacity. They can produce downstream progenitors, which are restricted to the production of a specific lineage. CLP and CMP are still considered progenitors as they can generate multiple cell types, however they are restricted to the lymphoid or myeloid arms of hematopoiesis. The CLP produces cells that are committed to lymphoid fates such as B cells, NK cells, T cells and dendritic cells. The CMP produces both GMP and MEP. GMP then give rise to granulocytes, monocytes and macrophages, while MEP only give rise to red cells and platelets. Dendritic cells can originate from either CL or CM progenitors.

HSC Microenvironment

The shift between multiple anatomical sites during hematopoietic development might permit different tissue microenvironments to alter HSC priorities between expansion and quiescence. Fetal HSC are largely cycling, however LT-HSC found in the adult bone marrow are primarily in G0 phase[109]. The HSC microenvironment or "niche" appears to play an important role in controlling this HSC homeostasis. Furthermore, proper migration to and seeding of the anatomical locations most likely depends on the proper establishment of the respective niches.

In 1978, Schofield first proposed the concept of a physiological microenvironment that could support HSC homeostasis[110]. Recent studies have established the niche as a complex tissue, encompassing multiple cell types that work together to support hematopoiesis. The niche cells are in intimate contact with HSC and produce many growth factors important in determining stem cell fate, including leukemia inhibitory factor (LIF), IL-6, IL-8, SCF, and Flt3 ligand. These cytokines are key regulators in the niche's control of HSC self-renewal and differentiation[111-113]. Specifically, a combination of TPO and Ftl3 ligand can force limited HSC self-renewal[114].

Stromal cell derived factor-1 (SDF-1), which is released from endothelial-type cells and osteoblasts within the bone marrow niche, appears to be required for the HSC homing process. The CXCR4 receptor on the surface of HSC induces migration towards an increasing SDF-1 gradient generated by stromal cells in the niche[115]. In fact, the treatment of mice with an anti-CXCR4 antibody

prior to transplantation results in failure of HSC engraftment, indicating this is a critical interaction for proper BM homing[116]. Additional studies have established that G-CSF, which is commonly used in clinic, mobilizes HSC to the peripheral blood by decreasing SDF-1 levels and disrupting the homing signal[117].

The players and mechanisms of the HSC microenvironment are complex and have yet to be fully defined. These interactions must function in concert for HSC to home to the bone marrow, remain in resting state in the niche, or mobilize to the periphery when needed. An emerging body of evidence suggests there are distinct microenvironments that regulate different HSC fates.

Many HSC in the BM reside near the endosteum, which is the inner surface in the bone at the boundary of bone and marrow. The cells that line the bone are heterogeneous, containing both osteoblasts and osteoclasts[118]. These endosteal cells secrete a variety of factors that regulate HSC maintenance including SCF, osteopontin, TPO, SDF-1, and angiopoietin[117,119-123]. In addition to the secretion of soluble factors, proper HSC maintenance may also require cell-to-cell contact with the endosteal surface. Osteoblasts express Jagged1, which can activate Notch signaling in HSC[124], indicating a direct contact interaction between HSC and osteoblasts. N-cadherin is an adhesion molecule that was believed to play a part in HSC lodgment at the endosteum, however, a recent study showed N-cadherin deficient HSC had normal function in the niche[125]. Additional work will be required to determine the importance of this cell contact interaction compared to soluble factors excreted by the endosteal cells in

regulating HSC. Regardless of the exact mechanism, the endosteal niche appears to promote HSC quiescence and maintenance[113,126,127].

During embryogenesis HSC are located in proximity to vasculature in the yolk sac, AGM and placenta[103,128]. These blood vessels have a crucial role in promoting the expansion of HSC throughout embryonic development and probably still contribute during adult hematopoiesis. The spleen is frequently a site of extramedullary hematopoiesis during adult life, indicating HSC can survive away from the endosteal (or osteoblastic) niche. Most HSC in the spleen are located near specialized blood vessels called sinusoids, implying extramedullary HSC are supported by a sinusoidal (or vascular) niche. In 2005, Morrison's group used an elegant immunofluorescence study to show that many HSC in adult BM were also found around sinusoids[129]. The concept of a vascular niche in the BM is further supported by the observation that HSC can mobilize into the circulation within minutes of administering IL-8[130]. The vascular niche is thus perceived to support HSC mobilization or activation, however the evidence is merely circumstantial. It remains to be determined if there are spatially distinct niches with distinct functional roles in HSC regulation or if they both support similar HSC function.

The histological complexity of the BM has made it challenging to pinpoint the anatomical location of HSC *in vivo*. The immunohistological techniques used by Morrison's group do not allow for functional evaluation of the HSC within their particular niches[129]. These *in vitro* studies are purely based on the phenotypic characterization of the cells using combinations of surface receptors. Recent

scientific advancements have been made using intra-vital microscopy to examine HSC within their *in vivo* niches[131,132]. In these studies, osteoblasts and blood vessels within the BM appear to be in very close proximity to one another and intertwined with HSC. This co-localization demonstrates it is anatomically improbable to have distinct osteoblastic and vasculaur niches in the BM[131]. Regardless of how and where HSC are supported in the microenvironment, normal niche function is required for regulated hematopoiesis.

HSC Functional Assays *In Vivo*

In order to establish HSC function, competitive repopulation models are often used. This system directly models the donor and host competition for hematopoietic engraftment *in vivo*[133]. After transplant donor cells home to the marrow, engraft and differentiate into myeloid and lymphoid cells. However, generating differentiated blood cells is not enough as most of these populations are short-lived. The engrafted HSC must also maintain the pool of progenitors in the host so that long-term hematopoiesis can be maintained. Short-term precursors disappear 1-4 months after transplantation[134], thereafter only long-term HSC (LT-HSC) will persist. Thus determination of donor repopulation after 4 months is essential in defining LT-HSC that can provide continuous hematopoiesis for the duration of the lifespan of the host. Using the competitive repopulating unit (CRU) assay, the function of LT-HSC is tested relative to normally functioning competitor cells at 4 months post-transplantation. The donor LT-HSC function is calculated using repopulating units (RU), where 1 RU

represents the repopulating ability of 100,000 competitor cells[133]. Using RU to determine the capacity of the donor HSC to repopulate host hematopoiesis, we can operationally define a functional HSC.

In addition to the functional analysis of HSC, the research community has invested much of its time in the phenotypic characterization of HSC using cell surface markers. Defined monoclonal antibodies to these surface markers have made it easier to isolate specific cell populations. It is important to note that there remains much discussion between investigators in determining which combination of surface markers most accurately isolates a pure LT-HSC population. Using combinations of these cell surface markers, fluorescence activated cell sorting (FACS) can be used to separate a purified LT-HSC population from the bone marrow. Using sorted cells that express an HSC phenotype, transplant competitions similar to the CRU assay can be performed to directly test the functional capacity of these phenotypic HSC. In the direct competition assay or DCA[135], phenotypic LT-HSC from donors are transplanted in competition with an equivalent dose of normal LT-HSC. Similar to the CRU assay, stem cell function can be determined at 4 months post-transplant. The DCA allows a more quantitative comparison of function on a per stem cell basis.

A Role For SHIP in HSC

The survival of an organism is dependent upon the ability of the HSC to replenish the blood compartment throughout life. For proper hematopoiesis to be sustained HSC must maintain a careful balance between self-renewal,

differentiation and apoptosis. HSC homeostasis is yet to be fully understood but we know HSC are at least in part regulated by extrinsic factors. Some of the external cues that engage receptors on HSC are SCF, SDF-1, TPO, and interleukins[111-115]. Several of these growth factors also stimulate PI(3,4,5)P3 formation by activating PI3K signaling. As previously described, SHIP plays a prominent role in reducing PI(3,4,5)P3 levels in hematopoietic cells, therefore we hypothesized SHIP might have a role in HSC homeostasis. Using SHIP knockout mice, we determined $SHIP^{-/-}$ purified HSC or whole bone marrow (WBM) failed to compete effectively with wild type (WT) HSC or WBM for long-term multi-lineage hematopoietic repopulation (LTMR)[136](Figure 4). This was determined using the described DCA or CRU assays, respectively.

The failure of $SHIP^{-/-}$ HSC to provide LTMR, combined with a significant expansion of phenotypic HSC numbers in $SHIP^{-/-}$ bone marrow and spleen (Table 1) indicated a loss of HSC homeostasis with SHIP-deficiency. We then determined the reduced LTMR function was not caused by accelerated senescence, as there were significantly fewer apoptotic cells in $SHIP^{-/-}$ bone marrow compared to WT. We hypothesized that a homing disruption might be preventing $SHIP^{-/-}$ HSC from making it to the bone marrow niche after transplant, thereby preventing proper LTMR. Using an in vivo homing assay, we determined $SHIP^{-/-}$ HSC could not home to the bone marrow as well as WT HSC. Appropriately, we also discovered several receptors key to the homing process were significantly down regulated on the surface of $SHIP^{-/-}$ HSC (Figure 5).

Combined, these results suggested a cell autonomous role for SHIP in HSC homing and repopulation.

The capacity of HSC to home to the correct microenvironment is an essential prerequisite for LTMR of transplanted hosts. Additionally, all LT-HSC in adult bone marrow that engraft after transplant are in G0 phase[109], whereas fetal HSC are largely cycling, which indicates, HSC only perform their proper functions when located within the appropriate niche. We therefore speculate that SHIP-deficiency might be disrupting the HSC niche and consequently lead to altered HSC function, arguing a non-autonomous role for SHIP in HSC.

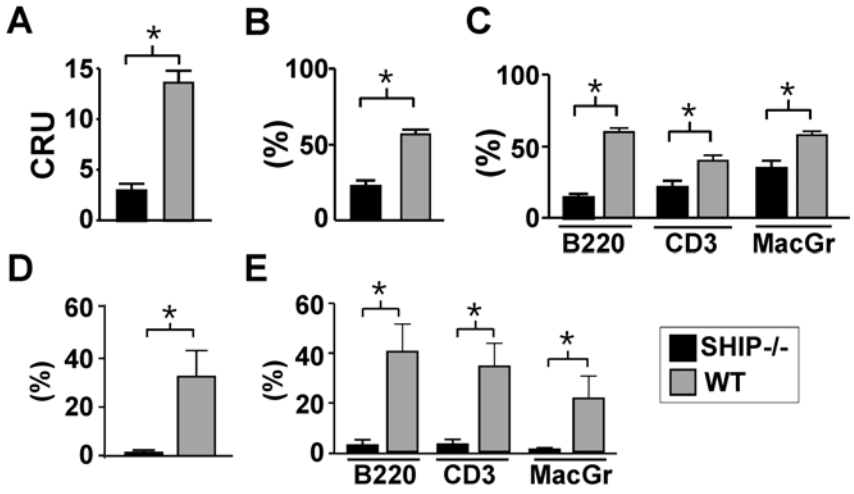

Figure 4: SHIP$^{-/-}$ WBM and purified HSC have compromised reconstituting activity.

(A) CRU activity calculated based on the percentage of global repopulation in the PB by donor WBM cells 4 months after transplant. (B) Percentage of global repopulation of PB by SHIP$^{-/-}$ or WT WBM cells 4 months after transplant. (C) Percentage of lymphoid and myeloid PB cells derived from SHIP$^{-/-}$ or WT WBM cells in the CRU assay 4 months after transplant. (D) Percentage of global repopulation by purified HSC from SHIP$^{-/-}$ or WT BM 4 months after transplant. (E) Percentage of lymphoid and myeloid PB cells derived from SHIP$^{-/-}$ or WT purified HSC cells in the DCA assay 4 months after transplant. Significance was established using the unpaired Student's T test (*$p<0.05$). Errors shown represent the SEM. [Black bars, cells derived from SHIP$^{-/-}$ BM; Grey bars, cells derived from WT BM] This research was originally published in Blood. Caroline Desponts, Amy L Hazen, Kim H T Paraiso and Wiliam G Kerr. SHIP deficiency enhances HSC proliferation and survival but compromises homing and repopulation. Blood. 2006; 107: 4338-4345. © the American Society of Hematology.

Table 1: Increased numbers of HSC cells in the BM and spleen of SHIP$^{-/-}$ mice compared to WT littermates.
This research was originally published in Blood. Caroline Desponts, Amy L Hazen, Kim H T Paraiso and William G Kerr. SHIP deficiency enhances HSC proliferation and survival but compromises homing and repopulation. Blood. 2006; 107: 4338-4345. © the American Society of Hematology.

Population		SHIP-/- (%)	WT (%)	P value
Lin-Sca1+cKit+Thy1^{low}	BM	0.4114 ± 0.0353	0.0725 ± 0.025	<0.0001
	spleen	0.0957 ± 0.0131	0.0142 ± 0.0040	0.004
Lin-cKit+Sca1+Flk2-	BM	0.2860 ± 0.0398	0.1340 ± 0.02015	0.0093
	spleen	0.0827 ± 0.0141	0.027 ± 0.002	0.0172
Lin-Sca1+cKit+CD48-	BM	0.019 ± 0.002	0.0068 ± 0.0006	0.0012
	spleen	0.0020 ± 0.0003	0.00023 ± 0.00005	0.0051

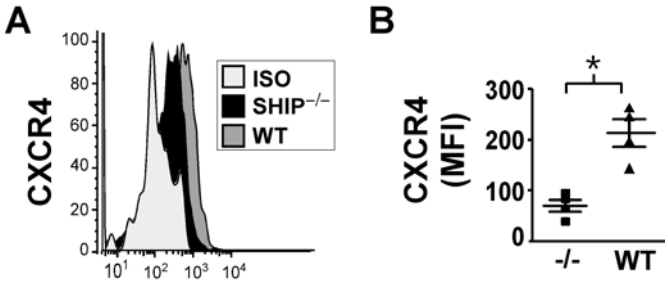

Figure 5: SHIP$^{-/-}$ HSC express lower levels of CXCR4.
(A) A representative histogram of CXCR4 expression on SHIP$^{-/-}$ or WT purified HSC. (B) The median fluorescence intensity (MFI) of CXCR4 expression on purified SHIP$^{-/-}$ or WT HSC. Significance was established using the unpaired Student's T test (*p<0.05). Errors shown represent the SEM. This research was originally published in Blood. Caroline Desponts, Amy L Hazen, Kim H T Paraiso and Wiliam G Kerr. SHIP deficiency enhances HSC proliferation and survival but compromises homing and repopulation. Blood. 2006; 107: 4338-4345. © the American Society of Hematology.

SHIP is Required for a Functional Hematopoietic Stem Cell Niche

Abstract

SH2-domain-containing Inositol 5'-Phosphatase-1 (SHIP) deficiency significantly increases the number of hematopoietic stem cells (HSC) present in the bone marrow (BM). However, the reconstitution capacity of these HSC is severely impaired suggesting that SHIP expression might be an intrinsic requirement for HSC function. To further examine this question, we developed a model in which SHIP expression is ablated in HSC while they are resident in a SHIP-competent milieu. In this setting we find that long-term repopulation by SHIP-deficient HSC is not compromised. Moreover, SHIP-deficient HSC from this model repopulate at levels comparable to wild type (WT) HSC upon serial transfer. However, when HSC from mice with systemic ablation of SHIP are transplanted they are functionally compromised for repopulation. These findings demonstrate SHIP is not an intrinsic requirement for HSC function, but rather that SHIP is required for the BM milieu to support functionally competent HSC. Consistent with these findings, cells that comprise the BM niche express SHIP and SHIP-deficiency profoundly alters their function.

Introduction

Because of their capacity for self-renewal and multi-lineage potential, HSC support blood cell production throughout life. HSC are thought to reside in specialized endosteal and vascular niches in the BM that support quiescence, self-renewal and/or differentiation[101,124,129,137]. Other HSC fates include mobilization to extramedullary sites and return to the BM[102]. Additionally, apoptosis which regulates the homeostasis of differentiated tissues[138], contributes to control of the HSC compartment size, where ~1-2% of HSC are apoptotic during steady-state hematopoiesis[136]. Thus, a careful balance between the above fates must be maintained to sustain a sufficient number of HSC to maintain blood cell production throughout life. We, and others, have found that stem cell restricted SHIP (s-SHIP)[41,139] and SHIP[136,140] play roles in the biology of pluripotent and adult tissue stem cells, respectively. Previously we showed that SHIP limits the HSC compartment size *in vivo*. However, following transplantation these HSC exhibit compromised BM homing and long-term multi-lineage repopulation[136].

SHIP or s-SHIP expression in adult physiology has been documented in HSC[41,139], most blood cell lineages[1,3,5,141], embryonic fibroblasts[136] and endothelial cells[142]. Through its enzymatic domain SHIP can hydrolyze the PI3K products, PI(3,4,5)P_3 and I(1,3,4,5)P_4, and thus is capable of regulating the activity of multiple PI3K effector pathways including the distal kinases Akt, Btk, MAP/ERK, PLC-γ and intracellular calcium. The context in which SHIP mediates these activities is determined by its expression, but also by its inducible

recruitment to various receptor-associated signaling complexes mediated by tyrosine phosphorylation of receptor motifs or NPXY sequences present in SHIP[1,3,143,144]. Due to the nearly ubiquitous expression of SHIP in differentiated hematopoietic cell types and its induced recruitment to a wide variety of receptor-associated signaling complexes, SHIP has the potential to regulate a wide variety of cellular functions in adult physiology.

SHIP is expressed throughout the hematopoietic system and in endothelial cells. From biochemical studies alone, it is difficult to determine if SHIP might play a critical role in normal mammalian physiology. Towards this end, genetic analysis of SHIP mutant mice has revealed a pivotal role for SHIP in a variety of differentiated cell types. SHIP plays a role in the control of the NK receptor repertoire and cytolytic function[11,145], B cell development and antibody production[146,147], the myeloid response to bacterial mitogens[148], development of marginal zone macrophages[82], osteoclast function[83], lymph node recruitment of dendritic cells[85], mast cell degranulation[149] and the homeostasis and function of myeloid immunoregulatory cells[85,86].

Previously we found that the poor repopulating capacity of SHIP-deficient HSC may be a result of their reduced BM homing capacity. We speculated that SHIP-deficient HSC might have normal repopulating function if they were not required to home to their BM niche. To test this hypothesis, we developed an *in situ* SHIP deletion model, where SHIP expression is ablated after HSC are resident in a SHIP-competent BM microenvironment. Analysis of the hematopoietic compartment in this model showed that SHIP-deficiency does not

diminish the capacity of HSC to self-renew or mediate multi-lineage repopulation after serial transfer to secondary hosts. Conversely, when SHIP expression is ablated systemically in MxCreSHIP$^{flox/flox}$ mice, we find that SHIP-deficiency compromises the repopulation potential of HSC in a similar fashion to that in germline SHIP-deficient mice. This demonstrates an unanticipated requirement for SHIP expression in the function of the HSC BM niche. Consistent with these results we show SHIP is expressed in cells that comprise the BM niche and SHIP-deficiency significantly alters their cell numbers, their production of chemokines and their ability to support HSC cycling.

Results

HSC Rendered SHIP-deficient in a SHIP-competent Niche Retain Multi-lineage Repopulation

To determine if the repopulation defect observed for SHIP$^{-/-}$ HSC is due to an inability to home efficiently to the BM HSC niche, we developed an *in situ* SHIP deletion model where SHIP expression is ablated after achieving HSC engraftment, bypassing the requirement of SHIP for BM homing. In this model, we co-transplant an equal dose of SHIP-competent BM cells in which Cre-mediated deletion of SHIP is not possible. This model enables quantitation of competitive repopulating activity (RU) for HSC rendered SHIP-deficient *in situ*. A similar approach was previously used to study the role of Rho family proteins in HSC function[150]. In our *in situ* SHIP deletion model, lethally irradiated CD45.1^{+}45.2^{+} recipients are transplanted with equal numbers of CD45.2^{+}CD45.1^{-}

MxCreSHIP$^{flox/flox}$ and CD45.1^{+}CD45.2^{-} SHIP$^{+/+}$ WBM cells. In these chimeras, equivalent repopulation from both the MxCreSHIP$^{flox/flox}$ (CD45.2^{+}CD45.1^{-}) and SHIP$^{+/+}$ (CD45.1^{+}CD45.2^{-}) BM donors was observed at 60 days post-transplant, indicating comparable levels of HSC engraftment from each donor (Figure 6). We then administered three intra-peritoneal polyinosinic-polycytidylic acid (polyI:C) injections to induce SHIP deletion in the MxCreSHIP$^{flox/flox}$ portion of these BM chimeras. Two months after deletion, CD45.2^{+}CD45.1^{-} and CD45.1^{+}CD45.2^{-} cells from the peripheral blood (PB) were FACS sorted to assess SHIP expression by Western blot analysis. SHIP deletion is highly efficient in polyI:C-treated MxCreSHIP$^{flox/flox}$ cells as indicated by the near complete absence of SHIP expression in the CD45.2^{+}CD45.1^{-} cells derived from MxCreSHIP$^{flox/flox}$ HSC (data not shown). For further confirmation, we harvested spleens from all chimeras upon their termination 5 months post-transplant. Western blot analysis of FACS sorted CD45.2^{+}CD45.1^{-} cells (Figure 7) confirmed nearly complete ablation of SHIP expression in the hematopoietic compartment derived from MxCreSHIP$^{flox/flox}$ HSC present in these BM chimeras.

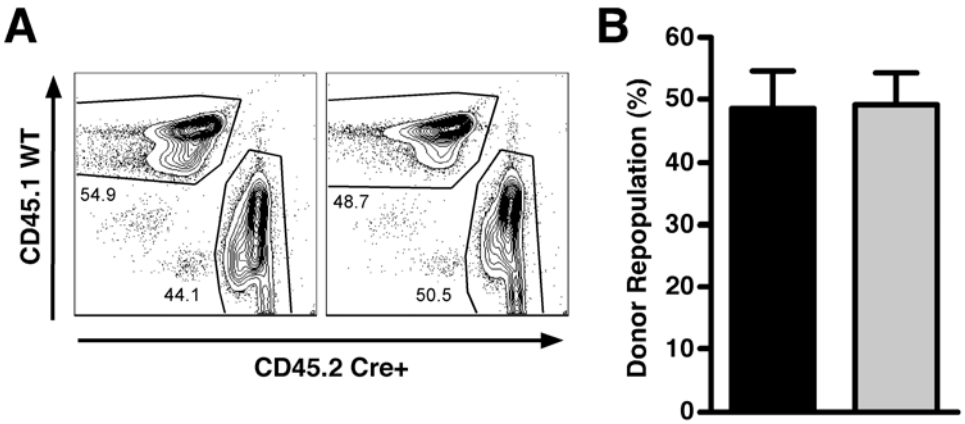

Figure 6: Equal engraftment by both donors after 60 days.
(A) Contour plots for CD45.1 vs. CD45.2 staining illustrating equal repopulation in PB at 60 days post-transplant prior to polyI:C treatment in two representative MxCreSHIP$^{flox/flox}$(CD45.2):WT-Ly5.1(CD45.1) BM chimeras. (B) Percentage of donor repopulation in the PB by MxCreSHIP$^{flox/flox}$(CD45.2) and WT-Ly5.1(CD45.1) HSC in MxCreSHIP$^{flox/flox}$(CD45.2):WT-Ly5.1(CD45.1) BM chimeras at 60 days post-transplant prior to polyI:C treatment. Significance was established using the unpaired Student's T test. Errors shown represent the SEM. [Black bars, cells derived from MxCreSHIP$^{flox/flox}$ BM; Grey bars, cells derived from WT-Ly5.1 BM]

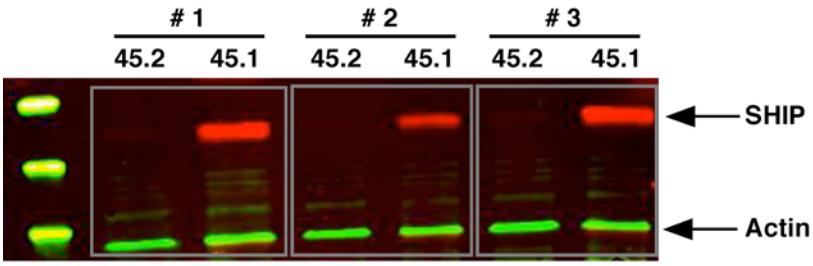

Figure 7: SHIP can be deleted *in situ* after transplant.
Representative SHIP Western blot from single positive $CD45.1^{+}CD45.2^{-}$ or $CD45.2^{+}CD45.1^{-}$ sorted cells isolated from splenocytes from $MxCreSHIP^{flox/flox}$(CD45.2):WT-Ly5.1(CD45.1) BM chimeras 5 months after polyI:C treatment. Single positive splenocytes were sorted and lysate were probed for SHIP expression.

At monthly intervals we monitored the degree of multi-lineage repopulation by $CD45.2^{+}CD45.1^{-}$ (SHIP-deficient) vs. $CD45.1^{+}CD45.2^{-}$ (SHIP-competent) cells in these chimeras. We found that SHIP-deleted HSC retain the ability to efficiently perform long-term, multi-lineage repopulation at levels comparable to the competing SHIP-competent HSC present in these chimeras. We observed no significant difference in global hematopoietic repopulation (Figure 8A) or RU activity (Figure 8B) between *in situ* SHIP-deleted and WT HSC up to 5 months following ablation of SHIP expression. In addition, repopulation of both the lymphoid and myeloid arms of hematopoiesis was observed out to 5 months following induction of SHIP-deficiency (Figure 8C). Thus, when HSC are established *in situ* and then rendered SHIP-deficient this does not significantly compromise their potential for long-term, multi-lineage repopulation. However, we did observe a small, but significant, reduction in T lymphocyte reconstitution

in the CD45.2^{+}CD45.1^{-} SHIP-deficient compartment despite normal repopulation of the B and NK lymphoid lineages (Figure 8D). Consistent with this finding, a reduction in peripheral T cell numbers is observed in germline SHIP$^{-/-}$ mice[81]. Because decreased T cell production is observed only in the SHIP-deficient portion of these chimeras and not in the other lymphoid lineages, we conclude that SHIP is required for the efficient development of T lymphocytes and this requirement is intrinsic to the T cell lineage.

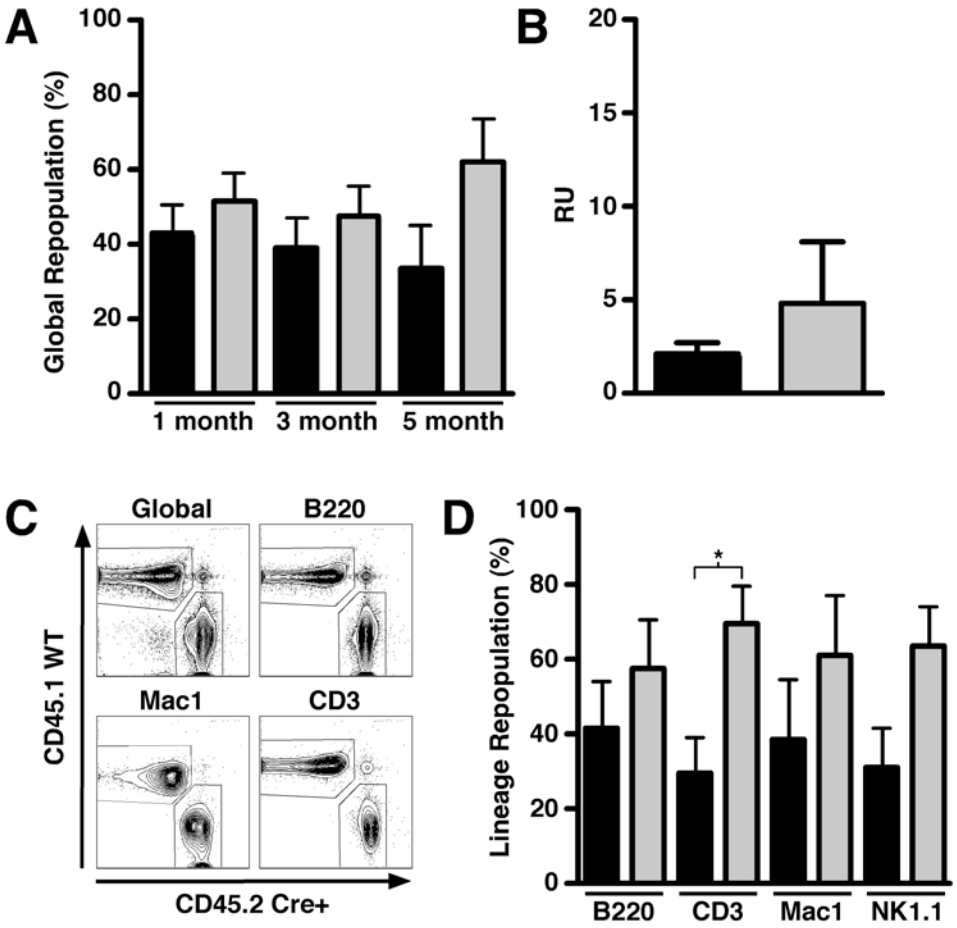

Figure 8: *In situ* deletion of SHIP does not compromise the capacity of HSC to mediate long-term multi-lineage repopulation.
(A) Percentage of global repopulation in the PB by MxCreSHIP$^{flox/flox}$(CD45.2) and WT-Ly5.1(CD45.1) HSC in MxCreSHIP$^{flox/flox}$(CD45.2):WT-Ly5.1(CD45.1) BM chimeras at the indicated times following polyI:C treatment (n≥5). At monthly intervals, the level of donor reconstitution was assessed in PB. (B) Repopulating Unit (RU) activity by MxCreSHIP$^{flox/flox}$(CD45.2) and WT-Ly5.1(CD45.1) HSC in the MxCreSHIP$^{flox/flox}$(CD45.2):WT-Ly5.1(CD45.1) BM chimeras 5 months after polyI:C treatment (n≥5). (C) Contour plots for CD45.1 vs. CD45.2 staining that illustrate multi-lineage repopulation in PB 20 weeks after polyI:C treatment in a representative MxCreSHIP$^{flox/flox}$(CD45.2):WT-Ly5.1(CD45.1) BM chimera. (D) Percentage repopulation of the indicated lymphoid and myeloid cell lineages by MxCreSHIP$^{flox/flox}$(CD45.2) and WT-Ly5.1(CD45.1) HSC in MxCreSHIP$^{flox/flox}$(CD45.2):WT-Ly5.1(CD45.1) BM chimeras 5 months after polyI:C treatment (n≥5). At sacrifice, the level of donor reconstitution was assessed in BM. Significance was established using the unpaired Student's T test (*$p<0.05$). Errors shown represent the SEM. [Black bars, cells derived from MxCreSHIP$^{flox/flox}$ BM; Grey bars, cells derived from WT-Ly5.1 BM]

SHIP-deficient HSC Derived from a SHIP-competent Niche Have Normal self-renewal Capacity

Analysis of the above chimeras demonstrated long-term, multi-lineage repopulation from the SHIP-deficient HSC compartment is intact when HSC are resident in a SHIP-competent niche. This finding suggested that self-renewal capacity might also be intact in SHIP-deficient HSC. To compare the self-renewal capacity of SHIP-deficient and SHIP-competent HSC in these chimeras we performed serial BM transfers from the initial chimeras to secondary recipients. Whole BM was harvested from the chimeras described above at 5 months following SHIP deletion and was then transplanted into lethally irradiated $CD45.1^{+}CD45.2^{+}$ secondary hosts. Prior to these serial transfers we first compared the proportion of SHIP-deficient ($CD45.2^{+}CD45.1^{-}$) to SHIP-competent ($CD45.1^{+}CD45.2^{-}$) cells in the HSC compartment by multi-parameter flow cytometric analysis of CD45.1 vs. CD45.2 staining on $Kit^{+}Lin^{-}Sca1^{+}CD48^{-}$ (KLSCD48) cells. This analysis revealed a statistically comparable level of contribution to the KLSCD48 HSC compartment by the SHIP-deficient and SHIP-competent HSC within the $MxCreSHIP^{flox/flox}$:WT-Ly5.1 BM chimeras (Figure 9A). SHIP-deficient HSC in these $MxCreSHIP^{flox/flox}$:WT-Ly5.1 BM chimeras were also found to represent a statistically comparable proportion of the KLSCD48 compartment as compared to $SHIP^{flox/flox}$ HSC in the $SHIP^{flox/flox}$:WT-Ly5.1 BM control chimeras analyzed in parallel (Figure 9B). We then monitored global repopulation in the secondary hosts for a period of four months and found that SHIP-deficient HSC from $MxCreSHIP^{flox/flox}$:WT-Ly5.1 BM chimeras competed

effectively in donor blood cell repopulation as compared to the WT-Ly5.1 HSC present in the same BM inoculum (Figure 10), demonstrating that SHIP-deficient HSC can effectively home and engraft upon transplant when they are derived from a SHIP-competent HSC niche. Thus, SHIP expression is not an intrinsic requirement for HSC homing to BM and self-renewal.

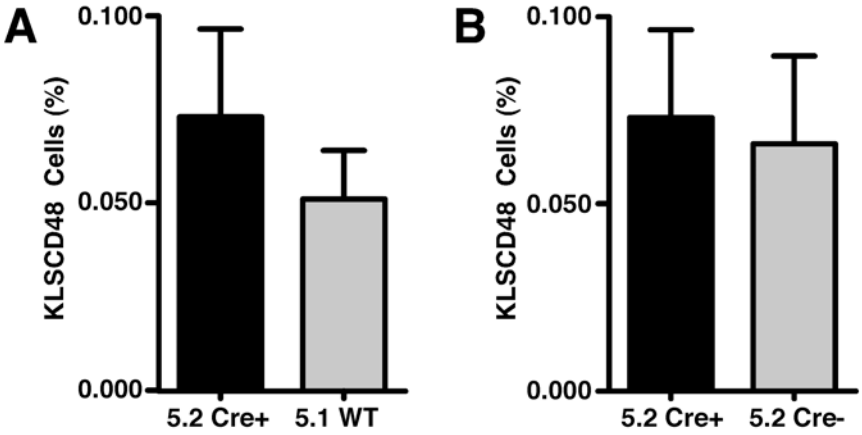

Figure 9: *In situ* deletion of SHIP does not compromise homing capacity of HSC.
(A) Flow cytometric quantitation of the relative contribution to KLSCD48 HSC by MxCreSHIP$^{flox/flox}$(CD45.2) or WT-Ly5.1(CD45.1) cells in the BM of MxCreSHIP$^{flox/flox}$(CD45.2):WT-Ly5.1(CD45.1) chimeras 5 months after polyI:C treatment (n≥3). BM cells were stained with markers for the Lineage$^{-/low}$c-Kit^{+}Sca1^{+}CD48^{-} (KLSCD48) phenotype[129]. (B) Flow cytometric quantitation of the relative contribution to KLSCD48 HSC by MxCreSHIP$^{flox/flox}$(CD45.2) cells in the BM of MxCreSHIP$^{flox/flox}$(CD45.2):WT-Ly5.1(CD45.1) chimeras vs. SHIP$^{flox/flox}$(CD45.2) cells in SHIP$^{flox/flox}$(CD45.2):WT-Ly5.1(CD45.1) control chimeras. Both sets of chimeras were analyzed 5 months after polyI:C treatment (n≥3). Significance was established using the unpaired Student's T test. Errors shown represent the SEM. [Black bars, cells derived from MxCreSHIP$^{flox/flox}$ BM (Cre+); Grey bars, cells derived from WT-Ly5.1 BM (WT) or SHIP$^{flox/flox}$ (Cre-)]

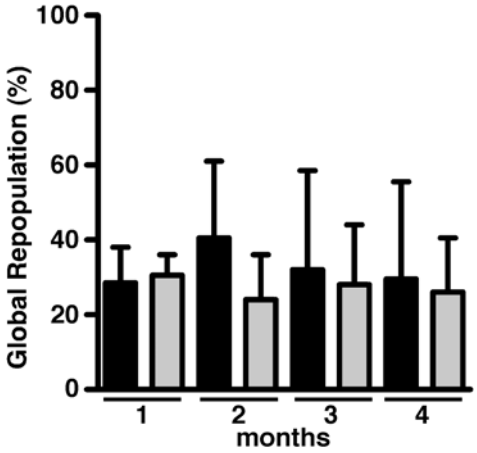

Figure 10: *In situ* deletion of SHIP does not compromise secondary repopulating capacity of HSC.
Percentage global repopulation of PB at the indicated times by MxCreSHIP$^{flox/flox}$(CD45.2) and WT-Ly5.1(CD45.1) HSC after serial transplantation of 1x10^6 WBM cells from MxCreSHIPflox/flox(CD45.2):WT-Ly5.1(CD45.1) chimeras 5 months after polyI:C treatment (n≥3). Significance was established using the unpaired Student's T test. Errors shown represent the SEM. [Black bars, cells derived from MxCreSHIP$^{flox/flox}$ BM (Cre+); Grey bars, cells derived from WT-Ly5.1 BM (WT)]

Systemic Induction of SHIP-deficiency in Adult Physiology is Detrimental to the Repopulating Capacity of BM HSC

SHIP is expressed in embryonic, fetal and adult tissues, including mesenchymal, endothelial and hematopoietic lineages[3,41,139,141]. Cells from all three of these tissues participate directly or indirectly in the HSC BM niche and thus their development may be impaired or altered during ontogeny in mice with germline SHIP-deficiency. Therefore, the HSC disruptions we observe could be due to developmental alterations of the niche by SHIP-deficiency. Alternatively, SHIP could be required in adult physiology for the normal function of the niche.

To test the latter possibility, we induced systemic SHIP-deficiency in adult mice and then asked whether this also impairs HSC function. Induction of SHIP-deficiency in the previous chimeras showed no intrinsic requirement of SHIP for BM homing, repopulation or self-renewal by HSC and thus, in the setting of induced, but systemic SHIP-deficiency we are testing whether SHIP-deficiency impairs the HSC niche in BM. For these studies, BM was harvested from MxCreSHIP$^{flox/flox}$ mice that had undergone systemic SHIP-ablation by three polyI:C injections (Figure 11). Induction of SHIP-deficiency was confirmed by Western blot analysis of PBMC (data not shown).

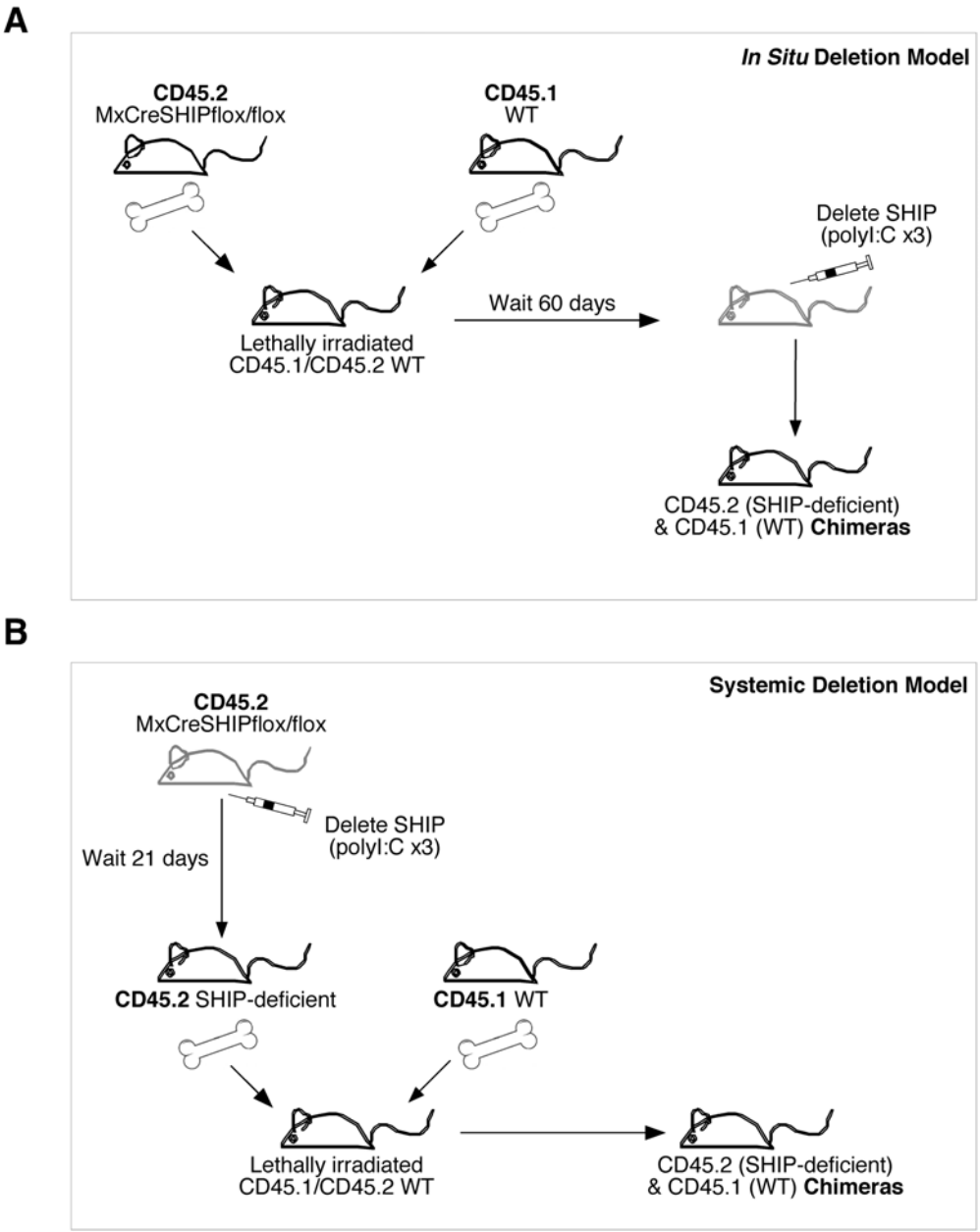

Figure 11: Schematic illustration of transplantation models.
(A) *In Situ* SHIP deletion BM transplants: MxCreSHIP$^{flox/flox}$(CD45.2^{+}) 5x10^{5} WBM cells were co-transplanted (i.v.) with 5x10^{5} WBM competitor cells from WT-Ly5.1(CD45.1^{+}) mice into lethally irradiated CD45.1^{+}45.2^{+} recipients. After 60 days recipient mice were treated with three poly I:C injections to delete SHIP in all cells derived from the MxCreSHIP$^{flox/flox}$ graft. (B) Systemic SHIP deletion BM transplants: MxCreSHIP$^{flox/flox}$(CD45.2^{+}) mice were pre-treated with three poly I:C injections to systemically delete SHIP. After SHIP deletion was confirmed, 5x10^{5} WBM cells from MxCreSHIP$^{flox/flox}$(CD45.2^{+}) mice were co-transplanted (i.v.) with 5x10^{5} WBM competitor cells from WT-Ly5.1(CD45.1^{+}) mice into lethally irradiated CD45.1^{+}45.2^{+} recipients.

Prior to transplant we observed that cells of the KLSCD48 HSC phenotype were significantly expanded in mice with induced SHIP-deficiency relative to $SHIP^{flox/flox}$ controls that underwent an equivalent regimen of polyI:C injections (Figure 12). Furthermore, the absolute number of KLSCD48 cells in mice with induced SHIP-deficiency was significantly expanded compared to $SHIP^{flox/flox}$ controls (data not shown). This expansion seems to be restricted to more primitive KLSCD48 and KLS progenitor cells and was not found in $cKit^{+}Lineage^{-}$ cells (data not shown). Because we observed no significant expansion of the SHIP-deficient KLSCD48 cells in chimeras with a SHIP-competent niche (Figure 9), we conclude then that SHIP expression is required by the adult BM niche to limit the size of the KLSCD48 HSC compartment. To analyze the repopulating ability of BM HSC in mice with systemic induction of SHIP deficiency, we co-transplanted equal numbers of WBM cells from SHIP-deleted ($CD45.2^{+}CD45.1^{-}$) and SHIP-competent ($CD45.1^{+}CD45.2^{-}$) donors into lethally irradiated WT ($CD45.2^{+}CD45.1^{+}$) recipients. As before, monthly peripheral blood monitoring was used to assess engraftment. Using both global repopulation (Figure 13A) and RU (Figure 13B) as measures of engraftment, the HSC from donors with induced SHIP-deficiency did not compete effectively against HSC from SHIP-competent donors.

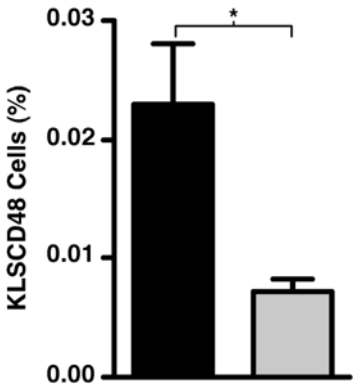

Figure 12: Systemic induction of SHIP-deficiency compromises homeostasis of the HSC compartment.
Flow cytometric quantitation of KLSCD48 HSC in the BM of MxCreSHIP$^{flox/flox}$(CD45.2) mice and SHIP$^{flox/flox}$(CD45.2) controls 21 days after polyI:C treatment (n≥3). Significance was established using the unpaired Student's T test (*p<0.05). Errors shown represent the SEM. [Black bars, cells derived from MxCreSHIP$^{flox/flox}$ BM; Grey bars, cells derived from SHIP$^{flox/flox}$]

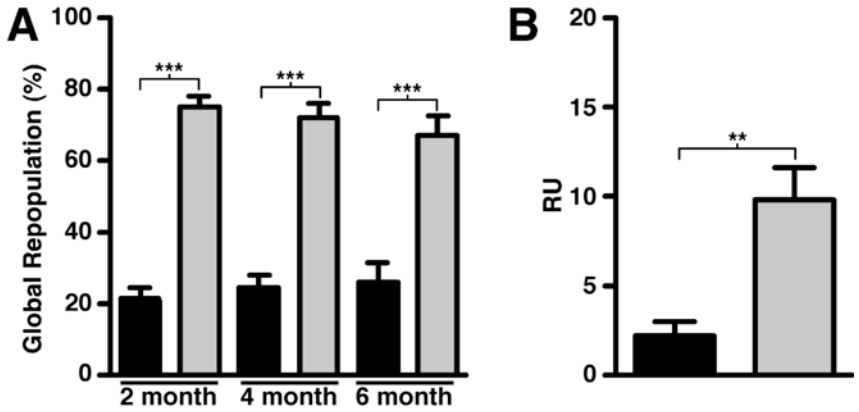

Figure 13: Systemic induction of SHIP-deficiency compromises the capacity of HSC to mediate repopulation over time.
(A) Percentage of global repopulation in PB at the indicated times post-transplant by WBM cells from SHIP-ablated MxCreSHIP$^{flox/flox}$(CD45.2) donors and WT-Ly5.1(CD45.1) control donors (n≥9). (B) Repopulation Unit (RU) activity from SHIP-ablated MxCreSHIP$^{flox/flox}$(CD45.2) donors and WT-Ly5.1(CD45.1) control donors (n≥9). Significance was established using the unpaired Student's T test (**p<0.005; ***p<0.0001). Errors shown represent the SEM. [Black bars, cells derived from MxCreSHIP$^{flox/flox}$ BM; Grey bars, cells derived from WT-Ly5.1 BM]

Furthermore, multi-lineage reconstitution appears to be significantly compromised for all lymphoid lineages in the PB (Figure 14A-B) and in myelo-erythroid lineages in the BM (Figure 14C). However, despite significantly decreased myelopoiesis, megakaryopoiesis and erythropoiesis in the BM by HSC from mice with induced SHIP-deficiency (Figure 14C), we observed statistically comparable myeloid reconstitution in the peripheral blood and spleen from these HSC (Figure 14B and data not shown). This sustained peripheral myelopoiesis by the SHIP-deficient BM graft that occurs in spite of significantly compromised central myelopoiesis is likely due to robust extramedullary myelopoiesis that we and others observe in the spleens of $SHIP^{-/-}$ mice[81].

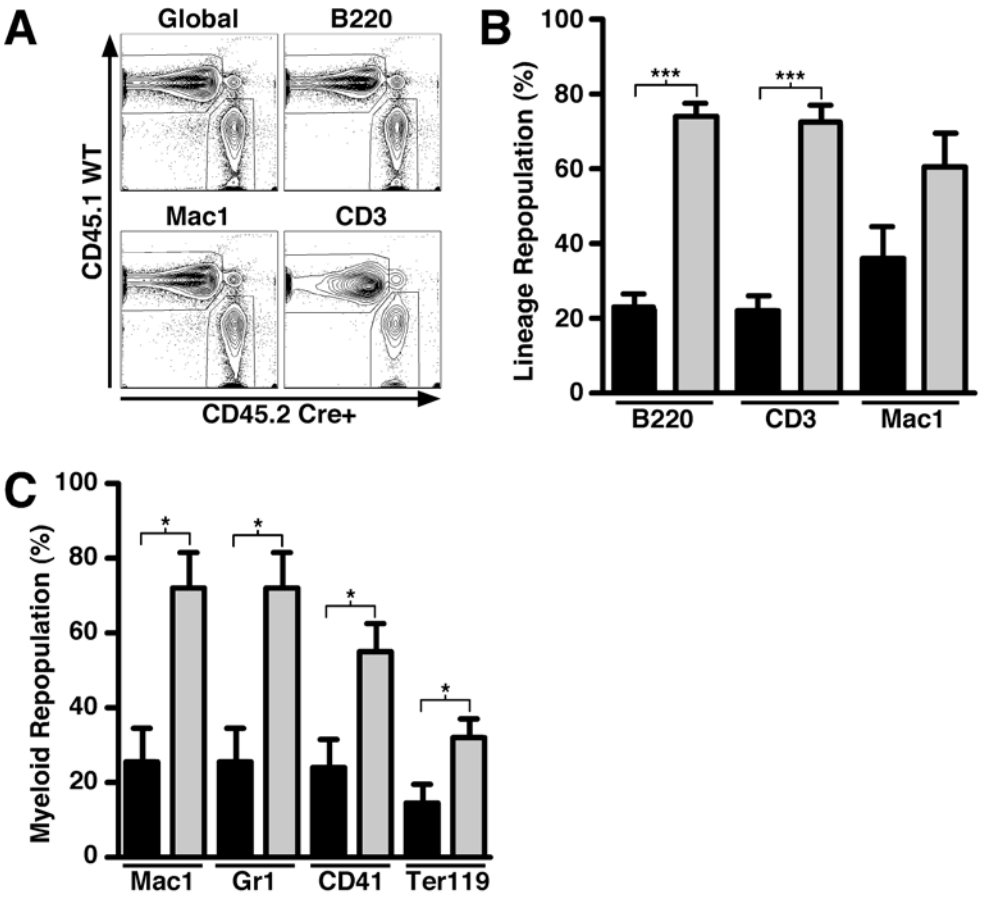

Figure 14: Systemic induction of SHIP-deficiency compromises the capacity of HSC to mediate long-term multi-lineage repopulation.
(A) Representative dual color contour plots that illustrate the level of PB reconstitution at 24 weeks post-transplant from SHIP-ablated MxCreSHIP$^{flox/flox}$(CD45.2) BM donors and WT-Ly5.1(CD45.1) BM competitor donors. (B) Percentage PB repopulation for the indicated lymphoid or myeloid lineage by WBM cells in a competitive transplant of SHIP-ablated MxCreSHIP$^{flox/flox}$(CD45.2) and WT-Ly5.1(CD45.1) BM competitor cells (n≥9). Prior to sacrifice, the level of donor reconstitution was assessed in PB. (C) Percentage BM repopulation for the indicated myeloid (Mac1), granulocytic (Gr1), megakaryocytic (CD41) or erythroid (Ter119) lineage by WBM cells in a competitive transplant of SHIP-ablated MxCreSHIP$^{flox/flox}$(CD45.2) and WT-Ly5.1(CD45.1) BM competitor cells (n≥9). At sacrifice, the level of donor reconstitution was assessed in BM. Significance was established using the unpaired Student's T test (*$p<0.05$; ***$p<0.0001$). Errors shown represent the SEM. [Black bars, cells derived from MxCreSHIP$^{flox/flox}$ BM; Grey bars, cells derived from WT-Ly5.1 BM]

A SHIP-deficient BM Microenvironment Expands Phenotypic HSC and Reduces Surface Expression of CXCR4

Expansion of the phenotypic HSC compartment and functional impairment of HSC in mice following the induction of systemic SHIP-deficiency described above was reminiscent of our previous findings for HSC in germline SHIP$^{-/-}$ mice. To examine whether CXCR4 surface expression on HSC might also be altered by the SHIP status of the BM niche, we assessed CXCR4 surface expression on *in situ* SHIP-deleted HSC where the niche remains SHIP-competent and in HSC from mice following induction of systemic SHIP-deficiency where the BM microenvironment is also rendered SHIP-deficient. In the *in situ* SHIP-deleted model described in Figures 6-9, we found that the SHIP-deficient KLSCD48 cells do not show significant reductions in CXCR4 surface expression as compared to SHIP-competent KLSCD48 cells present in the same mice (Figure 15A-B).

However, when we analyzed the surface expression of CXCR4 on KLSCD48 cells in mice with induced systemic SHIP-deficiency, we found that the CXCR4 surface expression is significantly reduced relative to SHIP$^{flox/flox}$ controls that received an equivalent regimen of polyI:C (Figure 16A-B). As shown in Figure 12, KLSCD48 cells are also significantly expanded in mice when systemic SHIP-deficiency is induced. Thus, expansion of the phenotypic HSC compartment and down-modulation of CXCR4 are triggered only by induced, systemic SHIP-deficiency, demonstrating regulation of these HSC properties by the BM niche in adult physiology.

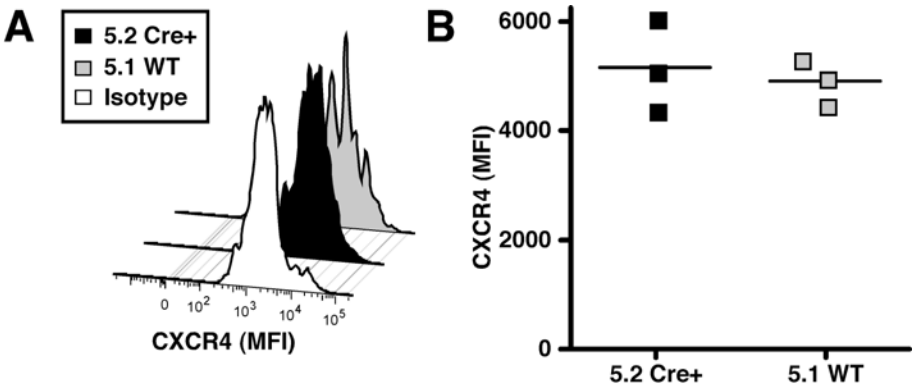

Figure 15: *In situ* deletion of SHIP does not alter CXCR4 surface expression on KLSCD48 HSC.
(A) A representative histogram of CXCR4 surface expression on KLSCD48 HSC cells derived from MxCreSHIP$^{flox/flox}$(CD45.2) or WT-Ly5.1(CD45.1) donors in the BM of MxCreSHIP$^{flox/flox}$(CD45.2):WT-Ly5.1(CD45.1) chimeras 5 months after polyI:C treatment. (B) Median Fluorescence Intensity (MFI) of CXCR4 staining on KLSCD48 HSC cells derived from MxCreSHIP$^{flox/flox}$(CD45.2) or WT-Ly5.1(CD45.1) donors in the BM of MxCreSHIP$^{flox/flox}$(CD45.2):WT-Ly5.1(CD45.1) chimeras 5 months after polyI:C treatment. [Black boxes, cells derived from MxCreSHIP$^{flox/flox}$ BM (Cre+); Grey boxes, cells derived from WT-Ly5.1 BM (WT)]

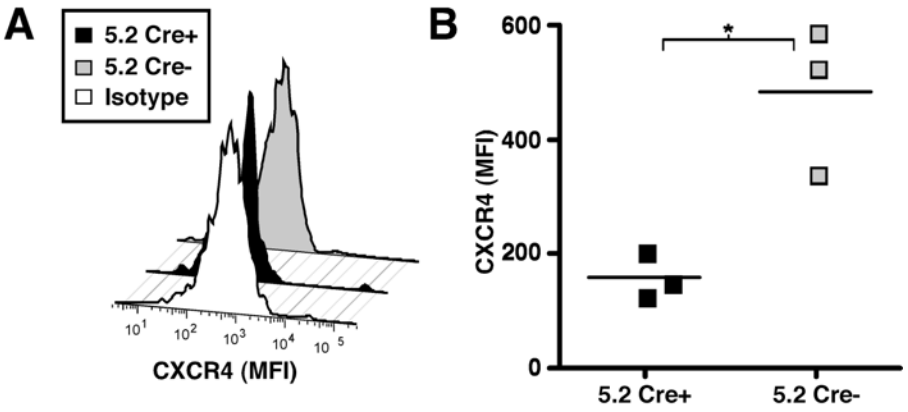

Figure 16: Systemic deletion of SHIP significantly impairs CXCR4 surface expression on KLSCD48 HSC.
(A) Representative histograms of CXCR4 surface expression on KLSCD48 HSC in the BM of MxCreSHIP$^{flox/flox}$(CD45.2) mice or SHIP$^{flox/flox}$(CD45.2) controls 21 days after polyI:C treatment. (B) MFI of CXCR4 staining on KLSCD48 HSC in the BM of MxCreSHIP$^{flox/flox}$(CD45.2) or SHIP$^{flox/flox}$(CD45.2) controls 21 days after polyI:C treatment. Significance was established using the unpaired Student's T test (*$p<0.05$). [Black boxes, cells derived from MxCreSHIP$^{flox/flox}$ BM (Cre+); Grey boxes, cells derived from SHIP$^{flox/flox}$ (Cre-)]

Production of Soluble Factors that Influence HSC Behavior are Altered in SHIP-deficient Mice

Although the BM niche can influence the behavior of HSC by elaborating cell bound ligands for HSC receptors, it also mediates effects through the production of soluble factors that influence HSC proliferation, survival, mobilization, and BM homing. Consistent with our proposed disruption of niche function by SHIP-deficiency, $SHIP^{-/-}$ mice exhibit significantly increased plasma levels of several growth and survival factors for HSC (TPO, G-CSF, IL-6) (Table 2). The increase in these factors and others may contribute to the increased number of HSC present in both the medullary and extramedullary compartments of $SHIP^{-/-}$ mice. We also observe increased concentrations of soluble factors that promote HSC mobilization, including G-CSF, IL-5 (Table 2), MMP-9 (Figure 17A) and soluble VCAM-1 (Figure 17B).

In addition, homing and retention of HSC by the SHIP-deficient BM niche may be compromised by reduced production of SDF-1/CXCL12. We find significantly reduced SDF-1/CXCL12 in both the blood and BM plasma of SHIP-deficient mice (Figure 18A-B). SDF-1/CXCL12 is produced by both the osteoblastic and vascular niche in BM[101,117]. In fact, decreased SDF-1 production in the SHIP-deficient BM niche could be triggered by increased G-CSF production, as G-CSF is known to reduce SDF-1 expression in BM niche cells[151]. Taken together, these findings provide evidence for several significant perturbations in the SHIP-deficient BM niche.

Table 2: Disrupted cytokine distribution in peripheral blood of SHIP-deficient mice.
Various factors were measured in serum obtained from PB by ELISA. The data is pooled from multiple assays derived from at least 4 different plasma samples for each genotype. Significance was established using the unpaired Student's T test.

Cytokine	SHIP -/-	(SEM,N)	WT	(SEM,N)	P value
TPO (ng/ml)	13.36	(± 0.3636, N=11)	11.79	(± 0.2143, N=14)	0.0007
G-CSF (pg/ml)	749.1	(± 39.13, N=4)	161.9	(± 24.62, N=4)	<0.0001
IL-6 (pg/ml)	39.82	(± 6.201, N=11)	13.67	(± 0.5205, N=13)	0.0001
IL-5 (ng/ml)	0.2147	(± 0.02350, N=11)	0.1511	(± 0.01634, N=14)	0.0314

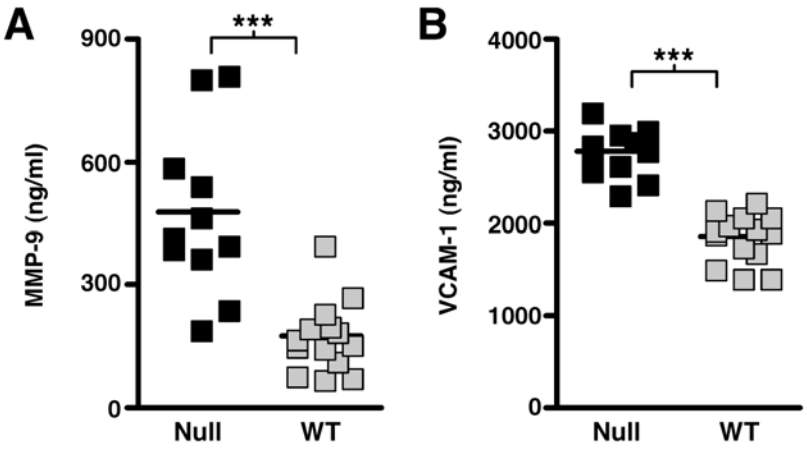

Figure 17: SHIP-deficiency alters production of HSC mobilization factors. (A) Scatter plots indicating the mean and range for the concentration of MMP-9 in the blood plasma of SHIP$^{-/-}$ and WT littermates. (B) Scatter plots indicating the mean and range for the concentration of VCAM-1 in the blood plasma of SHIP$^{-/-}$ and WT littermates. The data is pooled from multiple assays derived from a minimum of 7 different samples for each genotype. Significance was established using the unpaired Student's T test (***p<0.0001). [Black boxes, SHIP$^{-/-}$ samples; Grey boxes, WT samples].

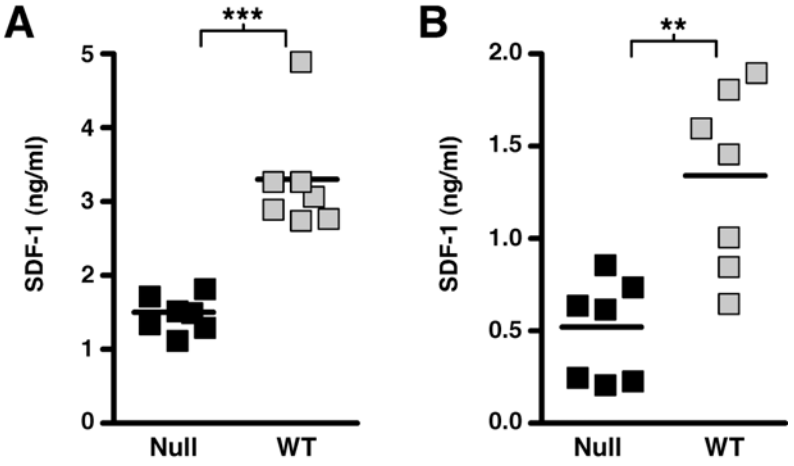

Figure 18: SHIP-deficiency alters production of HSC homing factors. (A) Scatter plots indicating the mean and range for the concentration of SDF-1/CXCL12 in the blood plasma of SHIP$^{-/-}$ and WT littermates. (B) Scatter plots indicating the mean and range for the concentration of SDF-1/CXCL12 in the BM plasma of SHIP$^{-/-}$ and WT littermates. The data is pooled from multiple assays derived from a minimum of 7 different samples for each genotype. Significance was established using the unpaired Student's T test (**p<0.005; ***p<0.0001). [Black boxes, SHIP$^{-/-}$ samples; Grey boxes, WT samples].

A Role for SHIP in BM Microenvironment Signaling and Function

Our transplantation studies, described above, indicated SHIP deficiency disrupts the BM niche that supports normal HSC function and BM homing. SHIP is expressed primarily in hematopoietic tissues in both humans and mice; however, direct analysis of SHIP expression in cells that constitute BM niche cell types was not directly tested[1,3,5,141,152]. We sought more direct evidence of a role for SHIP in the BM microenvironment by assessing whether it is expressed in cells that constitute key non-hematopoietic cell types in the BM niche. Thus, we prepared osteoblast (OB) and stromal cell cultures from SHIP$^{-/-}$ and WT BM. There were no substantive differences in morphology of stromal cells between the two genotypes. However, in OB cultures we consistently observe readily apparent differences with SHIP$^{-/-}$ OB exhibiting elongated and non-randomly oriented protrusions (Figure 19: day 11) and organized growth along axes (Figure 19: days 13 and 23).

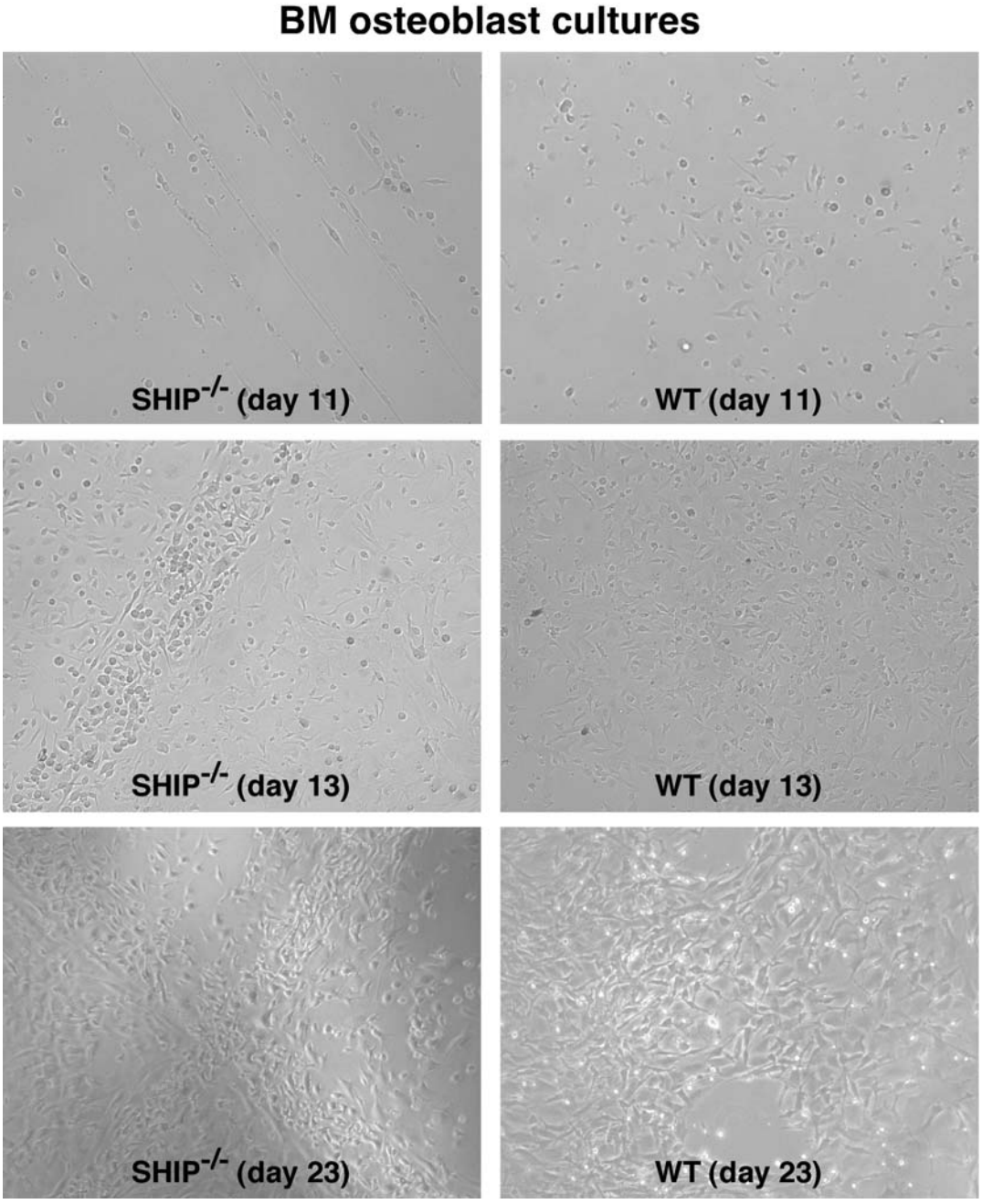

Figure 19: SHIP$^{-/-}$ OB cultures exhibit elongated and non-randomly oriented protrusions and organized growth along axes.
Representative OB cells propagated from SHIP$^{-/-}$ and WT femurs after 11, 13, and 23 days in culture. All images were generated using a Nikon TE2000 inverted microscope with a 10x 0.25NA PlanFluor objective lens and a Retiga 1300 12bit CCD QImaging camera. The images were acquired using IP Lab v3.6 software (Scanalytics of BD Biosciences).

We readily detect SHIP protein expression in WT stromal (Figure 20A) and OB cultures (Figure 20B). In addition, we detect tyrosine phosphorylation of SHIP in WT BM stromal cells indicating SHIP participates in signaling pathways active in cells of the BM niche (Figure 20C). Consistent with our detection of SHIP expression in BM niche cell cultures, we confirmed that SHIP protein expression is also readily detected in stromal cultures derived from the BM of $SHIP^{flox/flox}$ mice but not $MxCreSHIP^{flox/flox}$ mice treated with polyI:C (Figure 20D). These results indicate SHIP is expressed and participates in signaling in BM niche cells and thus is capable of influencing their function.

A lack of hematopoietic lineage markers combined with positive selection of vascular cell adhesion molecule-1 (VCAM1) is used to delineate mesenchymal stem/progenitor cells and endothelial cells in the BM microenvironment[153-155]. We find significantly more $VCAM1^{+}Lin^{-}$ cells in the BM of mice with germline or induced SHIP deficiency, relative to their SHIP competent counterparts (Figure 21A-B). Thus, SHIP expression is required for the homeostasis of stromal cells in the BM compartment during adult physiology.

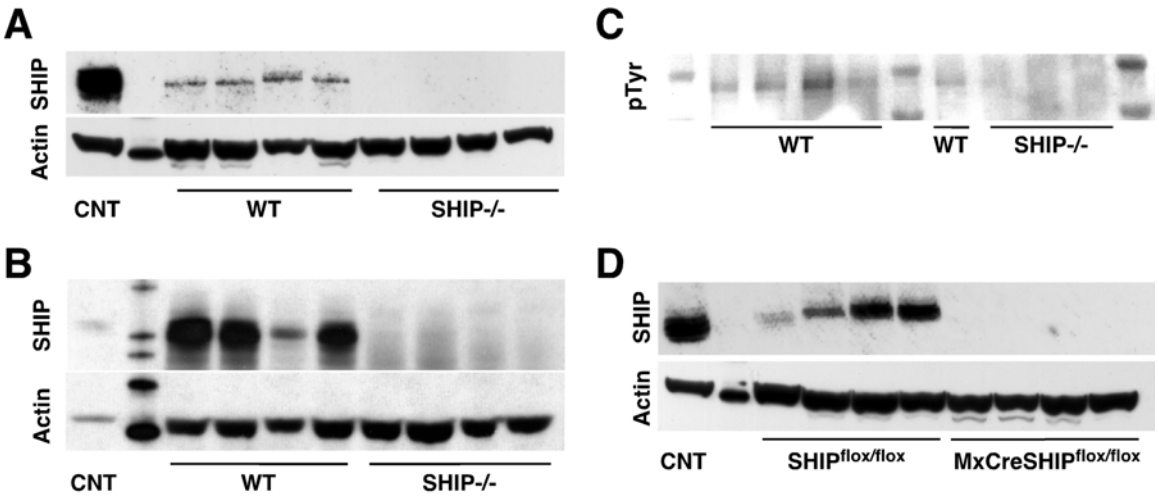

Figure 20: SHIP is expressed and phosphorylated in BM niche cells.
(A) Representative SHIP Western blot from stromal cells cultured from the BM of SHIP$^{-/-}$ and WT littermates. (B) SHIP Western blot from osteoblast cells cultured from the BM of SHIP$^{-/-}$ and WT littermates. (C) pTyr Western blot on a SHIP immunoprecipitation of stromal cells cultured from the BM of SHIP$^{-/-}$ and WT littermates. (D) SHIP Western blot from stromal cells cultured from the BM of MxCreSHIP$^{flox/flox}$ and SHIP$^{flox/flox}$ littermates. Each lane on the Western blots represents a culture lysate derived from an independent mouse.

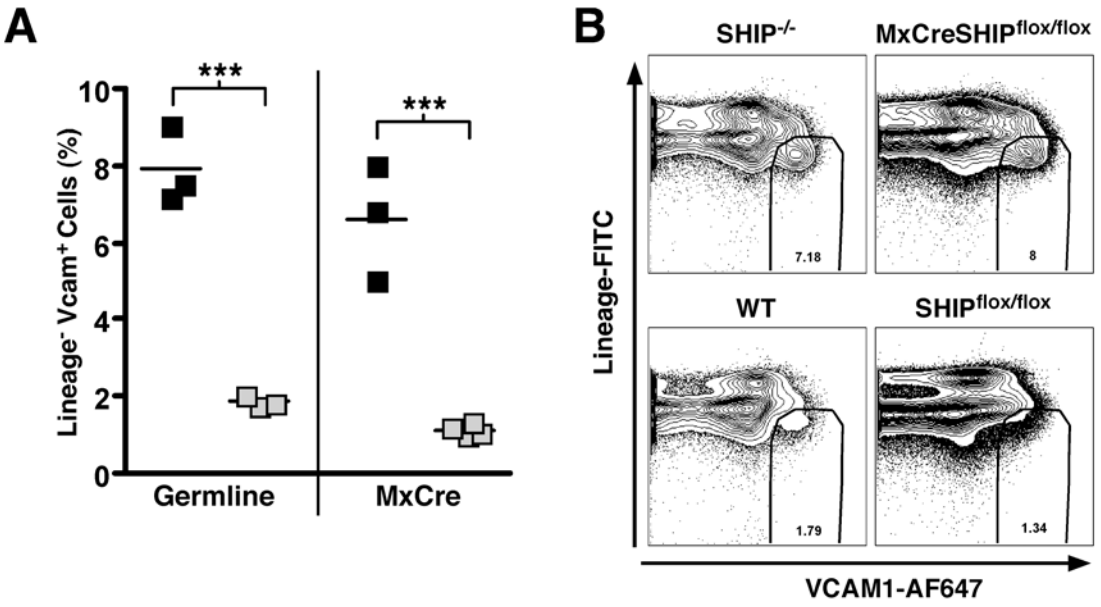

Figure 21: SHIP defficency alters cell numbers in the BM niche.
(A) Scatter plots indicating the mean and range of $VCAM1^{+}Lin^{-}$ cells present in the BM of $SHIP^{-/-}$ and WT (Germline) or $MxCreSHIP^{flox/flox}$ and $SHIP^{flox/flox}$ (MxCre) littermates as indicated. (B) Dual color contour plots illustrating the $VCAM^{+}Lin^{-}$ cells present in the BM of $SHIP^{-/-}$ and WT (LEFT) or polyI:C treated $MxCreSHIP^{flox/flox}$ and $SHIP^{flox/flox}$ littermates (RIGHT). Significance was established using the unpaired Student's T test (*$p<0.05$; **$p<0.005$; ***$p<0.0001$). [Black boxes, $SHIP^{-/-}$ samples (A, LEFT) or $MxCreSHIP^{flox/flox}$ samples (A, RIGHT); Grey boxes, WT samples (A, LEFT) or $SHIP^{flox/flox}$ samples (A, RIGHT)].

To further assess a functional role for SHIP in the BM microenvironment, we assayed SHIP$^{-/-}$ and WT OB for alkaline phosphatase (ALP) activity. SHIP-deficient OB exhibit significantly less ALP activity compared to WT OB (Figure 22A-B), indicating they are immature as ALP activity is closely correlated with maturation in the OB lineage[156-159]. As a further test of SHIP-deficient BM niche function, we examined the cell cycle kinetics of WT hematopoietic stem/progenitor cells (HS/PC) placed on BM stromal layers prepared from either SHIP$^{-/-}$ or WT mice. When we place 1 million HS/PC in co-culture with confluent SHIP$^{-/-}$ stromal layers and measure proliferation by loss of CFSE, we find a clear defect in the ability of SHIP$^{-/-}$ BM stroma to support normal proliferation of WT HS/PC (Figure 23C-D). These results demonstrate a significant and qualitative change in BM stromal cells that lack SHIP expression such that they are unable to support normal proliferation by SHIP-competent HS/PC.

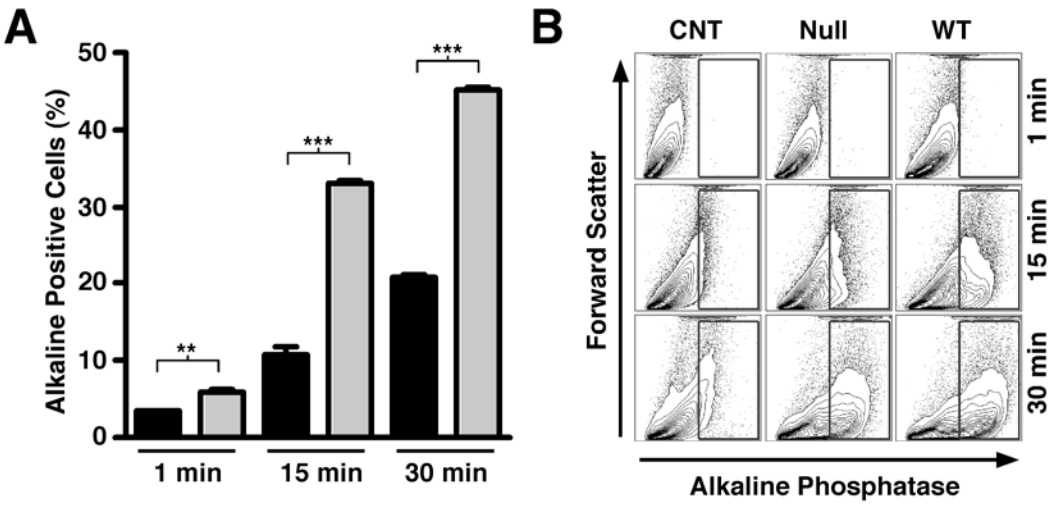

Figure 22: SHIP-deficiency alters the function of osteoblasts from the BM niche.
(A) Alkaline phosphatase positive cells from cultures of SHIP$^{-/-}$ and WT osteoblasts showing altered phosphatase kinetics at 1 minute, 15 minutes, and 30 minutes. (B) Representative FACS plots illustrating gating strategy for ALP positive cells based on ALP negative BM controls and showing ALP kinetics at increasing time points. Significance was established using the unpaired Student's T test (**p<0.005; ***p<0.0001). [Black, SHIP$^{-/-}$ osteoblasts(A); Grey, WT osteoblasts(A)].

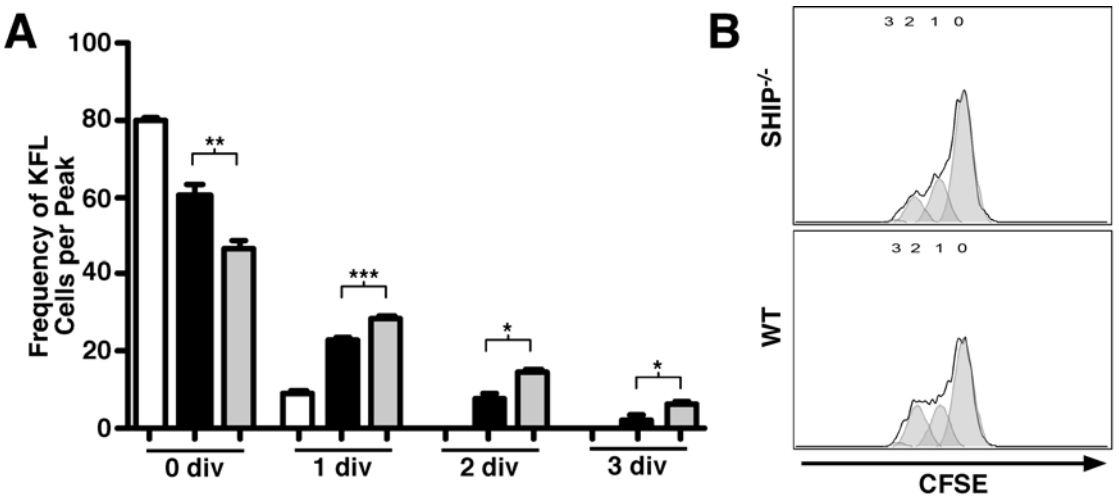

Figure 23: SHIP-deficiency alters the ability of stromal cells from the BM niche to support normal HSC function.
(A) Frequency of $Lin^{-}cKit^{+}Flk2^{-}$ (KFL) stem/progenitor cells among Lin-depleted BM cells (HPC) cultured alone (White), or with $SHIP^{-/-}$ (Black) or WT (Grey) stromal cells in each cell division after 36hrs. (B) Representative histograms showing decreased proliferation of $CFSE^{+}$ KFL cells cultured with $SHIP^{-/-}$ stromal cells (TOP) as compared to those cultured with WT stromal cells (BOTTOM). Significance was established using the unpaired Student's T test (*p<0.05; **p<0.005; ***p<0.0001). [White, WT HPC alone(A); Black, HPC cultured with $SHIP^{-/-}$ stroma(A); Grey, HPC cultured with WT stroma(A)].

Additionally, we analyzed the supernatants of multiple independent SHIP-deficient and WT stromal cultures for SDF-1 production and found profoundly compromised SDF-1 production in all SHIP-deficient cultures analyzed as compared to WT cultures analyzed in parallel (Figure 24A). Consistent with this, we saw a similar defect in SDF-1 production by stromal cells derived from MxCreSHIP$^{flox/flox}$ mice as compared to SHIP$^{flox/flox}$ controls (Figure 24B). Thus, SDF-1 production by BM niche cells is significantly impaired by SHIP-deficiency. As SDF-1 is pivotal for BM homing and retention of HSC, the impaired production of SDF-1 by SHIP$^{-/-}$ stroma is consistent with increased peripheralization of HSC to the blood and spleen of SHIP$^{-/-}$ mice[136]. Accordingly, immunohistology on femur sections from SHIP$^{-/-}$ mice show little to no SDF-1 present in the BM (Figure 25ii). In fact, levels appear to be similar to those in isotype control sections (Figure 25iii) indicating an almost complete lack of SDF-1 in SHIP-deficient BM. When taken together these results demonstrate that SHIP is required for multiple functions of BM niche cells, including production of factors that mediate BM recruitment, HSC retention and HSC proliferation.

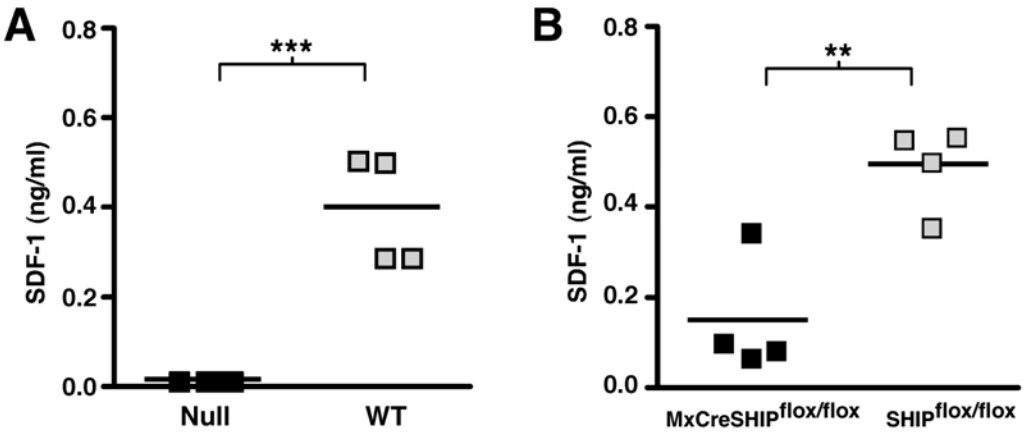

Figure 24: SHIP-deficiency alters cytokine production by cells from BM niche.
(A) Scatter plots indicating the mean and range for the concentration of SDF-1/CXCL12 in the cell culture supernatant of SHIP$^{-/-}$ and WT BM stromal cells. (B) Scatter plots indicating the mean and range for the concentration of SDF-1/CXCL12 in the cell culture supernatant of MxCreSHIP$^{flox/flox}$ and SHIP$^{flox/flox}$ BM stromal cells from polyI:C treated mice. Results are representative of independent stromal cultures derived from independent mice. Significance was established using the unpaired Student's T test (**p<0.005; ***p<0.0001). [Black, SHIP$^{-/-}$ samples(A); Grey, WT samples(A); Black, MxCreSHIP$^{flox/flox}$ samples(B); Grey, SHIP$^{flox/flox}$ samples(B)].

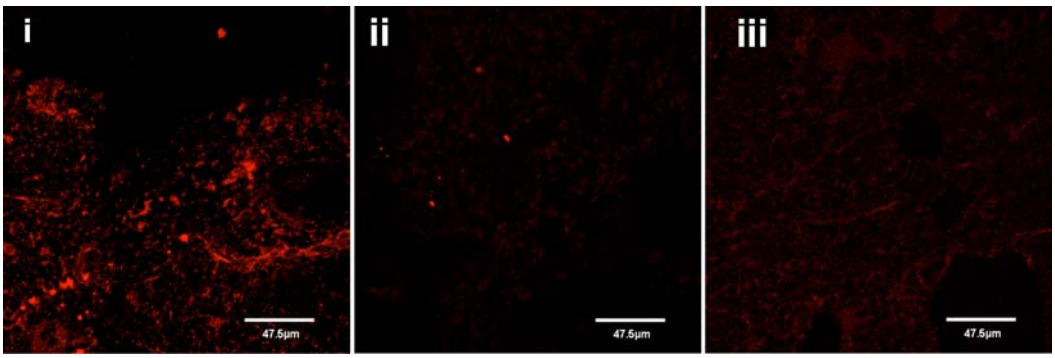

Figure 25: SHIP-deficiency ablates *in vivo* SDF-1 production in the BM niche.
Representative photomicrographs (63X) of frozen sections prepared from adult femurs of WT (i) and SHIP$^{-/-}$ mice (ii) that were stained with biotinylated mouse anti-SDF-1 Ab (i, ii) or a biotinylated mouse IgG1k control antibody (iii). Staining by the anti-SDF-1 or the IgG1k control was revealed by a secondary stain of SA-AlexaFluor 546. The background SDF-1 staining observed with SHIP$^{-/-}$ BM sections was consistently comparable to staining observed in isotype control stains performed on both SHIP$^{-/-}$ and WT femurs (iii and data not shown).

Discussion

In this study we show that induction of SHIP deficiency in the adult compromises HSC function only when SHIP-deficiency is systemic, indicating a requirement for SHIP expression by the HSC niche. In fact, when adult HSC residing in a SHIP-competent niche are rendered SHIP-deficient, they completely retain their capacity for multi-lineage repopulation and self-renewal. Thus, SHIP expression is not an intrinsic requirement for control of HSC homeostasis or function in the BM, but is required for normal function by the BM niche. Consistent with this, we find that SHIP is expressed and tyrosine phosporylated in niche cells and plays an intrinsic role in their production of chemokines, homeostasis and function. Furthermore, we find that following induction of systemic SHIP-deficiency in the adult, the SHIP-deficient BM microenvironment promotes expansion of cells of the KLSCD48 HSC phenotype. Despite this phenotypic expansion, BM HSC from these donors are fundamentally altered such that they are no longer able to mediate efficient multi-lineage repopulation following intravenous transplantation.

We find that three polyI:C injections results in highly efficient SHIP deletion in MxCreSHIP$^{flox/flox}$ cells. In the event that a small percentage of cells in the *in situ* deletion chimeras remained SHIP-competent and repopulated as well as their WT counterparts in the serial transplants shown in Figure 10, then it also logically follows that we should observe comparable repopulation with BM from systemically deleted MxCreSHIP$^{flox/flox}$ mice (Figure 13). On the contrary, we observe significantly compromised repopulation by this SHIP-deficient graft

despite the potential presence of residual SHIP-competent cells. These data combined with robust SHIP deletion in splenocytes (Figure 7) in the *in situ* deletion model strongly suggest that normal repopulation by *in situ* SHIP deleted HSC is not due to residual, undeleted HSC clones.

Our findings demonstrate the HSC BM niche is profoundly altered by SHIP-deficiency. SHIP expression has previously been documented in primary fibroblasts and endothelial cells, indicating the potential for SHIP to regulate the activity of these cell types[139,142]. Here we document that SHIP is expressed in OB and stromal cells derived from the BM niche. SHIP has previously been implicated in the regulation of osteoclast function and their resorption of osteoblasts[83]. However, SHIP expression in primary osteoclasts has not been demonstrated, suggesting the possibility that accelerated bone resorption exhibited by $SHIP^{-/-}$ osteoclasts could be caused by some of the cytokine alterations that we observe in $SHIP^{-/-}$ mice.

The immature state of $SHIP^{-/-}$ OB is consistent with the deregulated cell cycle kinetics and repopulation defect we previously reported for $SHIP^{-/-}$ HSC as mature OB are required to maintain HSC in a quiescent state[160-163] in which their reconstituting potential is maximal[109,162-164]. Consistent with this functional OB impairment, we see a significant expansion of the $VCAM1^{+}Lin^{-}$ niche in $SHIP^{-/-}$ mice, yet a functional defect in their ability to support normal HSC cycling, indicating an inability to support normal HSC function in a SHIP-deficient niche.

A previous report found that VEGF-A can induce SHIP expression in endothelial cells[142], and thus SHIP expression, or function, could be induced in

niche cells to limit effector functions of BM niche cells. This could include SHIP regulating the production of key factors produced by the niche, including G-CSF, TPO, IL-5 and SDF-1. Consistent with this, we observe increased levels of G-CSF, TPO, IL-6 and MMP-9, and decreased SDF-1/CXCL12 in the plasma of SHIP-deficient mice. Furthermore, we show direct evidence of compromised SDF-1 production by SHIP-deficient BM niche cells. This likely contributes to the profound mobilization and peripheralization of phenotypic HSC that we previously observed in SHIP-deficient mice. It has not escaped our attention that increased G-CSF production by SHIP-deficient microenvironment cells could in turn down-regulate SDF-1 production by other microenvironment cells. This would cause HSC mobilization while simultaneously reducing HSC recruitment to niche cells such as OB that maintain HSC quiescence.

The cellular and molecular pathways in the BM microenvironment altered by SHIP-deficiency remain to be defined. Nonetheless, these findings are the first to implicate inositol phospholipid-signaling pathways as being critical to the function of the BM microenvironment that supports HSC function. It remains to be determined whether other members of phosphoinositide signaling pathways also impact niche function or whether they have an impact solely through intrinsic effects in HSC. The analysis of PTEN-deficient mice suggests PTEN plays an intrinsic role in the control of HSC homeostasis and function[165,166]. Thus, PTEN is likely the *dominant* inositol phosphatase that opposes effector pathways distal to PI3K in HSC, while SHIP appears to be a dominant inositol phosphatase in cells of the BM niche that support HSC. It will be intriguing to determine whether this

segregation of PTEN and SHIP function between “seed” and “soil” is also conserved in other stem cell populations and their supporting milieu. Functional segregation of these signaling components suggests that selective targeting of these two phosphoinositide signaling enzymes might be of value in clinical settings where specific modulation of HSC or niche function is warranted.

Methods

Mice

Production of $SHIP^{-/-}$ and $MxCreSHIP^{flox/flox}$ mice has been previously described[11,86]. Briefly, $SHIP^{-/-}$ mice were generated by deletion of the promoter and first exon of SHIP via a Cre-LoxP strategy and backcrossed to a C57BL6/J background. $MxCreSHIP^{flox/flox}$ mice were generated using $SHIP^{flox/flox}$ and MxCre mice (Jackson Laboratory, Bar Harbor, ME). $MxCreSHIP^{flox/flox}$:WT-Ly5.1 and $SHIP^{flox/flox}$:WT-Ly5.1 BM chimeras were created by co-transplanting $5X10^5$ WBM cells from $MxCreSHIP^{flox/flox}(CD45.2^+)$ or $SHIP^{flox/flox}(CD45.2^+)$ plus $5X10^5$ cells from WT-Ly5.1($CD45.1^+$) mice into lethally irradiated $CD45.1^+45.2^+$ recipients. All animal experiments were conducted with approval of the Univ. of South Florida IACUC.

Cell Isolation

Bone marrow (BM) cells were flushed from femurs and tibias, red blood cell (RBC) lysed, centrifuged and resuspended in staining media (SM) composed of Dulbecco phosphate-buffered saline (D-PBS), 3%FBS, and 10mM HEPES. For

transplantation, WBM was simply flushed, washed and resuspended in sterile PBS. Spleens were manually crushed then treated like BM cells. Peripheral blood (PB) was collected in microtainers with K_2EDTA (BD, Franklin Lakes, NJ). RBC lysis was performed twice to obtain PB mononuclear cells (PBMC).

Conditional Deletion of SHIP

MxCreSHIP$^{flox/flox}$(CD45.2^{+}) mice and MxCreSHIP$^{flox/flox}$:WT-Ly5.1 BM chimeras were conditionally ablated for SHIP expression through intra-peritoneal injection of polyinosinic-polycytidylic acid (polyI:C) (Sigma-Aldrich, St. Louis, MO). Mice were injected three times with 625μg of polyI:C on days 1, 4, and 7.

Flow Cytometry

All antibodies were from BD Biosciences (San Jose, CA), eBioscience (San Diego, CA) or CalTag/Invitrogen (Carlsbad, CA). PBMC, splenocytes or BM cells were treated with CD16/CD32 mouse Fc block(2.4G2) on ice for 20 minutes then stained with a panel of antibodies. Global reconstitution was assessed by staining with: CD45.1-PE(A20) and CD45.2-FITC(104) or CD45.1-PE(A20) and CD45.2-PercpCy5.5(104). Multi-lineage reconstitution was assessed by staining with: CD45.1-PE(A20), CD45.2-PercpCy5.5(104), B220-AlexaFluor700(RA3-6B2), CD3-PECy7(145-2C11), Mac1-APCCy7(M1/70) and NK1.1-APC(PK136). Myeloid, erythroid and megakaryocytic reconstitution was assessed by staining with: CD45.1-PE(A20), CD45.2-PercpCy5.5(104), Mac1-APCCy7(M1/70), Gr1-FITC(RB6-8C5), or CD41-FITC(MWReg30) and Ter119-APC(TER-119).

Phenotypic HSC were assessed by staining with: CD45.1-Purified(A20) conjugated to Pac Orange using Zenon technology, CD45.2-PerCPCy5.5(104), Sca1-PECy7(D7), c-Kit-APC-AF750(2B8), CD48-APC(HM48-1), CXCR4-PE(2B11/CXCR4), and a lineage (Lin) panel on FITC; CD2(RM2-5), CD3ε(145-2C11), CD4(GK1.5), CD5(53-7.3), CD8α(53-6.7), B220(RA3-6B2), Gr-1(RB6-8C5), Mac-1(M1/70), NK1.1(PK136) and Ter119(TER-119) or Sca1-FITC(E13-161.7), c-Kit-PECy7(2B8), CD48-APC(HM48-1), CXCR4-biotin(2B11/CXCR4), and a Lin panel on PE; CD2(RM2-5), CD3ε(145-2C11), CD4(GK1.5), CD5(53-7.3), CD8α(53-6.7), B220(RA3-6B2), Gr-1(RB6-8C5), Mac-1(M1/70), NK1.1(PK136), and Ter119(TER-119) followed by a secondary stain of Steptavidin-AF700. Microenvironment cells were assessed in BM by: CD2-FITC(RM2-5), CD3e-FITC(145-2C11), CD4-FITC(GK1.5), CD5-FITC(53-7.3), CD8a-FITC(53-6.7), CD41-FITC(MWReg30), B220-FITC(RA3-6B2), Ter119-FITC(TER-119), NK1.1-FITC(PK136), Mac1-FITC(M1/70), GR1-FITC(RB6-8C5), and VCAM1-AF647(429). After 20 minutes of staining on ice the cells were washed and resuspended in SM containing 75ng/ml of 4',6-diamidino-2-phenylindole dihydrochloride (DAPI) (Sigma, Saint Louis, MO) for dead cell exclusion. All flow cytometry acquisition was done on a FACS LSRII (BD Biosciences), a FACS ARIA (BD), or a FACS Vantage (BD). Data was analyzed using FlowJo® software (Tree Star, Inc. Ashland, OR).

In Situ SHIP Deletion BM Transplants

$5x10^5$ MxCreSHIP$^{flox/flox}$(CD45.2$^+$) or SHIP$^{flox/flox}$(CD45.2$^+$) WBM cells were co-transplanted (i.v.) with $5x10^5$ WBM competitor cells from WT-Ly5.1(CD45.1$^+$) mice into lethally irradiated CD45.1$^+$45.2$^+$ recipients. Recipients received a split dose of 11-Gy at least 2-hours before transplantation. After 60 days recipient mice were treated with the polyI:C series.

Secondary BM Transplants from *In Situ* SHIP Deleted Mice

Five months after polyI:C treatment of MxCreSHIP$^{flox/flox}$:WT-Ly5.1 and SHIP$^{flox/flox}$:WT-Ly5.1 BM chimeras, mice were sacrificed and $1x10^6$ WBM cells were transplanted (i.v.) into lethally irradiated CD45.1$^+$45.2$^+$ recipients.

Systemic SHIP Deletion BM Transplants

MxCreSHIP$^{flox/flox}$(CD45.2$^+$) mice and SHIP$^{flox/flox}$(CD45.2$^+$) mice were pre-treated with the polyI:C series. SHIP deletion was confirmed by Western blot of PBMC. $5x10^5$ WBM cells from MxCreSHIP$^{flox/flox}$(CD45.2$^+$) or SHIP$^{flox/flox}$(CD45.2$^+$) mice were co-transplanted (i.v.) with $5x10^5$ WBM competitors from WT-Ly5.1(CD45.1$^+$) mice into lethally irradiated CD45.1$^+$45.2$^+$ recipients.

Western Blot Detection of SHIP and β-actin Expression

Cell lysates were prepared from cultured or sorted cells using modified RIPA lysis buffer (Upstate Cell Signaling, Millipore, Billerica, MA). Lysate supernatants were resolved on a 4-12% Bis-Tris gel, and transferred to a Hybond-ECL

nitrocellulose membrane (Amersham Biosciences, Piscataway, NJ). For Odyssey technology, the membrane was blocked with Odyssey blocking buffer (LICOR Biosciences, Lincoln, NE) and probed with 1-5μg/ml P1C1 (Santa Cruz Biotechnology, Santa Cruz, CA) then anti-mouse IR-700 at 1:8,000 (Molecular Probes, Carlsbad, CA). Probed blots were scanned using an Odyssey infrared imager. For chemi-luminescence, the membrane was blocked with 5% non-fat milk in PBS with 0.1% Tween-20 (PBS-T) and probed with 1μg/ml P1C1 or 1μg/ml Actin:C-11 (Santa Cruz Biotechnology) followed by anti-mouse IgG-HRP or anti-goat IgG-HRP at 1:1,000 (eBioscience). Protein was detected using SuperSignal West Femto Substrate (Thermo Scientific, Rockford, IL).

Calculation of Repopulation Units

Repopulating units (RU) were calculated as per Harrison et al.[167]: (C*CD45.2 repopulation(%))/(100-CD45.2 repopulation(%)), where 1C= 10^5 competitor cells. Since we used $5x10^5$ competitor cells, we used this equation:

RU = (5 * CD45.2 repopulation(%))/(100 – CD45.2 repopulation(%)).

ELISA Detection of Cytokines

Serum was isolated from PB and stored at -20ºC or sent for analysis by a service from Charles Rivers Laboratories Inc., where ELISA for multiple cytokines was performed. BM plasma was assayed for cytokines by flushing cleaned femurs with 500μl PBS. The PBS was then centrifuged at 1800 rpm for 5 minutes at 4ºC. The supernatant was removed to a new tube and stored at -20ºC. Cell culture

supernatants were harvested at regular intervals and stored at -20ºC. Stored supernatants were then assayed for stromal cell derived factor-1 (SDF-1) using the Quantikine® Immunoassay (R&D Systems, Minneapolis, MN).

Isolation and Culture of Stromal Cells

Bone marrow was flushed from intact femurs and tibias into tissue culture flasks containing alpha-modified MEM with nucleotides (α-MEM)[168]. The α-MEM was supplemented with 15% FBS, 50 units penicillin-G/mL, 50μg streptomycin/mL, 0.3μg amphotericin-B/mL, and 50μg ascorbate/mL. After culturing cells for three days undisturbed, media was changed and non-adherent cells removed.

Isolation and Culture of Osteoblasts

Cleaned and flushed femurs and tibias were scraped using a scalpel to remove remaining soft tissue[169]. The bones were cut into 1-2mm^2 pieces and incubated with shaking in a solution of 2 mg collagenase-II/mL in modified DMEM at 37°C for 2 hours. Complete culture medium (cCM) was added to stop the collagenase action. The cCM consisted of DMEM (pH 7.4) supplemented with 2.2g $NaHCO_3$/L, 10% FBS, 50 units penicillin-G/mL, 50μg streptomycin/mL, 50 μg gentamycin/mL, 1.25μg amphotericin-B/mL, and 100μg ascorbate/mL. The bone pieces were washed three times with cCM and cultured in 25cm^2 tissue culture flasks.

SHIP Immunoprecipitation and Western Blot for Phosphotyrosine

Stromal cell cultures were lysed in modified RIPA buffer. SHIP was immunoprecipitated overnight with 0.2μg P1C1 and protein A/G-agarose beads from precleared lysate supernatants. The immunoprecipitated protein was blotted and the membrane blocked using the protocol above. It was then probed using an anti-phosphotyrosine, HRP-conjugated monoclonal antibody (4G10, Santa Cruz Biotechnology) diluted 1:1000 with 3% milk in PBS-T. Phosphorylated tyrosine was detected using SuperSignal West Femto Substrate diluted 1:5 with Pierce ECL Western Blotting Substrate (Thermo Scientific).

ELF97 Alkaline Phosphatase Assay

Alkaline phosphatase (ALP) activity was measured using an ELF97 assay (Invitrogen) modified for flow cytometry[160]. Osteoblasts were fixed overnight in 70% EtOH at 4°C. Cells were then washed and transferred into FACS tubes. After pre-incubation with developing buffer, phosphate substrate was added to the cells. The cells were incubated at room temperature for 1-30 minutes before adding a phosphatase inhibitor, levamisole (10mM), to stop the reaction.

Co-culture Proliferation Assay

Hematopoietic progenitor cells[160] (HPC) were isolated from WT mice by lineage depletion of BM using an antibody cocktail on PE: CD3ε(145-2C11), CD4(GK1.5), CD5(53-7.3), B220(RA3-6B2), Gr-1(RB6-8C5), Mac-1(M1/70), and Ter119(TER-119) followed by a magnetic enrichment using anti-PE microbeads

(Mitenyi Biotec, Auburn, CA). HPC were loaded with 5μM carboxyfluorescein succinimidyl ester (CFSE). WT $CFSE^{+}$ HPC were co-cultured with confluent $SHIP^{-/-}$ or WT stromal cells for 36hrs. Proliferation was assayed based on loss of CFSE in $Lin^{-}cKit^{+}Flk2^{-}$ cells by staining with: a Lineage-PE panel (CD3, CD4, CD5, B220, Ter119, Mac1, Gr1), cKit-APC (Miltenyi Biotec), Flk2-PE(A2F10.1) and DAPI.

Histology

Femurs were embedded in O.C.T. compound (Tissue-Tek, Torrance, CA), snap-frozen in liquid nitrogen and stored at -80°C. Cryostat sections (10μm) were fixed, pre-incubated in blocking buffer (PBS, 3% BSA, anti-CD32/CD16(2.4G2)), and stained with antibodies. Sections were embedded in Fluorescent Mounting Medium (Dako Cytomation, Denmark) and analyzed by confocal microscopy (Leica TCS-SL, Leica, Bannockburn, IL) using a 63x objective. Image processing was performed with the Leica Confocal Software. Cryostat sectioning, staining and microscopy were jointly performed by Oliver Winter and Katrin Moser from the German Rheumatism Research Center in Berlin Germany.

Statistical Analysis

All statistical analyses were performed using Prism® (GraphPad, San Diego, CA).

Functional HSC in the Periphery of SHIP-Deficient Mice

Abstract

Previously we showed that SHIP-deficiency compromises the function of HSC and their supporting cells in the BM. This leads to splenomegaly and increased numbers of splenocytes possessing an HSC phenotype suggesting the spleen of SHIP$^{-/-}$ mice could be a source of definitive hematopoiesis. Consistent with this hypothesis, we show that SHIP$^{-/-}$ splenocytes possess all major functions of *bona fide* HSC, including radioprotection, long-term multi-lineage repopulation and self-renewal. Moreover, we find that purified splenic SHIP$^{-/-}$ HSC have equivalent stem cell capacity to that of SHIP-competent BM HSC. Analysis of Akt activation and inhibition of PI3K signaling *in vivo* indicates dysregulated PI3K/Akt signaling enables SHIP$^{-/-}$ HSC to function normally outside the confines of their niche in BM. These findings suggest that targeting of SHIP could be used to safely evacuate a functional HSC compartment to the spleen in the event of damage to the BM niche.

Introduction

Phosphoinositide 3-kinase (PI3K) signaling plays a crucial role in the fate of a cell[170]. When this signaling pathway is disrupted by loss of an inositol

phoshatase, key steps such as the hydrolysis of PI(3,4,5)P3 are lost and control of downstream signaling becomes aberrant[43,170,171]. The SH2-domain containing inositol phosphatase (SHIP) is an enzyme that removes the 5' phosphate from PI(3,4,5)P3 and generates PI(3,4)P2[1-3,5,60]. This activity regulates PI(3,4,5)P3 levels in the cell and thus contributes to the controls of survival signaling by limiting the downstream activation of PKB/Akt. Consistent with this we have previously shown that SHIP promotes turnover of peripheral NK cells *in vivo* by limiting Akt activation and expression[11].

SHIP is primarily expressed in the hematopoietic system[1,3,5], although its expression has also been documented in osteoblasts, bone marrow (BM) stromal cells, embryonic fibroblasts and endothelial cells[139,142,172]. Several perturbations of mature hematopoietic cells as well as hematopoietic stem cells (HSC), have been documented in SHIP-deficient mice. It has a significant role in NK cells[11,145,173], B lymphocytes[147,174], myeloid cells[148], macrophages[82], osteoclasts[83], dendritic cells[85] and immunoregulatory cells[85,86,175,176]. Furthermore, we previously showed a crucial role for SHIP in the regulation of the BM HSC compartment[136,172]. Initial transplant studies showed that SHIP$^{-/-}$ BM HSC were compromised in their ability to provide long term multi-lineage blood repopulation in competition with wild type (WT) BM HSC suggesting an intrinsic role for SHIP in HSC function[136]. However, our recent studies have also revealed a crucial role for SHIP in the function of niche cells that support HSC in the BM[172]. Taken together these studies reveal a complex role for SHIP in the control

of HSC function with both cell autonomous and extrinsic *in vivo* effects being possible.

In an *in situ* SHIP deletion model, in which BM resident HSC are rendered SHIP-deficient while they are resident in a SHIP-competent milieu, we observed significant HSC peripheralization to the spleen and splenomegaly suggesting a cell autonomous role for SHIP in limiting HSC function to the BM. Although not the primary supply during adulthood, the spleen can be a significant source of HSC and definitive hematopoiesis early in ontogeny[177]. Here we show that lack of SHIP causes relocation of a functional HSC compartment to the spleen. Furthermore, we show that increased PI3K/Akt signaling in SHIP$^{-/-}$ HSC preferentially sustains this peripheralized HSC compartment.

Results

SHIP$^{-/-}$ Splenocytes Exhibit All Major Features of *Bona Fide* HSC

We recently found that MxCreSHIP$^{flox/flox}$:WT BM chimeras develop splenomegaly after induction of SHIP-deficiency (Figure 26), suggesting there might be significant HSC activity and definitive hematopoiesis in the spleen when SHIP-deficient HSC are present in an animal.

To determine if there was significant HSC activity in the spleens of SHIP$^{-/-}$ mice we transplanted lethally irradiated Ly5 congenic hosts with 0.5x10^6 splenocytes from SHIP$^{-/-}$ or WT donors. Consistent with the presence of significant HSC numbers, SHIP$^{-/-}$ splenocytes protected >90% of lethally irradiated recipients while only <30% that received WT splenocyte grafts survived

for at least 30 days (Figure 27A). Analysis of blood cell repopulation in BM, spleen and blood at 4 months post-transplant showed that global donor hematopoietic repopulation was ~50% for mice transplanted with SHIP$^{-/-}$ splenocytes (Figure 27B and data not shown). SHIP$^{-/-}$ splenocytes also contributed significantly to repopulation of multiple lineages including the B lymphoid, T lymphoid and myeloid/granulocytic lineages (Figure 27B). Thus, the splenic HSC compartment in SHIP-deficient donors is capable of radioprotection and extended multi-lineage repopulation. The mice reconstituted with SHIP$^{-/-}$ splenocytes also exhibited splenomegaly at 4 months post-transplant (Figure 28), indicating peripheralized HSC retain the bias toward extramedullary hematopoiesis even after transplant into SHIP-competent mice.

Figure 26: SHIP-deficient HSC are peripherally biased.
Splenomegaly in MxCreSHIP$^{flox/flox}$/Ly5.1-BL6 BM chimeras post-deletion. MxCreSHIP$^{flox/flox}$:WT (-/-:WT) and SHIP$^{flox/flox}$:WT (+/+:WT) BM chimeras were established in Ly5.1^{+}5.2^{+} hosts and then SHIP was deleted by three injections of polyI/C. Five months later the spleens were removed and photographed. Three representative spleens from each type of chimera are shown.

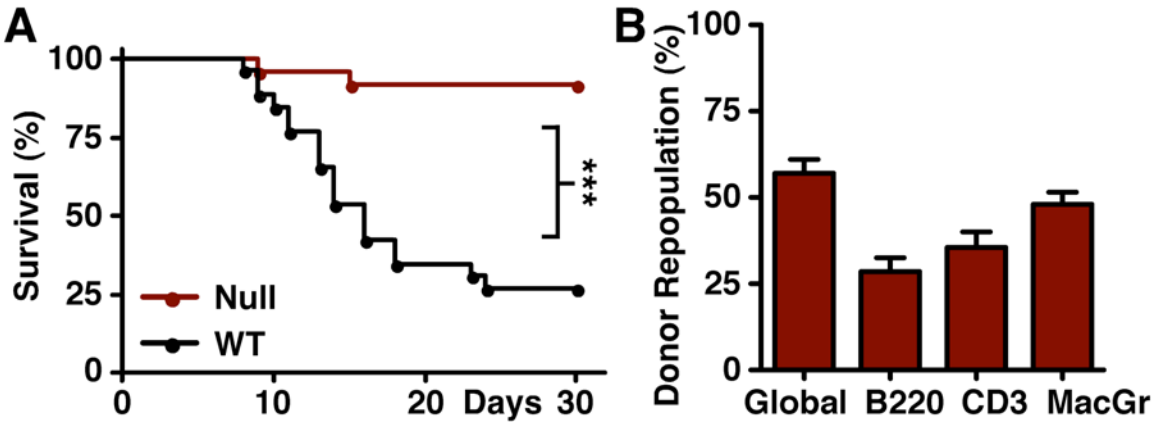

Figure 27: SHIP-deficient splenocytes have significant repopulating activity.
(A) A representative survival curve of lethally irradiated Ly5.1^{+}5.2^{+} hosts that received a splenocyte graft (0.5x10^{6} cells/mouse) from either a SHIP$^{-/-}$ donor (n=24) or a WT donor (n=26). (B) Global hematopoietic and lineage-specific donor repopulation at 4 months post-transplant for SHIP$^{-/-}$ splenocyte transplanted mice based on Ly5.2^{+}5.1^{-} staining of total PBMC (Global), Ly5.2^{+}5.1^{-} staining of B220^{+} B lymphoid cells (B220), of CD3^{+} T lymphoid cells (CD3) of Mac1^{+} or Gr1^{+} myeloid cells (MacGr). Survival differences were assessed by the Kaplan-Meier log-rank test. The significance of differences in repopulation were assessed by a Student's T-test and unless indicated are not significant. [***p<0.001] [SHIP$^{-/-}$ graft, RED; WT graft, BLACK]

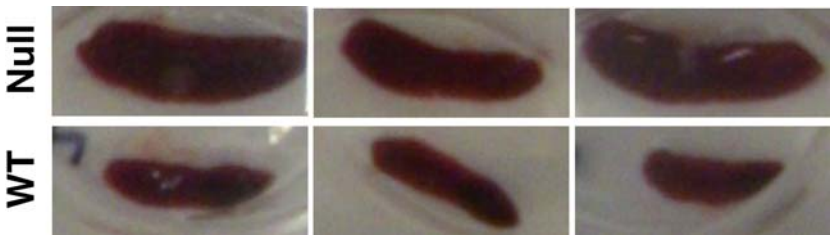

Figure 28: SHIP-deficient splenocytes provide hematopoiesis but remain peripherally biased.
Splenomegaly at four months post-transplant in recipients reconstituted with $SHIP^{-/-}$ splenocytes (Null) as compared to mice reconstituted with WT splenocytes (WT). Three representative spleens from each transplant group are shown.

The unique feature of the HSC is its ability to self-renew as measured by its ability to repopulate multiple-lineages upon serial transplantation. As an initial indication of self-renewal by HSC present in the $SHIP^{-/-}$ splenocyte graft we observed greater donor reconstitution of the $cKit^{+}Lin^{-}Scai^{+}CD48^{-}$ (KLSCD48)[178] HSC compartment in the spleens of primary recipients reconstituted with $SHIP^{-/-}$ splenocytes as compared to primary recipients reconstituted with WT splenocytes (Figure 29). This finding is consistent with the splenomegaly and extramedullary hematopoiesis observed in Figure 28.

To further assess self-renewal, we then serially transplanted secondary recipients with $0.5X10^{6}$ splenocytes from the primary recipients. As with the primary transplants, the serial transfer of splenocytes from primary recipients that received $SHIP^{-/-}$ splenocytes were significantly more radioprotective than splenocytes from primary recipients that received WT splenocytes (Figure 30A). Analysis of peripheral blood at 4 months post-transplant in these secondary recipients confirmed that the mice had significant multi-lineage and global hematopoietic repopulation derived from the original primary $SHIP^{-/-}$ splenocyte graft (Figure 30B). These findings demonstrate the existence of a robust extramedullary HSC compartment in $SHIP^{-/-}$ mice that is capable of radioprotection, long-term multi-lineage repopulation and self-renewal.

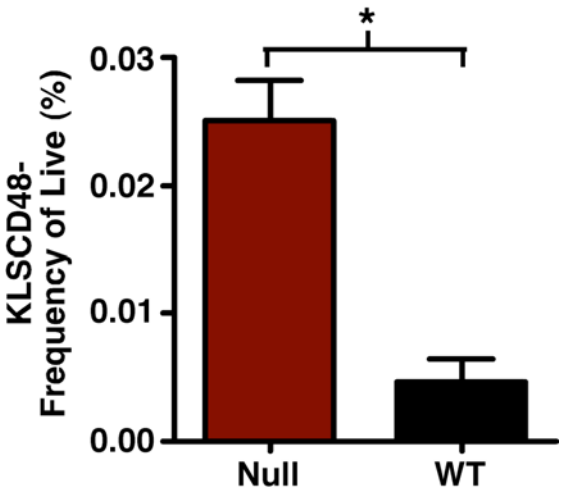

Figure 29: SHIP-deficient splenocytes have significant HSC activity. Donor HSC repopulation at 4 months post-transplant for mice based on a $Ly5.2^{+}5.1^{-}$ gate on the KLSCD48 HSC present in viable splenocytes. Mice originally received either a $SHIP^{-/-}$ (Null) splenoctye graft or a wild type (WT) splecnocyte graft. The significance of differences in repopulation were assessed by a Student's T-test. [*p<0.05] [$SHIP^{-/-}$ graft, RED; WT graft, BLACK]

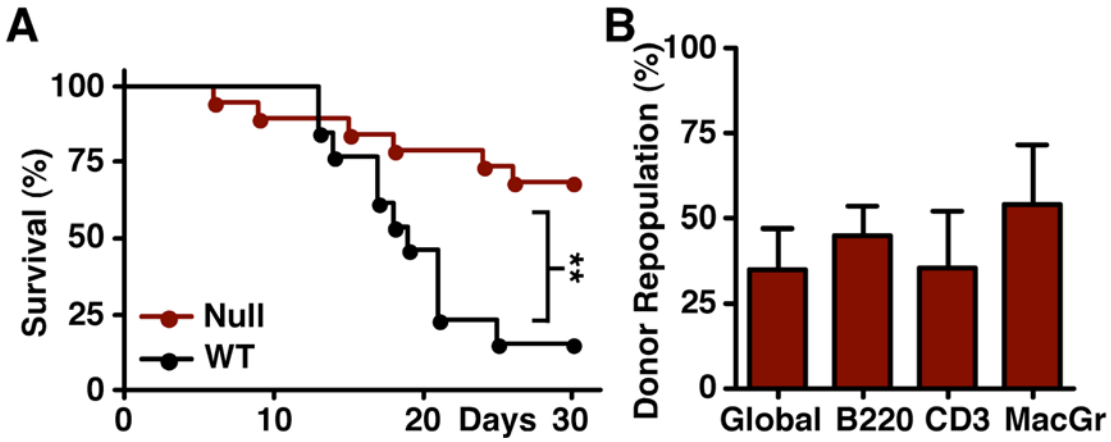

Figure 30: SHIP-deficient splenocytes have significant HSC self-renewal. (A) A representative survival curve of lethally irradiated $Ly5.1^{+}5.2^{+}$ secondary hosts that received a splenocyte graft ($0.5x10^{6}$ cells/mouse) from primary donors reconstituted with $SHIP^{-/-}$ (Null) splenocytes (n=19) or WT (WT) splenocytes (n=13). (B) Global hematopoietic and lineage specific donor repopulation at 4 months post-transplant for secondary mice that received a splenocyte graft from a primary host, which originally received a $SHIP^{-/-}$ graft. Survival differences were assessed by the Kaplan-Meier log-rank test. [**p<0.005] [$SHIP^{-/-}$ graft, RED; WT graft, BLACK]

SHIP$^{-/-}$ Splenic HSC are Equally Potent to *Bona Fide* SHIP-competent BM HSC

The above studies established the presence of a robust HSC compartment in the spleens of SHIP-deficient mice. Our previous study found increased mobilization, poor homing and compromised function by BM HSC in SHIP$^{-/-}$ mice[136], suggesting that a significant portion of the HSC compartment might be relocated to the spleen of these mice. To examine this question we directly compared the function of splenic SHIP$^{-/-}$ HSC to that of BM HSC from normal mice. To accomplish this we sorted equal numbers of KLSCD48 HSC from spleens of SHIP$^{-/-}$ and WT mice as well as KLSCD48 HSC from the BM of WT mice (Figure 31). Equal numbers of these three HSC populations were transplanted into lethally irradiated mice without the aid of supporting BM cells to directly compare their capacity to radioprotect lethally irradiated hosts. SHIP$^{-/-}$ splenic HSC protected >80% of lethally irradiated hosts, which in fact provides a comparable level of radioprotection as that provided by *bona fide* WT BM HSC (Figure 32). However, we find that KLSCD48 HSC sorted from the spleens of WT mice are incapable of significant radioprotection (Figure 32). These findings indicate a functional BM HSC compartment is not only relocated to the spleen in SHIP-deficient mice, but is qualitatively comparable to WT BM HSC.

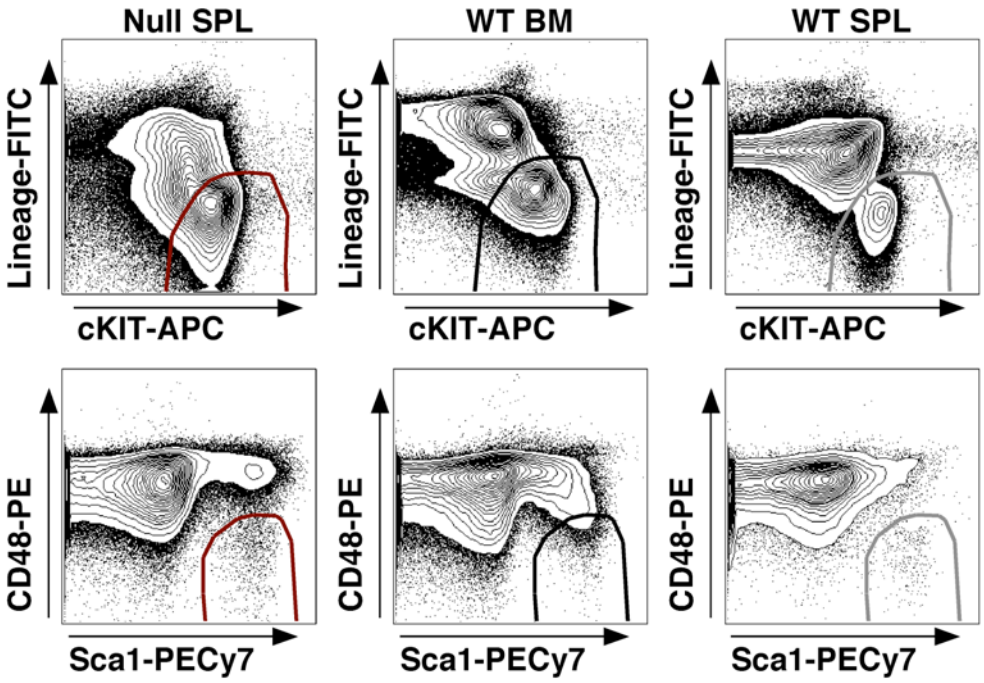

Figure 31: Purification of HSC from SHIP$^{-/-}$ spleen, WT BM and WT spleen.
Representative FACS plots demonstrating the isolation of KLSCD48 HSC for transplantation from SHIP$^{-/-}$ spleen (LEFT), WT BM (CENTER) or WT spleen (RIGHT).

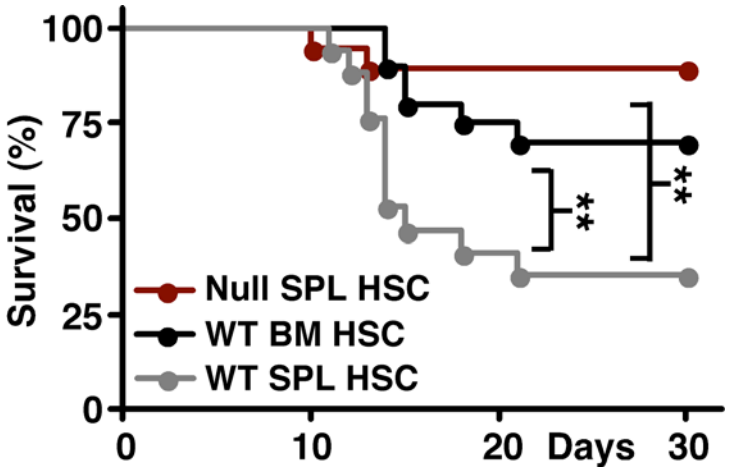

Figure 32: SHIP$^{-/-}$ splenic HSC have radioprotective capacity equivalent to WT BM HSC.
A representative survival curve of lethally irradiated Ly5.1^{+}5.2^{+} hosts that received a KLSCD48 HSC graft (200 cells/mouse) purified from either SHIP$^{-/-}$ spleen (n=19), WT spleen (n=17) or WT BM (n=20) as indicated. Survival differences were assessed by the Kaplan-Meier log-rank test. [**p<0.005] [SHIP$^{-/-}$ spleen graft, RED; WT BM graft, BLACK; WT spleen graft, GRAY]

Analysis of peripheral blood at 4 months post-transplant in the surviving recipients confirmed that the mice had significant multi-lineage and global hematopoietic repopulation derived from the original primary SHIP$^{-/-}$ splenic KLSCD48 HSC or WT BM KLSCD48 HSC graft (Figure 33 and data not shown). These findings demonstrate the existence of a robust extramedullary HSC compartment in SHIP$^{-/-}$ mice that is qualitatively comparable to a *bona fide* BM HSC.

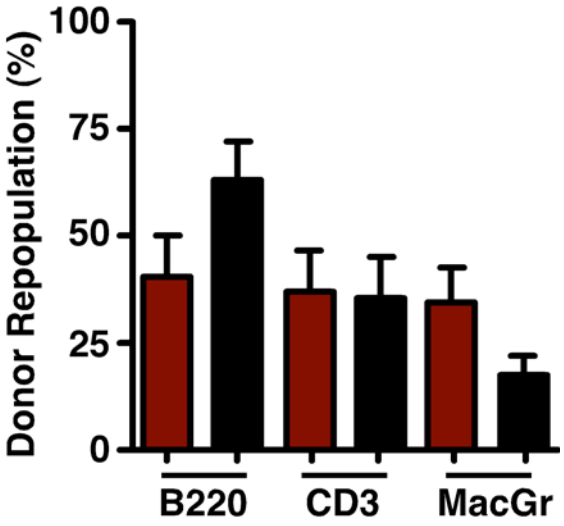

Figure 33: SHIP$^{-/-}$ splenic HSC have reconstituting capacity equivalent to WT BM HSC.
Lineage-specific donor repopulation at 4 months post-transplant form surviving SHIP$^{-/-}$ spleen KLSCD48 HSC and WT BM KLSCD48 HSC transplanted mice based on staining of PBMC for Ly5.2^{+}5.1^{-} and staining of B220^{+} B lymphoid cells (B220), of CD3^{+} T lymphoid cells (CD3) and of Mac1^{+} or Gr1^{+} myeloid cells (MacGr). The significance of differences in repopulation were assessed by a Student's T-test and unless indicated are not significant. [SHIP$^{-/-}$ spleen graft, RED; WT BM graft, BLACK]

Induction of SHIP-deficiency in Normal Adult Physiology Evacuates HSC to the Spleen

The above experiments did not address whether SHIP-deficiency causes a developmental defect that enables fetal and neonatal HSC to continue to reside in the spleen rather than completing their migration to the BM during ontogeny. If this were the case, then induction of SHIP-deficiency in adult mice would not result in relocation of HSC to the spleen. To test this possibility, we induced SHIP-deficiency in MxCreSHIP$^{flox/flox}$ mice by injection of polyinosinic-polycytidylic acid (polyI/C) and then quantitated HSC in the spleen and blood 21 days later using the KLSCD48 HSC phenotype. Similar to our observations in MxCreSHIP$^{flox/flox}$:WT BM chimeras (Figure 26), MxCreSHIP$^{flox/flox}$ mice develop splenomegaly after induction of SHIP-deficiency (Figure 34), again suggesting hematopoiesis in the spleen.

As we observed with germline SHIP-deficient mice[136], HSC numbers are significantly increased in both the blood and spleen of MxCreSHIP$^{flox/flox}$ mice relative to their SHIP$^{flox/flox}$ controls treated with an identical polyI/C regimen (Figure 35A-B). These findings demonstrate that during adult physiology SHIP is required for BM retention of HSC.

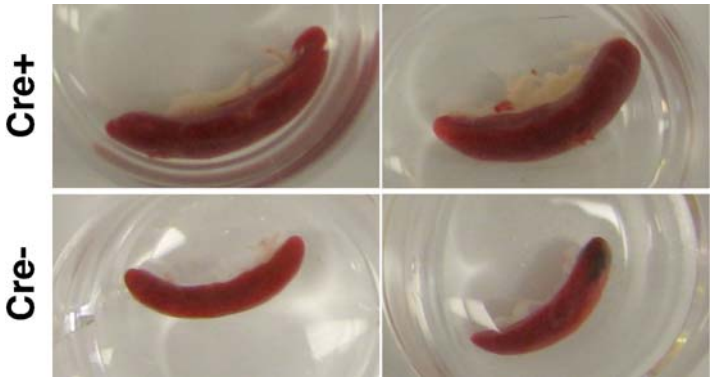

Figure 34: Induced SHIP deficiency in the adult causes extramedullary hematopoiesis.
Splenomegaly in MxCreSHIP$^{flox/flox}$ but not SHIP$^{flox/flox}$ controls after polyI/C treatment. Two representative spleens from MxCreSHIP$^{flox/flox}$ (CRE+) or SHIP$^{flox/flox}$ (CRE-) controls are shown.

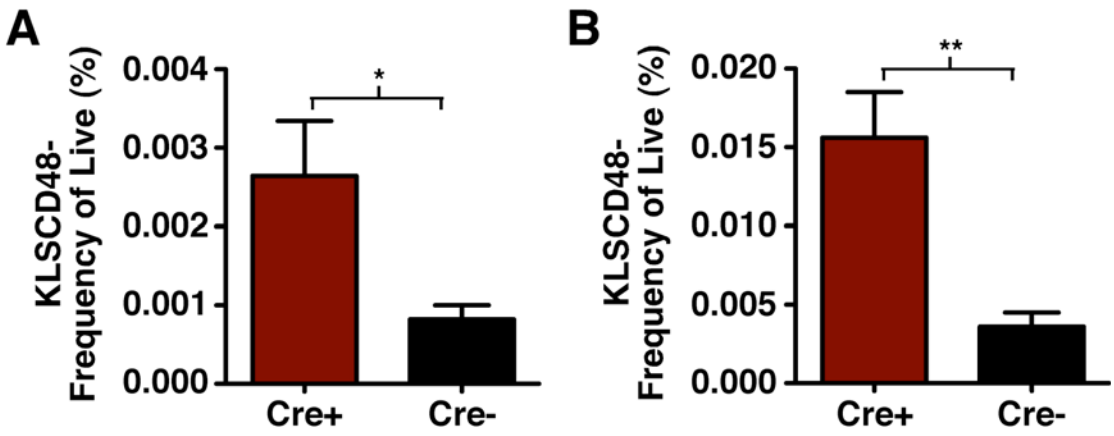

Figure 35: Induced SHIP deficiency in the adult mobilizes HSC to the blood and spleen.
(A) Representative flow cytometric quantitation of KLSCD48 HSC in PB of MxCreSHIP$^{flox/flox}$ and SHIP$^{flox/flox}$ controls after polyI/C stimulated deletion of SHIP. Mice received three polyI/C injections on days 1, 4 and 7 and then HSC were quantitated in the indicated tissues 21 days later by flow cytometry. (B) A similar flow cytometric quantitation of KLSCD48 HSC in Spleen of MxCreSHIP$^{flox/flox}$ and SHIP$^{flox/flox}$ controls after polyI/C. The significance of differences were assessed by a Student's T-test. [*$p<0.05$, **$p<0.005$] [MxCreSHIP$^{flox/flox}$, RED; SHIP$^{flox/flox}$, BLACK]

Aberrant PI3K/Akt Signaling Sustains the Peripheralized HSC Compartment in SHIP$^{-/-}$ Mice

Like its s-SHIP isoform expressed in pluripotent stem cells[41,139], SHIP can be recruited to key growth factor receptor complexes to oppose PI3K and thus limit HSC proliferation and/or survival. We proposed then that SHIP-deficient HSC may have higher levels of PI3K/Akt signaling that enables their survival outside the BM milieu where suboptimal concentrations of key HSC growth and survival factors are present. Consistent with this hypothesis, we observe elevated levels of Akt phosphorylation in SHIP-deficient hematopoietic stem/progenitor cells (HS/PC) (Figure 36).

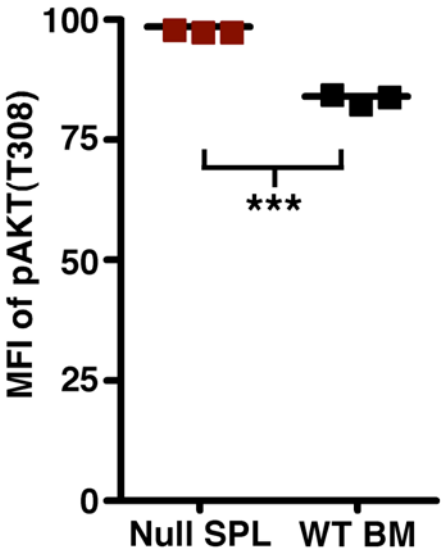

Figure 36: SHIP-deficiency results in aberrant PI3K/Akt signaling in HSC. Representative median fluorescence intensity (MFI) values for phosphorylated AKT levels in KLS cells from SHIP$^{-/-}$ spleens or WT BM as assessed by flow cytometry. The significance of differences were assessed by a Student's T-test. [***p<0.005] [SHIP-/-, RED; WT, BLACK]

In addition, inhibition of PI3K signaling *in vivo* by treatment with a potent PI3K inhibitor, Wortmannin, leads to a significant reduction in spleen size, total splenocytes and splenic HSC numbers in wortmannin-treated SHIP$^{-/-}$ mice as compared to the vehicle-treated group (Figure 38A-B). Taken together, these findings demonstrate that aberrant PI3K/Akt signaling sustains the splenic SHIP$^{-/-}$ HSC compartment and their hematopoietic output.

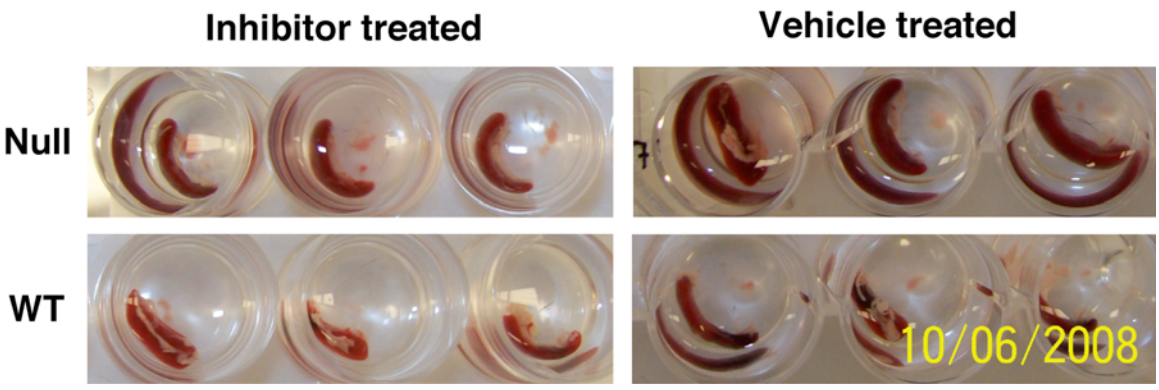

Figure 37: Aberrant PI3K/Akt signaling contributes to splenomegaly in SHIP$^{-/-}$ mice.
Images of spleens showing reduced splenomegaly in SHIP$^{-/-}$ mice treated with 0.7mg/kg Wortmannin (Inhibitor) compared to Vehicle (Vehicle) for 7 days.

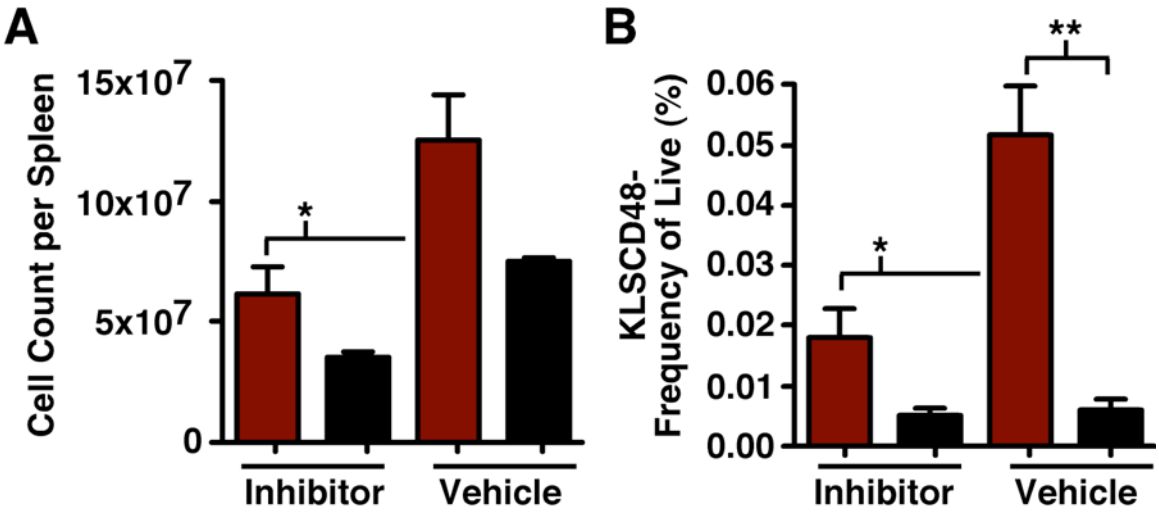

Figure 38: Aberrant PI3K/Akt signaling contributes to peripheral existence of SHIP$^{-/-}$ HSC.

(A) Quantitative comparison of viable cell counts from spleens of Wortmannin (Inhibitor) or Vehicle (Vehicle) treated SHIP$^{-/-}$ and WT mice. (B) Flow cytometric quantitation of KLSCD48 HSC in spleen of SHIP$^{-/-}$ and WT mice treated for 7 days with 0.7mg/kg Wortmannin (Inhibitor) or Vehicle (Vehicle) alone. The significance of differences were assessed by a Student's T-test and unless indicated are not significant. [*$p<0.05$, **$p<0.01$] [SHIP-/-, RED; WT, BLACK]

Discussion

The variety of phenotypes associated with SHIP-deficiency indicate SHIP has diverse roles in mammalian biology[11,82,83,85,86,136,145,147-149,173-175]. A complete understanding of the role that SHIP plays in HSC biology at both the molecular and cellular level has yet to be fully defined. We recently showed that SHIP plays a crucial role in the function of BM niche cells that support HSC activity[172]. Deregulated production of G-CSF, compromised SDF-1 production and suppression of CXCR4 expression by the altered BM niche may all contribute to the peripheralization of HSC to the spleen in SHIP$^{-/-}$ mice[136,172]. However, the findings shown here indicate an additional cell autonomous role for SHIP in HSC function. We find that SHIP-deficient HSC are capable of a sustained existence in the spleen of SHIP-competent hosts and, moreover, that deregulated PI3K/Akt signaling contributes to this sustained peripheral existence.

Recently work has been done to indicate there might be an extramedullary HSC niche in the spleen consisting of megakaryocyte like cells (MLC)[179]. These MLC express several factors important to the osteoblastic niche in BM, such as N-Cadherin and SDF-1. Interestingly, our group has shown that SHIP$^{-/-}$ spleens contain increased numbers of megakaryocytes[180], indicating a potential extramedullary HSC niche. Here we show that these SHIP$^{-/-}$ extramedullary HSC are capable of providing comparable radioprotection to WT BM derived HSC in addition to long term multi-lineage repopulation when transplanted into lethally irradiated hosts. To our knowledge this is the first work to suggest a role for SHIP in the survival of HSC in the periphery.

In spite of the negative repercussions for loss of SHIP, a short-term inhibition of SHIP could prove beneficial in a setting of BM failure. It is tempting to speculate on the implications these findings may have for clinical application. We propose that reversible inhibition of SHIP could be utilized when medullary hematopoiesis is selectively compromised by exposure to infectious agents, radioisotopes or chemicals that selectively target BM. Our findings here demonstrate that induced SHIP-deficiency could evacuate a sufficient number of HSC to the spleen that are equally potent to BM HSC. This "refugee" HSC compartment could support definitive hematopoiesis until such time as the BM microenvironment recovers from acute stress allowing return of HSC to their normal niche. Previously we advocated the use of SHIP inhibition strategies to abrogate host-versus-graft and graft-versus-host immune responses in allogeneic BM transplantation[11]. Our findings here indicate that such an approach could be applicable to recovery and maintenance of autologous blood cell production in a variety of therapeutic settings.

Methods

Mice

The development and production of $SHIP^{-/-}$ and $MxCreSHIP^{flox/flox}$ mice has previously been described by our group[11,86]. $MxCreSHIP^{flox/flox}$:WT and $SHIP^{flox/flox}$:WT BM chimeras were created by co-transplanting $0.5X10^6$ WBM cells from $MxCreSHIP^{flox/flox}$ or $SHIP^{flox/flox}$ ($Ly5.2^+$) with $0.5X10^6$ WBM cells from WT ($Ly5.1^+$) mice into lethally irradiated $Ly5.1^+Ly5.2^+$ recipients[172]. Two months

later both cohorts received three injection of polyI/C as described below. The spleens pictured in Figure 26 were removed at least 4 months after deletion of SHIP from representative members of the MxCreSHIP$^{flox/flox}$:WT (-/-:WT) and SHIP$^{flox/flox}$:WT (+/+:WT) cohorts.

Splenocyte Transplants

0.5x10^6 germline SHIP-deficient (Ly5.2$^+$) splenocytes or 0.5x10^6 WT (Ly5.2$^+$) splenocytes were transplanted by retro-orbital (r.o.) injection into separate groups of lethally irradiated WT (Ly5.1$^+$Ly5.2$^+$) recipients. In all transplants, recipient mice were given antibiotic water prior to receiving a split dose of 11-Gy at least 2-hours before transplantation.

Secondary Splenocyte Transplants

At least 4 months after the primary splenocyte transplant, animals were sacrificed and 0.5x10^6 spleen cells were transplanted (r.o.) into lethally irradiated WT (Ly5.1$^+$Ly5.2$^+$) recipients.

HSC Transplants

KLSCD48 HSC were isolated by fluorescence-activated cell sorting (FACS) from WT BM, SHIP$^{-/-}$ spleen or WT spleen. Then 200 purified KLSCD48 cells from each group were transplanted (r.o.) into separate lethally irradiated WT (Ly5.1$^+$Ly5.2$^+$) recipients.

Conditional Deletion of SHIP

MxCreSHIP$^{flox/flox}$ mice were conditionally deleted for SHIP through the intra-peritoneal (i.p.) injection of polyinosinic-polycytidylic acid (polyI/C) (Sigma-Aldrich, St. Louis, MO). Mice were injected three times with 625µg of poly(I:C) on days 1, 4, and 7.

Assessment of Donor Reconstitution in PBMC

All antibodies were from BD Biosciences (San Jose, CA), eBioscience (San Diego, CA) or Invitrogen (Carlsbad, CA) unless otherwise noted. Peripheral blood was collected and red blood cell lysis performed as previously described[136]. Peripheral blood mononuclear cells (PBMC) were treated with CD16/CD32 mouse Fc block (2.4G2) on ice for 20 minutes then stained with a panel containing: CD45.1-PE (A20), CD45.2-FITC, B220-AlexaFluor700 (RA3-6B2), CD3-PECy7 (145-2C11), Mac1-APC (M1/70) and Gr1-APC (RB6-8C5). After a 20-minute incubation on ice the cells were washed and resuspended in media containing 75ng/ml of 4',6-diamidino-2-phenylindole dihydrochloride (DAPI) for dead cell exclusion (Sigma, Saint Louis, MO). Acquisition was done on a FACS LSRII (BD Biosciences) and data analyzed using FlowJo® software (Tree Star, Inc. Ashland, OR).

KLSCD48 HSC Sorting

C-kit^{+} splenocytes or BM were enriched using an AutoMACS magnetic enrichment system with anti-cKit (Miltenyi Biotec, Auburn, CA) magnetic beads.

The positive fraction was then stained for the Lineage$^{-/low}$c-Kit^{+}Sca1^{+}CD48^{-} (KLSCD48) phenotype[129] for 20 minutes on ice using the following antibody panel: cKit-APC (Miltenyi Biotec), Lineage panel-FITC, CD48-PE (HM48-1), Sca1-PECy7 (D7). The lineage panel consisted of: CD2 (RM2-5), CD3e (145-2C11), CD4 (GK1.5), CD5 (53-7.3), CD8a (53-6.7), B220 (RA3-6B2), Gr-1 (RB6-8C5), Mac-1 (M1/70), NK1.1 (PK136), CD41 and Ter119 (TER-119). After staining, the cells were washed and resuspended in staining medium containing 75ng/ml of DAPI for dead cell exclusion. Sorting was performed on a FACS Aria (BD Biosciences).

KLSCD48 HSC Analysis

Peripheral blood and splenocytes were harvested and red blood cell lysis was performed. PBMC and splenocytes were treated with CD16/CD32 mouse Fc block on ice for 20 minutes then stained with a panel for the KLSCD48^{-} phenotype containing: cKit-APC, Lineage panel-FITC, CD48-PE, Sca1-PECy7. The lineage panel was identical to the previously described panel. After staining, the cells were washed and resuspended in medium containing 75ng/ml of DAPI for dead cell exclusion. Acquisition was done on a FACS LSRII and data analyzed using FlowJo® software.

Intracellular Flow Cytometry

Tissues were harvested on ice in PBS with 5% serum. A single cell suspension was prepared, then cells were centrifuged (5 min, 300g) to pellet and resuspend

in 20 volumes of pre-warmed (37°C) Lyse/Fix buffer (BD Phosflow Lyse/Fix, BD Biosciences). Cells were incubated at 37°C for 10 mins. After fixation, cells were pelleted again and permeabilized by adding 1ml Perm/Wash buffer (BD Phosflow, Perm/Wash I, BD Biosciences) per 10 million cells. Cells were incubated at room temperature for 10 mins then washed twice in 5 ml Perm/Wash buffer. Cells were resuspend in BD Stain buffer (BD Stain Buffer, BD Biosciences) at 100ul/million and treated with CD16/CD32 mouse Fc block on ice for 20 minutes. Then cells were stained with a panel for both intracellular and extracellular antibodies at room temperature for 30 mins. The panel for the KLS phenotype consisted of: Lineage panel-FITC, cKit-PECy7 (2B8), Sca1-APC (D7). The lineage panel was identical to the previously described panel. In addition, the antibody pAKT(T308)-PE (BD Biosciences) was used to assess levels of activated Akt. After staining the cells were washed once in BD Stain buffer and resuspend for flow cytometric analysis. Acquisition was done on a FACS LSRII and data analyzed using FlowJo® software.

PI3K Inhibitor Studies

Cohorts of SHIP$^{-/-}$ or WT mice were weighed and treated daily, for 7 consecutive days, with 0.7mg/kg Wortmannin (Sigma-Aldrich, St Louis, MO) dissolved in a Tween-20 vehicle and diluted in 500ul sterile PBS per i.p. injection per mouse, for ease of injection. Separate cohorts of SHIP$^{-/-}$ or WT mice were weighed and treated daily with Tween-20 vehicle alone, which was also dissolved in 500ul

sterile PBS per i.p. injection per mouse. On day 8 all mice were sacrificed for further analysis.

Statistical Analysis

All statistical analyses were performed using Prism® (GraphPad, San Diego, CA).

Defining the Hematopoietic Kinome

Abstract

Most cellular processes are regulated by the reversible phosphorylation of proteins, rendering those proteins active or inactive. This phosphorylation occurs on the amino acids serine (S), threonine (T) and tyrosine (Y) by protein kinases. These kinases play a major role in regulating signaling cascades that determine cell cycle entry, survival and the differentiation fate of cells in the mammalian body, including the hematopoietic system. Therefore, an important goal is to define those proteins that participate in phosphorylation-regulated signaling pathways involved in hematopoietic development and differentiation. A massively parallel and unbiased determination of the different kinase activities present in hematopoietic cells would help elucidate fundamental molecular processes that determine the unique biological properties of stem cells. We have collaborated with a group that developed peptide array technology where 1,176 different peptide substrates of kinases are arrayed in duplicate on a single chip. Our collaborators have previously established that this technology can be applied to whole cell lysates prepared from rare cell populations purified via high-speed cell sorting. We have now begun to use this technology to conduct a parallel assessment of the kinase signature or “kinome” of long-term repopulating hematopoietic stem cells (LT-HSC), short-term repopulating HSC (ST-HSC),

natural killer (NK) cells, B cells, T cells and myeloid cells. Our initial comparison of the kinome profiles of LT-HSC and ST-HSC reveals a significant degree of overlap in their respective kinomes, which is expected due to their close proximity in the hematopoietic differentiation program. Similarly, fully differentiated mature hematopoietic cells show many kinase similarities. However, these comparisons do reveal several key differentially regulated kinases. Here, we present kinome signatures that are specific to these discrete subsets as well as the specific kinome signature of the HSC. A bioinformatic approach was used to group differentially regulated kinases into common functional categories allowing us to draw initial conclusions regarding the biological relevance of these key differences. These kinome studies may provide crucial information concerning the unique biological activities as hematopoietic cells differentiate, including potential signaling pathways that control lineage commitment.

Introduction

The transcriptome and proteome have been widely explored over the past five years, mainly due to the development of array-based technologies[181,182]. In particular, much analysis has been done to elucidate the genes important for "stemness". Several groups have done extensive array analyses and compiled massive databases to determine what genes are important in giving stem cells their unique properties[183-186]. Although many important genes came to light from these analyses, there remain significant discrepancies between the two data-

sets[185]. Regardless of these initial ambiguities, this discovery driven type of analysis can offer significant value to understanding the molecular mechanisms that govern not only self-renewal but also the unique processes needed to transition from HSC to fully differentiated immune cells. Until now, these array based studies focused on identifying key genes involved in signaling. However, equally important factors in regulation are the enzymes that are active in these particular signaling pathways. Enzymes that phosphorylate tyrosine, serine and threonine residues on proteins can determine survival and differentiation fates of cells in the hematopoietic system. Because of the ambiguity of the current stemness data, we applied a different approach to discover key signaling interactions. Understanding the differences in *active* proteins will provide critical information about cell biology. Toward this end, we have worked with a group that developed a kinome analysis technique and we have applied this technology to different subsets of hematopoietic cells including, LT-HSC, ST-HSC, B cells, T cells, myeloid cells and NK cells.

The kinome analysis implements an array technology to measure the enzymatic activity between whole cell lysates and protein substrates[187-190]. Arrays have been assembled that contain multiple consensus sequences for a broad range of protein kinases across the mammalian genome, allowing detection of phosphorylation events mediated by active kinases present in whole cell lysates. A comprehesive validation of this technology was done by evaluating the temporal kinetics of phosphorylation events induced by lipopolysaccharide (LPS) stimulation of human peripheral blood mononuclear cells[191]. Western blot

analysis of LPS stimulated cells and peptide array studies with kinase inhibitors demonstrated the usefulness of the technology for discovery driven signal transduction studies[191].

The recent application of advanced techniques, such as multi-color cell sorting and the production of transgenic and gene-knockout mice, has contributed to a better understanding of hematopoietic development from HSC to fully differentiated cell. Now that we can purify progenitors at different maturational stages during hematopoietic development, the challenge is to understand the processes that govern each developmental stage. It has been formally demonstrated that in the first few months after repopulation many different clones can contribute to hematopoiesis, but then as repopulation is completed and steady state hematopoiesis resumes, only a small number of clones are needed to maintain the blood compartment[134,192]. The HSC clones that prevail are considered long-term repopulating HSC (LT-HSC), whereas clones that are present early and then subside are considered short-term repopulating HSC (ST-HSC). Morrison and Weissman found that HSC with long-term repopulating activity could be identified in mice by the $Kit^{+}Thy1^{+}Lin^{-}Sca1^{+}$ (KTLS) phenotype[193,194] Christensen and Weissman extended these findings to show that such isolations could be enhanced by use of an additional marker, Flk2[195]. Thus, LT-HSC could be identified based on the absence of Flk2, on the $Kit^{+}Sca1^{+}Flk2^{-}Lin^{-}$ subset; whereas ST-HSC acquire Flk2 while retaining the other markers: $Flk2^{+}Kit^{+}Lin^{-}Sca1^{+}$. In this study, we used the phenotypes of Christensen and Weissman to isolate both LT and ST-HSC subsets from adult

mouse BM. Using these phenotypes we are able to obtain highly enriched HSC populations which serve as an attractive model for array based kinome profiling. We aim to better understand the key differences between these two cell types. Through statistical comparisons we have discovered a list of key kinases preferentially active in signal transduction pathways in LT and ST-HSC. In this study we also applied kinome profiling to fully differentiated hematopoietic cells including NK, B, T and myeloid cells to define lineage specific and basal hematopoietic kinomes. We have then used this basal kinome to explore the signaling differences that exist between HSC and their differentiated progeny.

Results

Our overall approach was to isolate purified cell populations, define their phosphorylation signatures using a kinase array method, and apply statistical methods to create comparisons between different stages of hematopoietic development.

Purification of Cell Populations

The first step in this study was to isolate various purified hematopoietic cell populations and generate whole cell lysates. From the spleen or bone marrow of C57BL6/J mice, we sorted LT-HSC, ST-HSC, myeloid, T, B and NK cells. Our method for the isolation of LT and ST-HSC was based on the KTLS phenotypes previously described by Christensen and Weissman[195]. Other differentiated hematopoietic cells were isolated based on the expression of cell

specific receptors: $B220^+$ for B cells, $CD3^+$ for T cells, $Mac1^+$ for myeloid cells and $NK1.1^+CD3^-$ for NK cells. Figure 39 shows representative FACS plots for each of the sorted HSC populations. Three independent sorts were performed for each cell type, consisting of a minimum of 100,000 target cells from which whole cell lysates (WCL) were prepared.

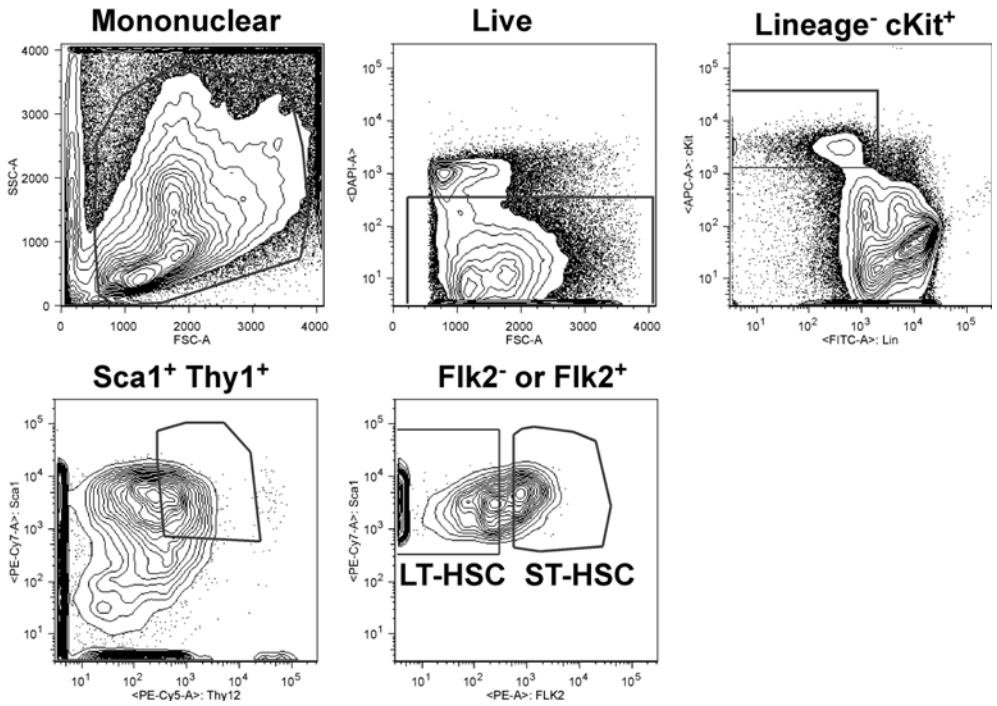

Figure 39: Representative gating for hematopoietic stem cell isolation. These dot plots show the sorting strategy for LT and ST-HSC. First mononuclear cells are included in the isolation gate, followed by viable cells. Then viable lineage negative cells that express cKit are included. Within this population we gate on Sca1 and Thy1 positive cells. This $Lin^{-}cKit^{+}Sca1^{+}Thy1^{+}$ population is then divided into Flk2 negative and Flk2 positive cells, representing LT and ST-HSC respectively.

PepChip™ Kinome Array

Each kinome array, or PepChip™, contained duplicate copies of 1,176 substrates. In order to measure kinase activity in the purified populations, WCL were applied to the PepChip™ in the presence of ^{33}P-ATP. After incubation of the WCL with the peptide arrays, the chips are exposed to a phophor-imaging screen. The resulting image contained 1,176 spots of varying intensity depending on the level of phosphorylation of the individual peptide (Figure 40). Three sets of chips were assayed from three independent isolations for each cell type, yielding six replicate phosphorylation assays for each peptide. All raw images from the phophor-imaging screen were analyzed using ScanAnalyze image analysis software. With this software, the intensity of phosphorylation of each peptide was measured and a corresponding numerical value was obtained. Using the values from the six replicates, we were able to generate a phosphorylation signature for each of the cell types examined.

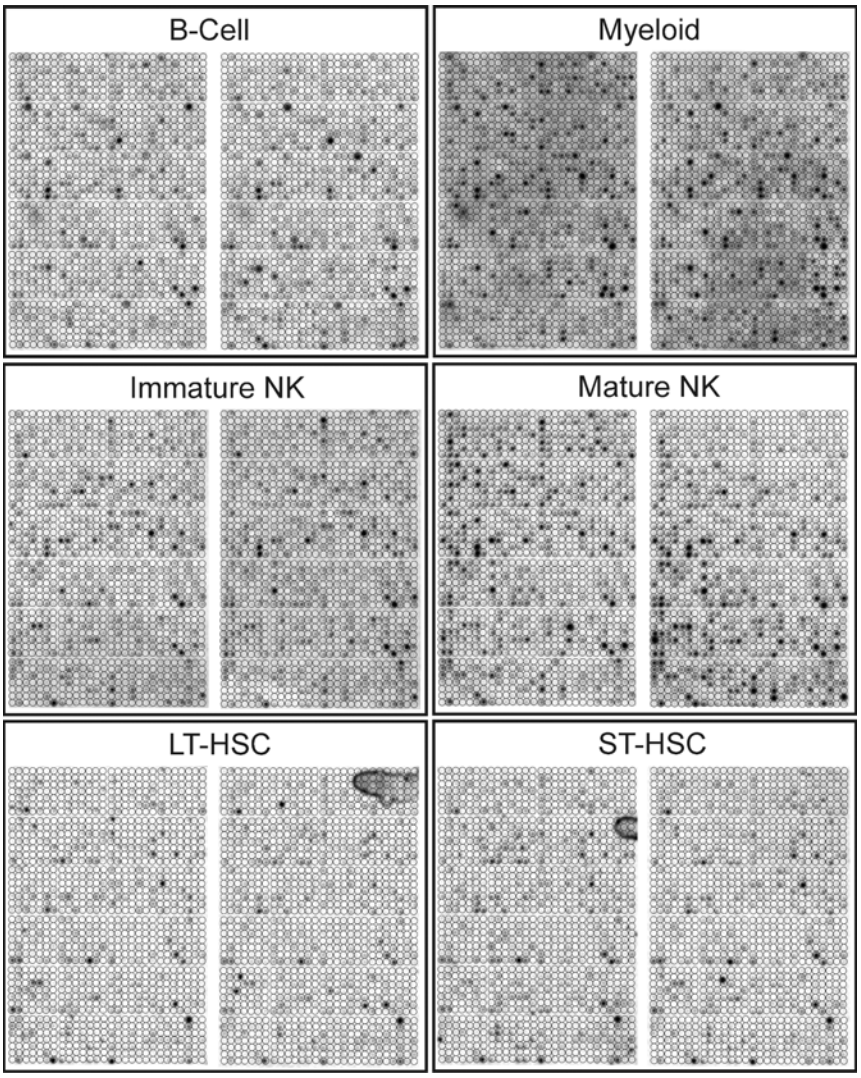

Figure 40: Representative replicate PepChip™ scans.
The resulting images after phosphor imaging screens are exposed to the PepChips™ and then developed. Two replicates for each hematopoietic cell type are shown.

Statistical Interpretation to Determine the Basal Hematopoietic Kinome

To create a basal hematopoietic kinome, we performed a Kruskal-Wallis statistical analysis to determine which peptides shared a common phosphorylation signature between B, T, NK and myeloid cells. From this analysis we were able to determine that, of the 1,176 peptides on the kinome chip, 492 have a common phosphorylation signature, leaving 684 peptides differentially phosphorylated between these fully differentiated cell types. These 492 peptides, or 42%, were designated part of the basal hematokinome (Figure 41) and represent peptides that are probably involved in basal cellular processes. Therefore, they have a lesser likelihood of yielding key differences between different cell lineages.

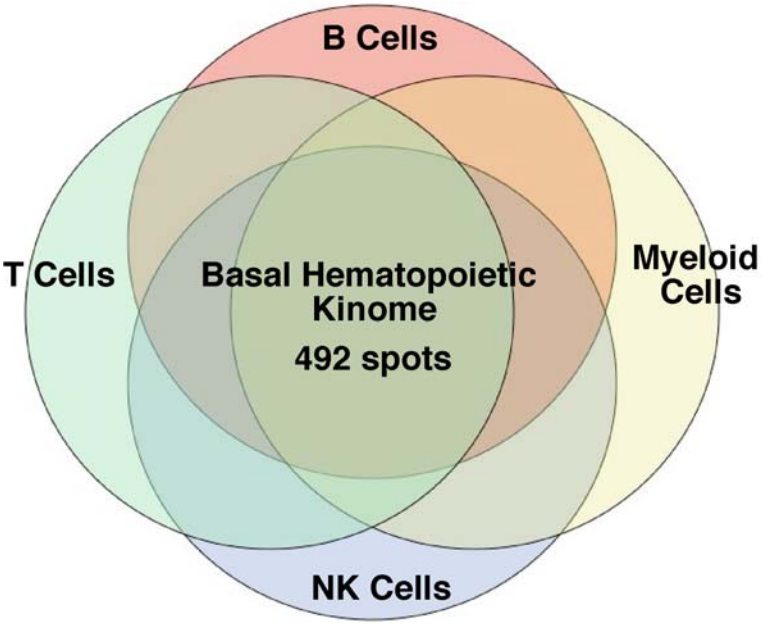

Figure 41: Venn diagram demonstrating basal hematopoietic kinome.
To create a basal hematopoietic kinome, we determined which peptides shared a common phosphorylation signature between B, T, NK and myeloid cells. The 492 peptides with a common phosphorylation signature are termed the basal hemtokinome and represent peptides that are probably involved in basal cellular processes.

Differential Kinomes of LT and ST-HSC

We extended our analysis of the basal hematokinome to the hematopoietic stem cell population. First, in order to gain insight to the functional differences between the LT and ST-HSC populations, we compared the kinome profiles of these two progenitor types and established a list of differentially phosphorylated peptides through a Wilcoxon Rank Sum analysis. We then categorized the significantly different spots based on biological function using a bioinformatics approach. In this analysis we found that 40 peptides were differentially regulated between LT and ST-HSC. In the design of the PepChip^{TM}, peptide sequences were chosen that corresponded to known or predicted phosphorylation sites across the mammalian kinome. Therefore all sites have a predicted protein that the peptide represents, although some overlap may exist between proteins with similar amino acid residues. We used a protein sequence alignment tool to cross-reference each of the 9-12 amino acid sequences to assure we had the most accurate representation of a specific protein in mouse. The protein with the strongest alignment was used, however in some instances we had to take into account the actual residue being phosphorylated. We first determined whether consensus sequences were more highly phosphorylated in LT or ST-HSC. We then assigned a biological function for each peptide using the human protein reference database (HPRD). Upon grouping of the functional categories we see that ST-HSC appear to have more activity in the cell growth pathways (Figure 42 TOP), which agrees with LT-HSC having a more quiescent behavior (Figure 42 BOTTOM).

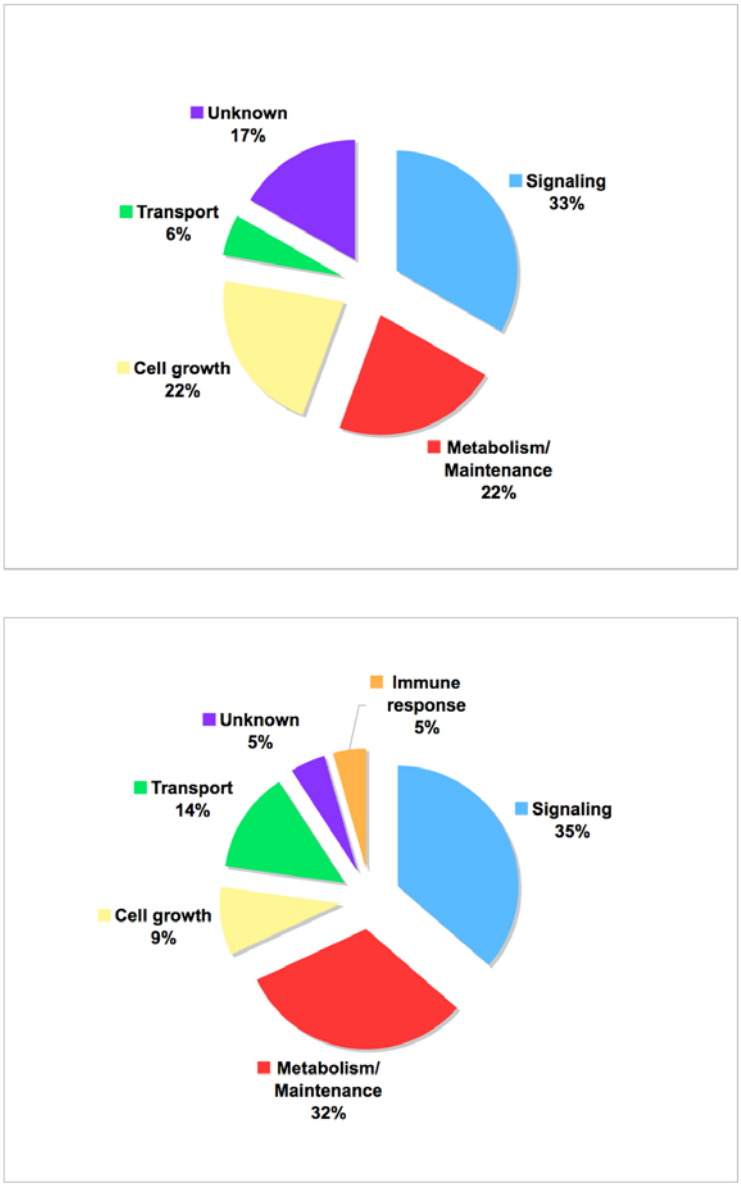

Figure 42: Functional annotation for LT and ST-HSC differences.
We compared the kinome profiles of LT and ST-HSC and established a list of differentially phosphorylated peptides. We then categorized the 40 peptides that were differentially regulated between LT and ST-HSC based on biological function. The top pie chart represents peptides with higher phosphorylation in ST-HSC. The bottom pie chart represents peptides with higher phosphorylation in LT-HSC.

The basal hematopoietic kinome profile was then compared to the list of peptides significant between LT and ST-HSC specific kinomes (Figure 43). Of the 492 basal hematopoietic kinase substrates, approximately 16 were significantly different between LT and ST-HSC. Despite the difference in regulation between LT and ST-HSC, these 16 kinase substrates are likely involved in basal cellular processes and were therefore excluded from the list of players that may be involved in key stem cell functions. In Table 3, we list the remaining 24 peptides that were more actively phosphorylated in ‘stem’ populations and might be involved in self-renewal.

Upon grouping of the functional categories we once again see that ST-HSC appear to have more activity in growth and signaling (Figure 44). The biological relevance of each of these kinases and their substrates will prove valuable in defining molecular processes active in stem cells such as self-renewal, long-term homeostasis and differentiation.

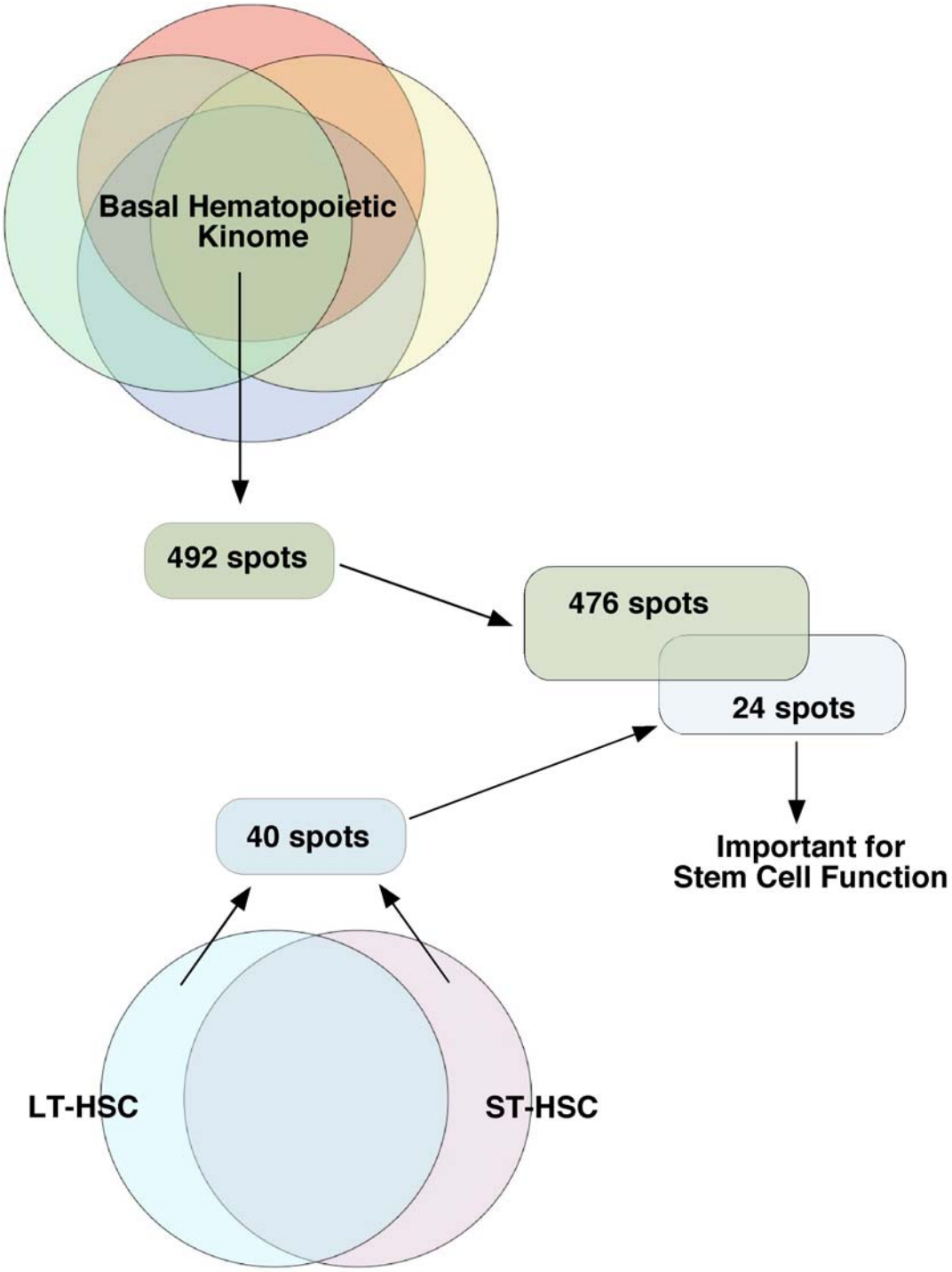

Figure 43: The 'stem' specific kinome.
The basal hematopoietic kinome profile was subtracted from the LT and ST-HSC specific kinomes. Of the 492 basal hematopoietic kinase substrates, only 16 are significantly different between LT and ST-HSC. These kinase substrates are likely involved in basal cellular processes and are therefore excluded from the list of 'stem' specific signaling events.

Table 3: Peptides sequences of proteins potentially involved in a 'stem' specific kinome.

Spot	Sequence	Putative Kinase	Protein Name
306	GSESTEDQA	CKII	Alpha-S1 casein
353	DRRVSVAAE	PKA	cAMP-dependent protein kinase II (PKA)
313	ARNDSVTVA	PKA	cAMP response element-binding protein CRE-BP1
314	DLFGSDEED	CKII	elongation factor 1-beta
354	GGRASDYKS	PKA,PKC	Myelin basic protein
350	PYKFPSSPLRIPGZ	na	unspecified protein
551	GTVPSDNID	GRK2,GRK5	Beta-2 adrenergic receptor
312	AARGSFDAS	RK	rhodopsin kinase
365	RLSISTESQ	AMP-PK	phosphorylase b kinase alpha
352	DAGASPVEK	PKC	myristolated alanine-rich C-kinase substrate
320	SIADTFVGT		Serine/threonine-protein kinase STE7
497	PYKFPSSPLRIPGZ	na	unspecified protein
339	QAGMTAPGT		calponin alpha and beta
789	HKIKSGAEA	PKC	DNA polymerase beta
802	GSRRR	PKC	protamine
211	RRAVSELDA	CaM-II	tyrosine 3-monooxygenase
438	QSPSSSPTH		phosphorylcholine transferase
596	GGVDYKNIH		Macrophage colony stimulating factor I receptor
420	LRANSI	PKA	cystic fibrosis transmembrane conductance regulator
800	SAYGSVKAY	PKC	Annexin II
807	SPKKSPRKA	sperm-specific	Histone H4
15	RRAVSEQDA	CaM-II	Tyrosine 3-monooxygenase
22	QLSTSEENS	CKI	Alpha-S2 casein
595	PYKFPSSPLRIPGZ	na	unspecified protein

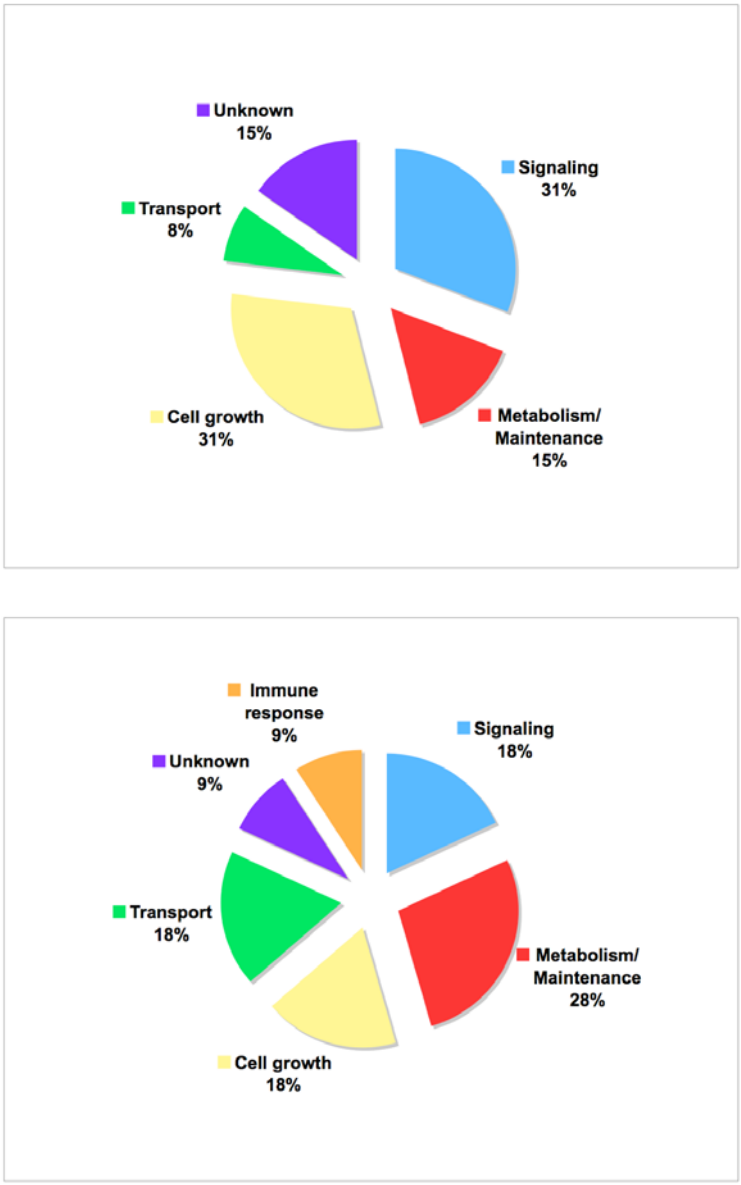

Figure 44: Functional annotation for the 'stem' specific kinome.
We functionally categorized the 24 peptides that were differentially regulated between LT and ST-HSC yet not involved in basal hematopoietic cell function. The top pie chart represents peptides with higher phosphorylation in ST-HSC. The bottom pie chart represents peptides with higher phosphorylation in LT-HSC.

Discussion

Unraveling the signaling pathways that control self-renewal, proliferation and differentiation of HSC will be important for gaining an understanding of how stem cell fate and homeostasis are controlled. Recently, similar systematic approaches have been taken to identify gene expression patterns unique to HSC[196]; however, most of the important signaling pathways that control cell physiology rely in large part on protein phosphorylation for control. Traditional genetic and biochemical approaches can certainly provide some of these answers, however, for technical and practical reasons these are typically pursued one gene or pathway at a time. Thus, a more comprehensive approach is needed in order to reveal signaling pathways active in HSC and their differentiated progeny. Furthermore, because HSC are rare cells, they do not readily lend themselves to traditional biochemical methods to reveal active signaling pathways. We have chosen to pursue an enzymatic approach that can quantitate the phosphorylation of a wide spectrum of kinase substrates to not only reveal kinases that are active in HSC, but also the substrates that are acted on in HSC.

Phosphorylation forms the basis of cell signaling and can regulate almost every property of a protein. Yet cataloging protein phosphorylation is a daunting task as protein kinases form the single largest family of enzymes and are coded by more than 2,000 genes[197,198]. Classical biochemical technologies such as peptide mapping and phosphoamino acid analysis are extremely laborious and often prove fruitless. In order to better tackle a problem of this magnitude,

peptide array chips or PepChips™ have been developed[191]. PepChips™ offer a convenient and rapid assay that requires a relatively small amount of cell lysate to generate a large amount of data. Using this technology, we can quickly build a broad picture of phosphorylation signatures within different cell subsets.

However, several disadvantages can slow down interpretation of the data. The primary issue is a processing bottleneck created by the magnitude of raw data generated[199]. New software tools specific for peptide arrays will help ease this problem. When comparing expression patterns, statistical analysis can help detect biologically relevant differences. However, frequently data points that give statistical significance have little biological interest. Similarly, lack of statistical significance can be a result of low sensitivity, not biological inactivity.

We have also used this novel kinase array technology to conduct a massively parallel analysis of kinase activities. We have identified phosphorylation signatures of LT and ST-HSC and by comparing these profiles, we hope to determine signaling events necessary for key stem cell functions. Our initial comparison reveals a significant degree of overlap in their respective kinomes and we would expect to see such a high correlation. However, we intend to examine the 3.4% difference more closely to see if it gives us some insight into the key players involved in the step down the lineage commitment tree that LT-HSC make to become ST-HSC. Interestingly, among these differences we found consensus sequences matching the potent tumor suppressor p53 were highly phosphorylated in LT-HSC. In 2007 several studies showed that lower p53 levels in HSC corresponded with defects in stem cell

regenerative capacity[200,201]. As LT-HSC differentiate into ST-HSC the proliferation activity increases[202] and self-renewal potential is believed to be reduced. Conformingly, a recent paper showed a role for p53 in the maintenance of HSC quiescence during steady-state hematopoiesis[203]. Therefore, we would expect p53 to be differentially regulated between these populations and our analysis validates this expectation.

Deciphering the complex network of phosphorylation-based signaling is crucial in understanding the cells internal workings. The majority of phosphorylation events can be considered housekeeping signaling and are needed to keep normal cell function going. In our study we have defined the basal hematopoietic kinome as the minimal transcriptome needed for hematopoietic cell function. It is unlikely that these phosphorylation events contribute to the identity of specific cell lineages. Using a systematic approach we have attempted to identify kinase activity unique between HSC and their fully differentiated progeny. A parallel analysis of the kinase activities of 'fully differentiated' hematopoietic cells compared to HSC could help elucidate molecular pathways involved in pluripotency and differentiation. We have conducted peptide array analysis on B cells, T cells, myeloid cells, and NK cells. These kinome profiles were then combined to create a 'fully differentiated' or 'basal hematopoietic' kinome. The kinases segregated into this group are believed to be involved in normal cellular processes and were therefore deducted from the stem cell comparison. Our initial comparison of the kinome profiles of HSC revealed few significant differences in their respective kinomes. The

biological relevance of the substrates with higher phosphorylation in LT-HSC may reveal important clues as to the molecular processes that control self-renewal and other unique stem cell properties. The functional relevance of these differences needs to be further investigated. However we feel that this technology provides an excellent discovery based method to identify signaling pathways that are preferentially active in lineage commitment and stem cel biology. This wealth of data offers a resource for further investigation of specific proteins involved in hematopoietic differentiation.

Methods

Mice

All mice were 8-10 week old wild type C57BL6/J mice from an in-house breeding colony or an approved vendor. On the day of cell purification the spleen and BM were removed from sufficient animals to obtain a minimum of 250,000 pure cells. Generally, this required 20 mice per experiment.

Purification of Cell Populations

LT and ST-HSC: BM was isolated from the legs, arms, hips and vertebrae of 20 C57BL6/J mice. A single cell suspension of BM mononuclear cells was obtained by filtration and red blood cell lysis. Red blood cell lysis was for 5 minutes at room temperature in a lysis buffer consisting of 0.15μM NH4Cl, 10mM KHCO3, and 0.1mM EDTA. Cells were treated with CD16/CD32 mouse Fc block on ice for 20 minutes. Then cells were stained with a panel of Lineage specific markers

followed by magnetic beads for enrichment using an AutoMACS (Miltenyi Biotec, Auburn, CA). The lineage-depleted portion of the BM was then stained with HSC specific markers, including: a lineage panel [CD2, CD3, CD4, CD5, CD8, Mac1, Gr-1, B220, NK1.1, Ter119], Flk-2, Thy1.1, c-Kit, and Sca-1. DAPI was used for dead cell exclusion. The LT and ST-HSC cell populations were sorted using a FACS Aria as follows: ST-HSC were $cKit^{+}Thy1^{+}Sca1^{+}Flk2^{+}Lin^{-}$ and LT-HSC were $cKit^{+}Thy1^{+}Sca1^{+}Flk2^{-}Lin^{-}$. *NK cells*: Spleens were removed and made into a single cell suspension by crushing, filtering and red blood cell lysis. After a 20 minute incubation with mouse Fc block, cells were stained on ice with NK1.1 and CD3. After 15 minutes, cells were washed and resuspended for FACS. DAPI was included for dead cell exclusion. Sorting of $NK1.1^{+}CD3^{-}$ cells was performed on a FACS Vantage (Beckton Dickson). *B, T, and Myeloid cells*: Similarly to NK cell isolation, a single cell suspension of splenocytes was obtained followed by 20 minutes of mouse Fc blocking. Cells were stained on ice with markers for B220, CD3, Gr1 and NK1.1. After 15 minutes, cells were washed and resuspended with media containing DAPI. Mature hematopoietic cells were sorted using a FACS Vantage. Dependent on the desired population, cells isolated were single positive for $B220^{+}$, $CD3^{+}$, or $Gr1^{+}$ markers. For PepChip analysis, a minimum of 100,000 cells were sorted from each cell population per experiment to obtain an appropriate signal. After sorting, the populations were pelleted and lysed, using an optimal kinase lysis buffer, at 500,000 cell equivalents per 50µl of buffer. The kinase lysis buffer consisted of 20mM Tris-HCl (pH 7.5), 150mM NaCl, 1mM Na2EDTA, 1mM EGTA, 1% Triton X-100, 2.5mM sodium pyrophosphate, 1mM

MgCl2, 1mM glycerophosphate, 1mM Na3VO4, 1mM NaF, 1 µg/ml leupeptin (Sigma Aldrich), 1 µg/ml aprotinin (Sigma Aldrich), 1mM PMSF. The cell lysate was cleared by centrifugation and flash frozen in liquid nitrogen.

Detection of Kinase Activity

Volumes of the cell lysates were equalized with autoclaved H2O. The cell lysates were then passed through a 0.22-µm low protein binding filter. 10µL of activation buffer was then added to the filtered cell lysates. The activation buffer consisted of 50% glycerol, 50µM ATP, 0.05% v/v Brij-35, 0.25 mg/ml bovine serum albumin, ^{33}P-γ-ATP (1000 kBq). The peptide array mix was then added to the PepChip™, and incubated at 37°C in a humidified chamber for 90 minutes. The activation and cell lysate mixture phosphorylates peptide motifs spotted on the chip. The peptide array was washed twice with Tris-buffered saline with 1% Tween-20, then twice in 2M NaCl, and then twice in demineralized H_2O and finally air-dried. The chips were exposed to a phospho-imaging screen inside a cassette for 72 hours. After 72 hours the phospho-imaging screens were scanned using a Storm Phospho-imager (GE Healthcare). From the Storm imager we obtained high-resolution image files that were imported into the ScanAlyze software program (Lawrence Berkley National Laboratory, CA) for analysis. ScanAlyze is an analysis software designed to process fluorescent microarray images. To obtain median spot density a 28 X 42 grid was overlaid onto the PepChip™ that delineated each individual peptide spot. The software program then calculated the median spot density for each square within the grid

thereby providing a value for the phosphorylation level for each peptide. (Detection of kinase activity was performed with the kind help of our collaborators Dr. Sander Diks and Dr. Maikel Peppelenbosch at the University of Groningen.)

Statistical Analysis

The median spot density for each spot on the chip was normalized across each chip. Normalization was achieved by correction of the spot density for the individual background to diminish inter-array variances thereby normalizing the total phosphorylation of the chip to be equal between all samples. This helped to compensate for differences in labeled ATP and protein levels thus facilitating normalization between experiments. This was done by taking the phosphorylation value for an individual spot dividing it by the sum of the total phosphorylation of all spots on the chip and then multiplying that by the total number of peptides (1,176). In order to be included in the kinome analysis the mean phosphorylation between the two replicates on one PepChip^{TM} had to have a correlation value of greater than +0.85. Any data that was inconsistent (i.e. SEM between data points >1.96) was excluded from further analysis. Both the correlation and standard deviation were calculated using Excel (Microsoft, Redmond, WA). Further statistical analyses were performed in Excel, Prism (GraphPad, San Diego, CA), or SAS (SAS Institute, Cary, NC) with the assistance of the Biostatistics Core Facility of H. Lee Moffitt Cancer Center. In brief, the basal hematokinome was determined using the Kruskal-Wallis test. The Kruskal-Wallis test is a non-parametric method to compare the equality of three

or more population groups. It is an extension of the more commonly known Wilcoxon Rank Sum test that applies to three or more groups. The HSC kinome was determined using a Wicoxon Rank Sum comparison. It is a non-parametric test used to determine whether two groups of observations come from the same distribution. This test is used in place of a T-test when the values of the populations being compared are not normally distributed.

Discussion

SHIP and the BM Niche

SHIP has a significant role in regulating growth and differentiation, but does not seem to be necessary for these processes as SHIP$^{-/-}$ mice are viable. Depending on the cell type, the absence of SHIP seems to have diverse roles in cell biology. Initial studies of HSC in SHIP$^{-/-}$ mice indicated an expansion of the progenitor compartment yet impaired repopulation ability[140]. These data suggested the alterations associated with SHIP-deficient HSC were transplantable and most likely cell intrinsic. Our lab extended these findings to demonstrate significant effects of SHIP deficiency on the ability of HSC to reach the BM niche after transplant. The capacity of HSC to home to the right environment is one of the essential requirements for successful repopulation of transplanted hosts. Using a combination of *in vivo* homing studies and surface receptor assessments, we determined that loss of SHIP impacts the ability of HSC to home and lodge in the BM niche[136]. These studies provided additional circumstantial evidence of a cell autonomous role for SHIP in HSC. However, they did not address possible extrinsic influences from other SHIP-deficient cells within the HSC BM niche.

Using an *in situ* deletion model where the BM microenvironment remains SHIP competent, we have provided unprecedented evidence that SHIP plays a crucial role in non-hematopoietic cells of the HSC microenvironment[172]. Our results suggest that a SHIP-deficient microenvironment can deregulate the capacity of HSC to home, lodge and engraft in the marrow space through extrinsic influences on HSC.

The directional migration of cells via signaling molecules, also called chemotaxis, is a key feature in the regulation of HSC homing and engraftment. BM stromal cells and osteoblasts are believed to support and maintain stem cell niches by interaction with HSC via various soluble factors. Specifically, the chemokine SDF-1 is involved in trafficking HSC in and out of the BM and plays a major role in successful HSC engraftment after transplant. Bone-lining cells produce a gradient of SDF-1, which provides a chemo-attractant signal. In turn, CXCR4, the receptor for SDF-1, navigates HSC through the blood to their specialized niche in the BM. This process is tightly regulated through the production of G-CSF, which induces the release of proteolytic enzymes such as matrix metalloproteinase 9 (MMP-9) to inactivate SDF-1 by cleaving from its N-terminus[204,205]. SDF-1 degradation in turn results in the release of HSC from the BM niche.

During hematopoietic homeostasis, most of the HSC compartment is located within specialized niches in the BM, however a small population of HSC are found circulating through the periphery. During situations of hematopoietic stress mobilization occurs and the circulating population greatly increases. The

cleavage of SDF-1 in the BM is a crucial process in breaking the anchorage of HSC from the cells of the niche[101,124,137], indicating a disruption in SDF-1 regulation could be detrimental to normal HSC homeostasis. Additionally, we know SDF-1 dependent migration is regulated by PI3K signaling[206]. Both mature and immature hematopoietic cells from SHIP$^{-/-}$ mice have increased chemotaxis toward SDF-1 *in vitro*[207]. Similarly, disruption of a single PTEN allele increases lymphocyte chemotaxis toward SDF-1[87]. Therefore, we anticipated SHIP deficiency might disrupt SDF-1 regulation of HSC *in vivo*.

Here we show that SHIP-deficient mice have significantly decreased SDF-1 levels in both blood and BM. Accordingly, we see a significant increase in G-CSF and MMP-9 levels in SHIP-deficient mice, which could be causing the SDF-1 reduction. Furthermore, G-CSF has been shown to inhibit osteoblast activity[151]. This supports our findings of a functional osteoblast impairment in SHIP-deficient mice. A recent study by a prominent Harvard group demonstrated that osteoblasts can directly modulate HSC function, implicating the importance of these bone-lining cells as HSC regulators[160]. Additionally, osteoclasts are the principal bone-resorbing cell and work in careful balance with osteoblasts in maintaining bone formation. We know SHIP regulates osteoclast precursors via the Akt pathway[208]. Therefore, SHIP is essential for normal bone homeostasis and its deficiency leads to severe osteoporosis [83]. Hyper-resorptive osteoclast behavior is consistent with our findings of immature osteoblasts, which characteristically can not support quiescent HSC[160].

Interestingly, increased G-CSF levels also correlate with increased reactive oxygen species (ROS)[209]. Accordingly, the Sharkis group has shown low levels of ROS correspond to a quiescent osteoblastic niche[210]. Combined these data suggest a requirement for the expression of SHIP for normal function of the BM niche. SHIP-deficiency profoundly alters the BM niche, disrupting HSC homeostasis, and causes a switch away from the quiescent osteoblastic niche.

Similar control of migration is seen in the normal development of megakaryocytes. Once differentiation begins, megakaryocyte precursors leave the osteoblastic BM niche and travel towards the sinusoidal vascular niche, where they release platelets into the circulation. In $SHIP^{-/-}$ mice, we see a significant increase of megakaryocytes in the spleen[180], indicating the cytokine disruption in SHIP deficiency also effects more mature hematopoietic cells.

SHIP and Peripheralized HSC

This work does not preclude SHIP from playing additional cell autonomous roles in HSC. When SHIP is lost, a portion of the HSC compartment becomes peripheralized. SHIP-deficient HSC mobilize to the blood and establish hematopoiesis elsewhere rather than returning to the BM. Similarly, patients receiving clinical G-CSF treatments to induce HSC mobilization can experience significant enlargement of the spleen[211].

Without the necessary SDF-1 signal for BM homing and retention, SHIP-deficient HSC set-up shop in a splenic niche and provide extramedullary hematopoiesis. Consistent with this, when SHIP-deficient HSC are present, we

consistently observe splenomegaly indicating SHIP expression is needed to retain HSC in the BM. The down modulation of CXCR4 expression on SHIP-deficient HSC[136] may also prevent recall of HSC to the BM osteoblastic niche[124,137]. Interestingly, in mice where osteoblasts have been ablated, the marrow no longer supports HSC and extramedullary hematopoiesis occurs[212].

In myeloid cells, SHIP functions to limit proliferation and PI(3,4,5)P3 production, which in turn regulates the activation of the serine/threonine kinase Akt[60]. Additionally, SHIP can control growth factor induced PI(3,4,5)P3 and Akt activation in mast cells, B cells[26], and neutrophils[213]. Consistent with this, SHIP-deficient mature hematopoietic cells exhibit elevated Akt levels and have an increased resistance to apoptosis. This was shown to be mediated through PI3K signaling using a potent inhibitor, wortmannin, which prevents PI(3,4,5)P3 from accumulating[36].

Here we show that SHIP has a critical responsibility in regulating PI3K signaling in HSC, thereby controlling anti-apoptotic/survival signals. It is important to note that the phospholipid regulation of Akt is complex and that Akt can interact with both PI(3,4,5)P3 and PI(3,4)P2[214]. Recent studies indicate the accumulation of PI(3,4,5)P3 is associated with Threonine 308 phosphorylation of Akt, whereas PI(3,4)P2 levels correspond with Serine 473 phosphorylation of Akt[215]. We have only seen evidence of increased Threonine 308 phosphorylation; however, it seems plausible that perturbation of several independent pathways could contribute to the ability of SHIP-deficient HSC to survive in environments

that are inhospitable for SHIP-competent HSC. Ultimately, we show that extramedullary SHIP-deficient HSC possess normal HSC activity.

Combined, these studies suggest SHIP expression is required to support normal HSC function in the BM niche; however, in the absence of SHIP normal HSC function is transferred to the periphery. Differential responsiveness to cytokines between BM and spleen derived HSC has previously been reported[216]. In embryogenesis, we see evidence of successive anatomical niches supporting different HSC functions, we speculate then that a peripheral HSC niche may exist in the spleen of SHIP-deficient animals. HSC located in this splenic niche have normal HSC function and can respond normally to chemokine signals after transplant. It will be interesting to examine CXCR4 surface expression on HSC isolated from $SHIP^{-/-}$ spleens, since it appears the splenic niche does not alter homing capacity of HSC like the $SHIP^{-/-}$ BM niche does.

Recent studies have begun to focus on the complex role of the niche in HSC regulation. One group has even generated a functionally supportive HSC niche within an ectopic site[217]. This supports our hypothesis of the existence of HSC niches in tissues outside the BM, such as the spleen. These types of studies will help elucidate a functional understanding of the niche.

We already know that when BM hematopoiesis is impaired by cancer or myeloablation, increased numbers of HSC can engage in hematopoiesis in the spleen. Therefore, it seems logical that a SHIP inhibition strategy could prove useful in temporarily relocating functional hematopoiesis to the spleen in hopes of rescuing hematopoiesis in settings of BM failure. There is certainly a concerted

effort to develop small molecule inhibitors of SHIP to temporarily render it inactive.

Scientific Significance

Inositol Phospholopid Signaling and Cancer

Cancer develops when the balance between new cell generation and cell death is lost. Therefore, the activation of survival signaling must be tightly regulated. In fact, evasion of apoptosis is considered to be a hallmark of cancer, because loss of apoptosis regulation invariably leads to tumorigenesis[218].

For over 20 years the PI3K pathway has been a focus in the cancer research field. Several components of the PI3K pathway, such as PTEN, are dysregulated in a wide spectrum of cancers. Inactivation of PTEN in BM HSC causes their rapid expansion followed by long-term decline[165]. Normal HSC become depleted and are replaced by leukemia initiating cells or cancer stem cells[165,166]. In humans, loss of PTEN function usually results in a myeloproliferative disorder and eventually leukemia[166]. Unlike PTEN, there is no explicit role for SHIP as a tumor suppressor. In fact, there is very little evidence that SHIP mutations are present in human cancers. A specific role for SHIP mutation in diseases appears limited to myeloproliferative disorders[81] and osteoporosis[83]. However, a Belgian group recently showed that SHIP has an important role in leukemic cell responses to ROS in terms of apoptosis resistance[219]. Both SHIP and SHIP2 have been shown to be constitutively phosphorylated and associated with Shc in leukemia progentitor cells[35]. Another

group discovered an inactivating mutation in the catalytic domain of SHIP within the blast cells of a patient with acute myelogenous leukemia (AML)[220]. However these findings are very preliminary and there is still no statistical evidence of a role for SHIP in leukemia.

The balance of HSC homeostasis is achieved by integrating a combination of external cues and intrinsic molecular signals. Understanding the molecular signaling relationship between self-renewal, proliferation and functional commitment is important to harnessing the full clinical potential of HSC. If we can determine key phosphorylation events responsible for influencing HSC fate choices, we can likely reveal the signaling pathways that underlie these events.

Our kinome results demonstrate the ability of peptide arrays to enhance our understanding of phosphorylation dependent signaling. This may give some understanding of the molecular changes that occur when an HSC undergoes lineage commitment and becomes irreversibly locked in its fate. However, generating pathways from lists of phosphorylated sequences will require linking these events with downstream signaling. Integration of extensive bioinformatics and improved statistical analysis is likely to improve the value of this data. Initial data from this study is promising, but array based technology provides a useful *starting point* and concrete validation will be required.

Not only is there a high therapeutic value in gaining a better understanding of HSC signaling, there are many other clinical applications for this technology. Tyrosine kinase activity is frequently deregulated in cancer and can drive tumor cells to proliferate inappropriately. By identifying the kinases involved in disrupted

signaling regulation, we can develop more effective cancer treatments. Since cancer cells share many functional properties with normal stem cells, it is crucial to understand the molecular signaling pathways involved in these properties. We need to identify ways to therapeutically target pathways that differentially impact the self-renewal of HSC and cancer cells. Implementing array based kinome technology could provide rapid elucidation of key differences.

Cancer Stem Cells

A selective growth advantage by cancer cells rapidly led to comparisons with somatic stem cells. Both cell types have self-renewal properties and can differentiate into heterogeneous populations. John Dick was first to describe the existence of "cancer stem cells" in 1994 in AML[221,222]. Since then, much work has surrounded the cancer stem cell hypothesis[165,223-225], which claims that there should be mechanistic similarities between the self-renewal and hierarchical differentiation of stem cells and cancer cells[226].

The question of whether a fraction of cancer stem cells have self-renewal potential has fundamental clinical implications, as cancer stem cells might be more resistant to chemotherapy than non-tumorogenic cancer cells. The evidence for cancer stem cells in leukemia remains convincing, however a recent publication challenges the cancer stem cell hypothesis in solid tumor models[227]. This study challenges the idea of a rare population within the tumor cells that can self-renew to continually regenerate cancer. When melanoma cells were transplanted into NOD/SCID mice lacking the IL-2 gamma receptor, as many as

one in four cells could generate a tumor, indicating self-renewing/tumorogenic cancer cells are not a rare event[227]. So is a cancer stem cell just a cancer cell? Critics of this work suggest that self-renewing cells don't need to be rare to be worthy of attention. Furthermore, perhaps most melanoma cells possess self-renewal up to a certain limit but only a few will persist. Regardless of the terminology used to describe these tumorogenic cells, the fact remains that a better understanding of the signaling and environment needed for self-renewal will help establish improved cancer treatments.

List of References

1. Lioubin MN, Algate PA, Tsai S, Carlberg K, Aebersold A, Rohrschneider LR. p150Ship, a signal transduction molecule with inositol polyphosphate-5-phosphatase activity. Genes Dev. 1996;10:1084-1095.

2. Kavanaugh WM, Pot DA, Chin SM, Deuter-Reinhard M, Jefferson AB, Norris FA, Masiarz FR, Cousens LS, Majerus PW, Williams LT. Multiple forms of an inositol polyphosphate 5-phosphatase form signaling complexes with Shc and Grb2. Curr Biol. 1996;6:438-445.

3. Damen JE, Liu L, Rosten P, Humphries RK, Jefferson AB, Majerus PW, Krystal G. The 145-kDa protein induced to associate with Shc by multiple cytokines is an inositol tetraphosphate and phosphatidylinositol 3,4,5-triphosphate 5-phosphatase. Proc Natl Acad Sci U S A. 1996;93:1689-1693.

4. Ono M, Bolland S, Tempst P, Ravetch JV. Role of the inositol phosphatase SHIP in negative regulation of the immune system by the receptor Fc(gamma)RIIB. Nature. 1996;383:263-266.

5. Kerr WG, Heller M, Herzenberg LA. Analysis of lipopolysaccharide-response genes in B-lineage cells demonstrates that they can have differentiation stage-restricted expression and contain SH2 domains. Proceedings of the National Academy of Sciences of the United States of America. 1996;93:3947-3952.

6. Damen JE, Liu L, Cutler RL, Krystal G. Erythropoietin stimulates the tyrosine phosphorylation of Shc and its association with Grb2 and a 145-Kd tyrosine phosphorylated protein. Blood. 1993;82:2296-2303.

7. Liu L, Damen JE, Cutler RL, Krystal G. Multiple cytokines stimulate the binding of a common 145-kilodalton protein to Shc at the Grb2 recognition site of Shc. Mol Cell Biol. 1994;14:6926-6935.

8. Valderrama-Carvajal H, Cocolakis E, Lacerte A, Lee EH, Krystal G, Ali S, Lebrun JJ. Activin/TGF-beta induce apoptosis through Smad-dependent expression of the lipid phosphatase SHIP. Nat Cell Biol. 2002;4:963-969.

9. Tridandapani S, Kelley T, Pradhan M, Cooney D, Justement LB, Coggeshall KM. Recruitment and phosphorylation of SH2-containing inositol phosphatase and Shc to the B-cell Fc gamma immunoreceptor tyrosine-based inhibition motif peptide motif. Mol Cell Biol. 1997;17:4305-4311.

10. Daws MR, Eriksson M, Oberg L, Ullen A, Sentman CL. H-2Dd engagement of Ly49A leads directly to Ly49A phosphorylation and recruitment of SHP1. Immunology. 1999;97:656-664.

11. Wang JW, Howson JM, Ghansah T, Desponts C, Ninos JM, May SL, Nguyen KH, Toyama-Sorimachi N, Kerr WG. Influence of SHIP on the NK repertoire and allogeneic bone marrow transplantation. Science. 2002;295:2094-2097.

12. Moran MF, Koch CA, Anderson D, Ellis C, England L, Martin GS, Pawson T. Src homology region 2 domains direct protein-protein interactions in signal transduction. Proc Natl Acad Sci U S A. 1990;87:8622-8626.

13. Ellis C, Moran M, McCormick F, Pawson T. Phosphorylation of GAP and GAP-associated proteins by transforming and mitogenic tyrosine kinases. Nature. 1990;343:377-381.

14. Liu L, Damen JE, Ware MD, Krystal G. Interleukin-3 induces the association of the inositol 5-phosphatase SHIP with SHP2. J Biol Chem. 1997;272:10998-11001.

15. Sattler M, Salgia R, Shrikhande G, Verma S, Choi JL, Rohrschneider LR, Griffin JD. The phosphatidylinositol polyphosphate 5-phosphatase SHIP and the protein tyrosine phosphatase SHP-2 form a complex in hematopoietic cells which can be regulated by BCR/ABL and growth factors. Oncogene. 1997;15:2379-2384.

16. Baran CP, Tridandapani S, Helgason CD, Humphries RK, Krystal G, Marsh CB. The inositol 5'-phosphatase SHIP-1 and the Src kinase Lyn negatively regulate macrophage colony-stimulating factor-induced Akt activity. J Biol Chem. 2003;278:38628-38636.

17. Huber M, Helgason CD, Damen JE, Scheid MP, Duronio V, Lam V, Humphries RK, Krystal G. The role of the SRC homology 2-containing inositol 5'-phosphatase in Fc epsilon R1-induced signaling. Current Topics in Microbiology & Immunology. 1999;244:29-41.

18. Burgering BM, Coffer PJ. Protein kinase B (c-Akt) in phosphatidylinositol-3-OH kinase signal transduction. Nature. 1995;376:599-602.

19. Franke TF, Yang SI, Chan TO, Datta K, Kazlauskas A, Morrison DK, Kaplan DR, Tsichlis PN. The protein kinase encoded by the Akt proto-oncogene is a target of the PDGF-activated phosphatidylinositol 3-kinase. Cell. 1995;81:727-736.

20. Yao R, Cooper GM. Requirement for phosphatidylinositol-3 kinase in the prevention of apoptosis by nerve growth factor. Science. 1995;267:2003-2006.

21. Freeburn RW, Wright KL, Burgess SJ, Astoul E, Cantrell DA, Ward SG. Evidence that SHIP-1 contributes to phosphatidylinositol 3,4,5-trisphosphate metabolism in T lymphocytes and can regulate novel phosphoinositide 3-kinase effectors. J Immunol. 2002;169:5441-5450.

22. Andjelkovic M, Maira SM, Cron P, Parker PJ, Hemmings BA. Domain swapping used to investigate the mechanism of protein kinase B regulation by 3-phosphoinositide-dependent protein kinase 1 and Ser473 kinase. Mol Cell Biol. 1999;19:5061-5072.

23. Toker A, Newton AC. Akt/protein kinase B is regulated by autophosphorylation at the hypothetical PDK-2 site. J Biol Chem. 2000;275:8271-8274.

24. Yang E, Zha J, Jockel J, Boise LH, Thompson CB, Korsmeyer SJ. Bad, a heterodimeric partner for Bcl-XL and Bcl-2, displaces Bax and promotes cell death. Cell. 1995;80:285-291.

25. Downward J. Lipid-regulated kinases: some common themes at last. Science. 1998;279:673-674.

26. Aman MJ, Lamkin TD, Okada H, Kurosaki T, Ravichandran KS. The inositol phosphatase SHIP inhibits Akt/PKB activation in B cells. J Biol Chem. 1998;273:33922-33928.

27. Carver DJ, Aman MJ, Ravichandran KS. SHIP inhibits Akt activation in B cells through regulation of Akt membrane localization. Blood. 2000;96:1449-1456.

28. Ong CJ, Ming-Lum A, Nodwell M, Ghanipour A, Yang L, Williams DE, Kim J, Demirjian L, Qasimi P, Ruschmann J, Cao LP, Ma K, Chung SW, Duronio V, Andersen RJ, Krystal G, Mui AL. Small-molecule agonists of SHIP1 inhibit the phosphoinositide 3-kinase pathway in hematopoietic cells. Blood. 2007;110:1942-1949.

29. van der Geer P, Wiley S, Gish GD, Lai VK, Stephens R, White MF, Kaplan D, Pawson T. Identification of residues that control specific binding of the Shc phosphotyrosine-binding domain to phosphotyrosine sites. Proc Natl Acad Sci U S A. 1996;93:963-968.

30. Laminet AA, Apell G, Conroy L, Kavanaugh WM. Affinity, specificity, and kinetics of the interaction of the SHC phosphotyrosine binding domain with asparagine-X-X-phosphotyrosine motifs of growth factor receptors. J Biol Chem. 1996;271:264-269.

31. van der Geer P, Pawson T. The PTB domain: a new protein module implicated in signal transduction. Trends Biochem Sci. 1995;20:277-280.

32. Carlberg K, Rohrschneider LR. Characterization of a novel tyrosine phosphorylated 100-kDa protein that binds to SHP-2 and phosphatidylinositol 3'-kinase in myeloid cells. J Biol Chem. 1997;272:15943-15950.

33. Zhang S, Broxmeyer HE. p85 subunit of PI3 kinase does not bind to human Flt3 receptor, but associates with SHP2, SHIP, and a tyrosine-phosphorylated 100-kDa protein in Flt3 ligand-stimulated hematopoietic cells. Biochem Biophys Res Commun. 1999;254:440-445.

34. Gupta N, Scharenberg AM, Fruman DA, Cantley LC, Kinet JP, Long EO. The SH2 domain-containing inositol 5'-phosphatase (SHIP) recruits the p85 subunit of phosphoinositide 3-kinase during FcgammaRIIb1-mediated inhibition of B cell receptor signaling. J Biol Chem. 1999;274:7489-7494.

35. Wisniewski D, Strife A, Swendeman S, Erdjument-Bromage H, Geromanos S, Kavanaugh WM, Tempst P, Clarkson B. A novel SH2-containing phosphatidylinositol 3,4,5-trisphosphate 5-phosphatase (SHIP2) is constitutively tyrosine phosphorylated and associated with src homologous and collagen gene (SHC) in chronic myelogenous leukemia progenitor cells. Blood. 1999;93:2707-2720.

36. Rohrschneider LR, Fuller JF, Wolf I, Liu Y, Lucas DM. Structure, function, and biology of SHIP proteins. Genes Dev. 2000;14:505-520.

37. Damen JE, Liu L, Ware MD, Ermolaeva M, Majerus PW, Krystal G. Multiple forms of the SH2-containing inositol phosphatase, SHIP, are generated by C-terminal truncation. Blood. 1998;92:1199-1205.

38. Lucas DM, Rohrschneider LR. A novel spliced form of SH2-containing inositol phosphatase is expressed during myeloid development. Blood. 1999;93:1922-1933.

39. Krystal G, Damen JE, Helgason CD, Huber M, Hughes MR, Kalesnikoff J, Lam V, Rosten P, Ware MD, Yew S, Humphries RK. SHIPs ahoy. Int J Biochem Cell Biol. 1999;31:1007-1010.

40. Horn S, Meyer J, Heukeshoven J, Fehse B, Schulze C, Li S, Frey J, Poll S, Stocking C, Jucker M. The inositol 5-phosphatase SHIP is expressed as 145 and 135 kDa proteins in blood and bone marrow cells in vivo, whereas carboxyl-truncated forms of SHIP are generated by proteolytic cleavage in vitro. Leukemia. 2001;15:112-120.

41. Tu Z, Ninos JM, Ma Z, Wang JW, Lemos MP, Desponts C, Ghansah T, Howson JM, Kerr WG. Embryonic and hematopoietic stem cells express a novel SH2-containing inositol 5'-phosphatase isoform that partners with the Grb2 adapter protein. Blood. 2001;98:2028-2038.

42. Rohrschneider LR, Custodio JM, Anderson TA, Miller CP, Gu H. The intron 5/6 promoter region of the ship1 gene regulates expression in stem/progenitor cells of the mouse embryo. Dev Biol. 2005;283:503-521.

43. Majerus PW, Kisseleva MV, Norris FA. The role of phosphatases in inositol signaling reactions. Journal of Biological Chemistry. 1999;274:10669-10672.

44. Hejna JA, Saito H, Merkens LS, Tittle TV, Jakobs PM, Whitney MA, Grompe M, Friedberg AS, Moses RE. Cloning and characterization of a human cDNA (INPPL1) sharing homology with inositol polyphosphate phosphatases. Genomics. 1995;29:285-287.

45. Pesesse X, Deleu S, De Smedt F, Drayer L, Erneux C. Identification of a second SH2-domain-containing protein closely related to the phosphatidylinositol polyphosphate 5-phosphatase SHIP. Biochem Biophys Res Commun. 1997;239:697-700.

46. Liu Q, Dumont DJ. Molecular cloning and chromosomal localization in human and mouse of the SH2-containing inositol phosphatase, INPP5D (SHIP). Amgen EST Program. Genomics. 1997;39:109-112.

47. Bruyns C, Pesesse X, Moreau C, Blero D, Erneux C. The two SH2-domain-containing inositol 5-phosphatases SHIP1 and SHIP2 are coexpressed in human T lymphocytes. Biol Chem. 1999;380:969-974.

48. Muraille E, Pesesse X, Kuntz C, Erneux C. Distribution of the src-homology-2-domain-containing inositol 5-phosphatase SHIP-2 in both non-haemopoietic and haemopoietic cells and possible involvement of SHIP-2 in negative signalling of B-cells. Biochem J. 1999;342 Pt 3:697-705.

49. Giuriato S, Pesesse X, Bodin S, Sasaki T, Viala C, Marion E, Penninger J, Schurmans S, Erneux C, Payrastre B. SH2-containing inositol 5-phosphatases 1 and 2 in blood platelets: their interactions and roles in the control of phosphatidylinositol 3,4,5-trisphosphate levels. Biochem J. 2003;376:199-207.

50. Sleeman MW, Wortley KE, Lai KM, Gowen LC, Kintner J, Kline WO, Garcia K, Stitt TN, Yancopoulos GD, Wiegand SJ, Glass DJ. Absence of the lipid phosphatase SHIP2 confers resistance to dietary obesity. Nat Med. 2005;11:199-205.

51. Stambolic V, Suzuki A, de la Pompa JL, Brothers GM, Mirtsos C, Sasaki T, Ruland J, Penninger JM, Siderovski DP, Mak TW. Negative regulation of PKB/Akt-dependent cell survival by the tumor suppressor PTEN. Cell. 1998;95:29-39.

52. Kishimoto H, Hamada K, Saunders M, Backman S, Sasaki T, Nakano T, Mak TW, Suzuki A. Physiological functions of Pten in mouse tissues. Cell Struct Funct. 2003;28:11-21.

53. Cantley LC, Neel BG. New insights into tumor suppression: PTEN suppresses tumor formation by restraining the phosphoinositide 3-kinase/AKT pathway. Proc Natl Acad Sci U S A. 1999;96:4240-4245.

54. Suzuki A, de la Pompa JL, Stambolic V, Elia AJ, Sasaki T, del Barco Barrantes I, Ho A, Wakeham A, Itie A, Khoo W, Fukumoto M, Mak TW. High cancer susceptibility and embryonic lethality associated with mutation of the PTEN tumor suppressor gene in mice. Curr Biol. 1998;8:1169-1178.

55. Krystal G. Lipid phosphatases in the immune system [In Process Citation]. Semin Immunol. 2000;12:397-403.

56. Rameh LE, Cantley LC. The role of phosphoinositide 3-kinase lipid products in cell function. J Biol Chem. 1999;274:8347-8350.

57. Huber M, Helgason CD, Damen JE, Scheid M, Duronio V, Liu L, Ware MD, Humphries RK, Krystal G. The role of SHIP in growth factor induced signalling. Prog Biophys Mol Biol. 1999;71:423-434.

58. Maehama T, Dixon JE. The tumor suppressor, PTEN/MMAC1, dephosphorylates the lipid second messenger, phosphatidylinositol 3,4,5-trisphosphate. J Biol Chem. 1998;273:13375-13378.

59. Matsuguchi T, Salgia R, Hallek M, Eder M, Druker B, Ernst TJ, Griffin JD. Shc phosphorylation in myeloid cells is regulated by granulocyte macrophage colony-stimulating factor, interleukin-3, and steel factor and is constitutively increased by p210BCR/ABL. J Biol Chem. 1994;269:5016-5021.

60. Liu Q, Sasaki T, Kozieradzki I, Wakeham A, Itie A, Dumont DJ, Penninger JM. SHIP is a negative regulator of growth factor receptor-mediated PKB/Akt activation and myeloid cell survival. Genes Dev. 1999;13:786-791.

61. Hunter MG, Avalos BR. Phosphatidylinositol 3'-kinase and SH2-containing inositol phosphatase (SHIP) are recruited by distinct positive and negative growth-regulatory domains in the granulocyte colony-stimulating factor receptor. J Immunol. 1998;160:4979-4987.

62. Hunter MG, Jacob A, O'Donnell L C, Agler A, Druhan LJ, Coggeshall KM, Avalos BR. Loss of SHIP and CIS recruitment to the granulocyte colony-stimulating factor receptor contribute to hyperproliferative responses in severe congenital neutropenia/acute myelogenous leukemia. J Immunol. 2004;173:5036-5045.

63. Drachman JG, Kaushansky K. Dissecting the thrombopoietin receptor: functional elements of the Mpl cytoplasmic domain. Proc Natl Acad Sci U S A. 1997;94:2350-2355.

64. Drachman JG, Griffin JD, Kaushansky K. The c-Mpl ligand (thrombopoietin) stimulates tyrosine phosphorylation of Jak2, Shc, and c-Mpl. J Biol Chem. 1995;270:4979-4982.

65. Marchetto S, Fournier E, Beslu N, Aurran-Schleinitz T, Dubreuil P, Borg JP, Birnbaum D, Rosnet O. SHC and SHIP phosphorylation and interaction in response to activation of the FLT3 receptor. Leukemia. 1999;13:1374-1382.

66. Zamorano J, Keegan AD. Regulation of apoptosis by tyrosine-containing domains of IL-4R alpha: Y497 and Y713, but not the STAT6-docking tyrosines, signal protection from apoptosis. J Immunol. 1998;161:859-867.

67. Jiang H, Harris MB, Rothman P. IL-4/IL-13 signaling beyond JAK/STAT. J Allergy Clin Immunol. 2000;105:1063-1070.

68. Chernock RD, Cherla RP, Ganju RK. SHP2 and cbl participate in alpha-chemokine receptor CXCR4-mediated signaling pathways. Blood. 2001;97:608-615.

69. Fong DC, Malbec O, Arock M, Cambier JC, Fridman WH, Daeron M. Selective in vivo recruitment of the phosphatidylinositol phosphatase SHIP by phosphorylated Fc gammaRIIB during negative regulation of IgE-dependent mouse mast cell activation. Immunology Letters. 1996;54:83-91.

70. D'Ambrosio D, Fong DC, Cambier JC. The SHIP phosphatase becomes associated with Fc gammaRIIB1 and is tyrosine phosphorylated during 'negative' signaling. Immunology Letters. 1996;54:77-82.

71. Smit L, de Vries-Smits AM, Bos JL, Borst J. B cell antigen receptor stimulation induces formation of a Shc-Grb2 complex containing multiple tyrosine-phosphorylated proteins. J Biol Chem. 1994;269:20209-20212.

72. Saxton TM, van Oostveen I, Bowtell D, Aebersold R, Gold MR. B cell antigen receptor cross-linking induces phosphorylation of the p21ras oncoprotein activators SHC and mSOS1 as well as assembly of complexes containing SHC, GRB-2, mSOS1, and a 145-kDa tyrosine-phosphorylated protein. Journal of Immunology. 1994;153:623-636.

73. Chacko GW, Tridandapani S, Damen JE, Liu L, Krystal G, Coggeshall KM. Negative signaling in B lymphocytes induces tyrosine phosphorylation of the 145-kDa inositol polyphosphate 5-phosphatase, SHIP. J Immunol. 1996;157:2234-2238.

74. Ravichandran KS, Lee KK, Songyang Z, Cantley LC, Burn P, Burakoff SJ. Interaction of Shc with the zeta chain of the T cell receptor upon T cell activation. Science. 1993;262:902-905.

75. Phee H, Jacob A, Coggeshall KM. Enzymatic activity of the Src homology 2 domain-containing inositol phosphatase is regulated by a plasma membrane location. J Biol Chem. 2000;275:19090-19097.

76. Sly LM, Rauh MJ, Kalesnikoff J, Buchse T, Krystal G. SHIP, SHIP2, and PTEN activities are regulated in vivo by modulation of their protein levels: SHIP is up-regulated in macrophages and mast cells by lipopolysaccharide. Exp Hematol. 2003;31:1170-1181.

77. Bolland S, Pearse RN, Kurosaki T, Ravetch JV. SHIP modulates immune receptor responses by regulating membrane association of Btk. Immunity. 1998;8:509-516.

78. Scharenberg AM, El-Hillal O, Fruman DA, Beitz LO, Li Z, Lin S, Gout I, Cantley LC, Rawlings DJ, Kinet JP. Phosphatidylinositol-3,4,5-trisphosphate (PtdIns-3,4,5-P3)/Tec kinase-dependent calcium signaling pathway: a target for SHIP-mediated inhibitory signals. Embo J. 1998;17:1961-1972.

79. Tridandapani S, Wang Y, Marsh CB, Anderson CL. Src homology 2 domain-containing inositol polyphosphate phosphatase regulates NF-kappa B-mediated gene transcription by phagocytic Fc gamma Rs in human myeloid cells. J Immunol. 2002;169:4370-4378.

80. Kimura T, Sakamoto H, Appella E, Siraganian RP. The negative signaling molecule SH2 domain-containing inositol-polyphosphate 5-phosphatase (SHIP) binds to the tyrosine-phosphorylated beta subunit of the high affinity IgE receptor. J Biol Chem. 1997;272:13991-13996.

81. Helgason CD, Damen JE, Rosten P, Grewal R, Sorensen P, Chappel SM, Borowski A, Jirik F, Krystal G, Humphries RK. Targeted disruption of SHIP leads to hemopoietic perturbations, lung pathology, and a shortened life span. Genes Dev. 1998;12:1610-1620.

82. Karlsson MC, Guinamard R, Bolland S, Sankala M, Steinman RM, Ravetch JV. Macrophages control the retention and trafficking of B lymphocytes in the splenic marginal zone. J Exp Med. 2003;198:333-340.

83. Takeshita S, Namba N, Zhao JJ, Jiang Y, Genant HK, Silva MJ, Brodt MD, Helgason CD, Kalesnikoff J, Rauh MJ, Humphries RK, Krystal G, Teitelbaum SL, Ross FP. SHIP-deficient mice are severely osteoporotic due to increased numbers of hyper-resorptive osteoclasts. Nat Med. 2002;8:943-949.

84. Huber M, Helgason CD, Damen JE, Liu L, Humphries RK, Krystal G. The src homology 2-containing inositol phosphatase (SHIP) is the gatekeeper of mast cell degranulation. Proc Natl Acad Sci U S A. 1998;95:11330-11335.

85. Ghansah T, Paraiso KH, Highfill S, Desponts C, May S, McIntosh JK, Wang JW, Ninos J, Brayer J, Cheng F, Sotomayor E, Kerr WG. Expansion of myeloid suppressor cells in SHIP-deficient mice represses allogeneic T cell responses. J Immunol. 2004;173:7324-7330.

86. Paraiso KH, Ghansah T, Costello A, Engelman RW, Kerr WG. Induced SHIP deficiency expands myeloid regulatory cells and abrogates graft-versus-host disease. J Immunol. 2007;178:2893-2900.

87. Fox JA, Ung K, Tanlimco SG, Jirik FR. Disruption of a single Pten allele augments the chemotactic response of B lymphocytes to stromal cell-derived factor-1. J Immunol. 2002;169:49-54.

88. Kuhn R, Schwenk F, Aguet M, Rajewsky K. Inducible gene targeting in mice. Science. 1995;269:1427-1429.

89. Jacobson LO, Marks EK, et al. The role of the spleen in radiation injury. Proc Soc Exp Biol Med. 1949;70:740-742.

90. Jacobson LO, Marks EK, et al. The effects of nitrogen mustard on induced erythroblastic hyperplasia in rabbits. J Lab Clin Med. 1949;34:902-924.

91. Jacobson LO, Simmons EL, Marks EK, Robson MJ, Bethard WF, Gaston EO. The role of the spleen in radiation injury and recovery. J Lab Clin Med. 1950;35:746-770.

92. Lorenz E, Uphoff D, Reid TR, Shelton E. Modification of irradiation injury in mice and guinea pigs by bone marrow injections. J Natl Cancer Inst. 1951;12:197-201.

93. Thomas ED, Blume KG. Historical markers in the development of allogeneic hematopoietic cell transplantation. Biol Blood Marrow Transplant. 1999;5:341-346.

94. Mikkola HK, Orkin SH. The journey of developing hematopoietic stem cells. Development. 2006;133:3733-3744.

95. McGrath KE, Palis J. Hematopoiesis in the yolk sac: more than meets the eye. Exp Hematol. 2005;33:1021-1028.

96. Palis J, Robertson S, Kennedy M, Wall C, Keller G. Development of erythroid and myeloid progenitors in the yolk sac and embryo proper of the mouse. Development. 1999;126:5073-5084.

97. Cumano A, Ferraz JC, Klaine M, Di Santo JP, Godin I. Intraembryonic, but not yolk sac hematopoietic precursors, isolated before circulation, provide long-term multilineage reconstitution. Immunity. 2001;15:477-485.

98. Johnson GR, Moore MA. Role of stem cell migration in initiation of mouse foetal liver haemopoiesis. Nature. 1975;258:726-728.

99. Morrison SJ, Hemmati HD, Wandycz AM, Weissman IL. The purification and characterization of fetal liver hematopoietic stem cells. Proc Natl Acad Sci U S A. 1995;92:10302-10306.

100. Christensen JL, Wright DE, Wagers AJ, Weissman IL. Circulation and chemotaxis of fetal hematopoietic stem cells. PLoS Biol. 2004;2:E75.

101. Ara T, Tokoyoda K, Sugiyama T, Egawa T, Kawabata K, Nagasawa T. Long-term hematopoietic stem cells require stromal cell-derived factor-1 for colonizing bone marrow during ontogeny. Immunity. 2003;19:257-267.

102. Wright DE, Wagers AJ, Gulati AP, Johnson FL, Weissman IL. Physiological migration of hematopoietic stem and progenitor cells. Science. 2001;294:1933-1936.

103. Gekas C, Dieterlen-Lievre F, Orkin SH, Mikkola HK. The placenta is a niche for hematopoietic stem cells. Dev Cell. 2005;8:365-375.

104. Medvinsky A, Dzierzak E. Definitive hematopoiesis is autonomously initiated by the AGM region. Cell. 1996;86:897-906.

105. Muller AM, Medvinsky A, Strouboulis J, Grosveld F, Dzierzak E. Development of hematopoietic stem cell activity in the mouse embryo. Immunity. 1994;1:291-301.

106. Choi K. The hemangioblast: a common progenitor of hematopoietic and endothelial cells. J Hematother Stem Cell Res. 2002;11:91-101.

107. Weissman IL, Shizuru JA. The origins of the identification and isolation of hematopoietic stem cells, and their capability to induce donor-specific transplantation tolerance and treat autoimmune diseases. Blood. 2008;112:3543-3553.

108. Luc S, Buza-Vidas N, Jacobsen SE. Delineating the cellular pathways of hematopoietic lineage commitment. Semin Immunol. 2008;20:213-220.

109. Passegue E, Wagers AJ, Giuriato S, Anderson WC, Weissman IL. Global analysis of proliferation and cell cycle gene expression in the regulation of hematopoietic stem and progenitor cell fates. J Exp Med. 2005;202:1599-1611.

110. Schofield R. The relationship between the spleen colony-forming cell and the haemopoietic stem cell. Blood Cells. 1978;4:7-25.

111. Spradling A, Drummond-Barbosa D, Kai T. Stem cells find their niche. Nature. 2001;414:98-104.

112. Fuchs E, Tumbar T, Guasch G. Socializing with the neighbors: stem cells and their niche. Cell. 2004;116:769-778.

113. Li L, Xie T. Stem cell niche: structure and function. Annu Rev Cell Dev Biol. 2005;21:605-631.

114. Miller CL, Eaves CJ. Expansion in vitro of adult murine hematopoietic stem cells with transplantable lympho-myeloid reconstituting ability. Proc Natl Acad Sci U S A. 1997;94:13648-13653.

115. Aiuti A, Webb IJ, Bleul C, Springer T, Gutierrez-Ramos JC. The chemokine SDF-1 is a chemoattractant for human CD34+ hematopoietic progenitor cells and provides a new mechanism to explain the mobilization of CD34+ progenitors to peripheral blood. J Exp Med. 1997;185:111-120.

116. Peled A, Petit I, Kollet O, Magid M, Ponomaryov T, Byk T, Nagler A, Ben-Hur H, Many A, Shultz L, Lider O, Alon R, Zipori D, Lapidot T. Dependence of human stem cell engraftment and repopulation of NOD/SCID mice on CXCR4. Science. 1999;283:845-848.

117. Petit I, Szyper-Kravitz M, Nagler A, Lahav M, Peled A, Habler L, Ponomaryov T, Taichman RS, Arenzana-Seisdedos F, Fujii N, Sandbank J, Zipori D, Lapidot T. G-CSF induces stem cell mobilization by decreasing bone marrow SDF-1 and up-regulating CXCR4. Nat Immunol. 2002;3:687-694.

118. Kiel MJ, Morrison SJ. Uncertainty in the niches that maintain haematopoietic stem cells. Nat Rev Immunol. 2008;8:290-301.

119. Kiel MJ, Morrison SJ. Maintaining hematopoietic stem cells in the vascular niche. Immunity. 2006;25:862-864.

120. Stier S, Ko Y, Forkert R, Lutz C, Neuhaus T, Grunewald E, Cheng T, Dombkowski D, Calvi LM, Rittling SR, Scadden DT. Osteopontin is a hematopoietic stem cell niche component that negatively regulates stem cell pool size. J Exp Med. 2005;201:1781-1791.

121. Nilsson SK, Johnston HM, Whitty GA, Williams B, Webb RJ, Denhardt DT, Bertoncello I, Bendall LJ, Simmons PJ, Haylock DN. Osteopontin, a key component of the hematopoietic stem cell niche and regulator of primitive hematopoietic progenitor cells. Blood. 2005;106:1232-1239.

122. Yoshihara H, Arai F, Hosokawa K, Hagiwara T, Takubo K, Nakamura Y, Gomei Y, Iwasaki H, Matsuoka S, Miyamoto K, Miyazaki H, Takahashi T, Suda T. Thrombopoietin/MPL signaling regulates hematopoietic stem cell quiescence and interaction with the osteoblastic niche. Cell Stem Cell. 2007;1:685-697.

123. Arai F, Hirao A, Ohmura M, Sato H, Matsuoka S, Takubo K, Ito K, Koh GY, Suda T. Tie2/angiopoietin-1 signaling regulates hematopoietic stem cell quiescence in the bone marrow niche. Cell. 2004;118:149-161.

124. Calvi LM, Adams GB, Weibrecht KW, Weber JM, Olson DP, Knight MC, Martin RP, Schipani E, Divieti P, Bringhurst FR, Milner LA, Kronenberg HM, Scadden DT. Osteoblastic cells regulate the haematopoietic stem cell niche. Nature. 2003;425:841-846.

125. Kiel MJ, Acar M, Radice GL, Morrison SJ. Hematopoietic Stem Cells Do Not Depend on N-Cadherin to Regulate Their Maintenance. Cell Stem Cell. 2008.

126. Adams GB, Scadden DT. The hematopoietic stem cell in its place. Nat Immunol. 2006;7:333-337.

127. Suda T, Arai F, Hirao A. Hematopoietic stem cells and their niche. Trends Immunol. 2005;26:426-433.

128. Ottersbach K, Dzierzak E. The murine placenta contains hematopoietic stem cells within the vascular labyrinth region. Dev Cell. 2005;8:377-387.

129. Kiel MJ, Yilmaz OH, Iwashita T, Yilmaz OH, Terhorst C, Morrison SJ. SLAM family receptors distinguish hematopoietic stem and progenitor cells and reveal endothelial niches for stem cells. Cell. 2005;121:1109-1121.

130. Laterveer L, Lindley IJ, Hamilton MS, Willemze R, Fibbe WE. Interleukin-8 induces rapid mobilization of hematopoietic stem cells with radioprotective capacity and long-term myelolymphoid repopulating ability. Blood. 1995;85:2269-2275.

131. Lo Celso C, Fleming HE, Wu JW, Zhao CX, Miake-Lye S, Fujisaki J, Cote D, Rowe DW, Lin CP, Scadden DT. Live-animal tracking of individual haematopoietic stem/progenitor cells in their niche. Nature. 2009;457:92-96.

132. Xie Y, Yin T, Wiegraebe W, He XC, Miller D, Stark D, Perko K, Alexander R, Schwartz J, Grindley JC, Park J, Haug JS, Wunderlich JP, Li H, Zhang S, Johnson T, Feldman RA, Li L. Detection of functional haematopoietic stem cell niche using real-time imaging. Nature. 2009;457:97-101.

133. Harrison DE. Competitive repopulation: a new assay for long-term stem cell functional capacity. Blood. 1980;55:77-81.

134. Jordan CT, Lemischka IR. Clonal and systemic analysis of long-term hematopoiesis in the mouse. Genes Dev. 1990;4:220-232.

135. Domen J, Cheshier SH, Weissman IL. The role of apoptosis in the regulation of hematopoietic stem cells: Overexpression of Bcl-2 increases both their number and repopulation potential. J Exp Med. 2000;191:253-264.

136. Desponts C, Hazen AL, Paraiso KH, Kerr WG. SHIP deficiency enhances HSC proliferation and survival but compromises homing and repopulation. Blood. 2006;107:4338-4345.

137. Zhang J, Niu C, Ye L, Huang H, He X, Tong WG, Ross J, Haug J, Johnson T, Feng JQ, Harris S, Wiedemann LM, Mishina Y, Li L. Identification of the haematopoietic stem cell niche and control of the niche size. Nature. 2003;425:836-841.

138. Kerr JF, Wyllie AH, Currie AR. Apoptosis: a basic biological phenomenon with wide-ranging implications in tissue kinetics. British Journal of Cancer. 1972;26:239-257.

139. Desponts C, Ninos JM, Kerr WG. s-SHIP associates with receptor complexes essential for pluripotent stem cell growth and survival. Stem Cells Dev. 2006;15:641-646.

140. Helgason CD, Antonchuk J, Bodner C, Humphries RK. Homeostasis and regeneration of the hematopoietic stem cell pool are altered in SHIP-deficient mice. Blood. 2003;102:3541-3547.

141. Geier SJ, Algate PA, Carlberg K, Flowers D, Friedman C, Trask B, Rohrschneider LR. The human SHIP gene is differentially expressed in cell lineages of the bone marrow and blood. Blood. 1997;89:1876-1885.

142. Zippo A, De Robertis A, Bardelli M, Galvagni F, Oliviero S. Identification of Flk-1 target genes in vasculogenesis: Pim-1 is required for endothelial and mural cell differentiation in vitro. Blood. 2004;103:4536-4544.

143. Sattler M, Verma S, Pride YB, Salgia R, Rohrschneider LR, Griffin JD. SHIP1, an SH2 domain containing polyinositol-5-phosphatase, regulates migration through two critical tyrosine residues and forms a novel signaling complex with DOK1 and CRKL. J Biol Chem. 2001;276:2451-2458.

144. Liu Y, Jenkins B, Shin JL, Rohrschneider LR. Scaffolding protein Gab2 mediates differentiation signaling downstream of Fms receptor tyrosine kinase. Mol Cell Biol. 2001;21:3047-3056.

145. Wahle JA, Paraiso KH, Costello AL, Goll EL, Sentman CL, Kerr WG. Cutting edge: dominance by an MHC-independent inhibitory receptor compromises NK killing of complex targets. J Immunol. 2006;176:7165-7169.

146. Brauweiler A, Tamir I, Dal Porto J, Benschop RJ, Helgason CD, Humphries RK, Freed JH, Cambier JC. Differential regulation of B cell development, activation, and death by the src homology 2 domain-containing 5' inositol phosphatase (SHIP). J Exp Med. 2000;191:1545-1554.

147. Helgason CD, Kalberer CP, Damen JE, Chappel SM, Pineault N, Krystal G, Humphries RK. A dual role for Src homology 2 domain-containing inositol-5-phosphatase (SHIP) in immunity: aberrant development and enhanced function of b lymphocytes in ship -/- mice. J Exp Med. 2000;191:781-794.

148. Sly LM, Rauh MJ, Kalesnikoff J, Song CH, Krystal G. LPS-induced upregulation of SHIP is essential for endotoxin tolerance. Immunity. 2004;21:227-239.

149. Huber M, Helgason CD, Scheid MP, Duronio V, Humphries RK, Krystal G. Targeted disruption of SHIP leads to Steel factor-induced degranulation of mast cells. Embo J. 1998;17:7311-7319.

150. Cancelas JA, Lee AW, Prabhakar R, Stringer KF, Zheng Y, Williams DA. Rac GTPases differentially integrate signals regulating hematopoietic stem cell localization. Nat Med. 2005;11:886-891.

151. Semerad CL, Christopher MJ, Liu F, Short B, Simmons PJ, Winkler I, Levesque JP, Chappel J, Ross FP, Link DC. G-CSF potently inhibits osteoblast activity and CXCL12 mRNA expression in the bone marrow. Blood. 2005;106:3020-3027.

152. Ware MD, Rosten P, Damen JE, Liu L, Humphries RK, Krystal G. Cloning and characterization of human SHIP, the 145-kD inositol 5-phosphatase that associates with SHC after cytokine stimulation. Blood. 1996;88:2833-2840.

153. Sudres M, Norol F, Trenado A, Gregoire S, Charlotte F, Levacher B, Lataillade JJ, Bourin P, Holy X, Vernant JP, Klatzmann D, Cohen JL. Bone marrow mesenchymal stem cells suppress lymphocyte proliferation in vitro but fail to prevent graft-versus-host disease in mice. J Immunol. 2006;176:7761-7767.

154. Anjos-Afonso F, Bonnet D. Nonhematopoietic/endothelial SSEA-1+ cells define the most primitive progenitors in the adult murine bone marrow mesenchymal compartment. Blood. 2007;109:1298-1306.

155. Miyake K, Medina K, Ishihara K, Kimoto M, Auerbach R, Kincade PW. A VCAM-like adhesion molecule on murine bone marrow stromal cells mediates binding of lymphocyte precursors in culture. J Cell Biol. 1991;114:557-565.

156. Quarles LD, Yohay DA, Lever LW, Caton R, Wenstrup RJ. Distinct proliferative and differentiated stages of murine MC3T3-E1 cells in culture: an in vitro model of osteoblast development. J Bone Miner Res. 1992;7:683-692.

157. Raouf A, Seth A. Ets transcription factors and targets in osteogenesis. Oncogene. 2000;19:6455-6463.

158. Vary CP, Li V, Raouf A, Kitching R, Kola I, Franceschi C, Venanzoni M, Seth A. Involvement of Ets transcription factors and targets in osteoblast differentiation and matrix mineralization. Exp Cell Res. 2000;257:213-222.

159. Stewart K, Walsh S, Screen J, Jefferiss CM, Chainey J, Jordan GR, Beresford JN. Further characterization of cells expressing STRO-1 in cultures of adult human bone marrow stromal cells. J Bone Miner Res. 1999;14:1345-1356.

160. Mayack SR, Wagers AJ. Osteolineage niche cells initiate hematopoietic stem cell mobilization. Blood. 2008;112:519-531.

161. Bradford GB, Williams B, Rossi R, Bertoncello I. Quiescence, cycling, and turnover in the primitive hematopoietic stem cell compartment. Exp Hematol. 1997;25:445-453.

162. Fleming WH, Alpern EJ, Uchida N, Ikuta K, Spangrude GJ, Weissman IL. Functional heterogeneity is associated with the cell cycle status of murine hematopoietic stem cells. J Cell Biol. 1993;122:897-902.

163. Glimm H, Oh IH, Eaves CJ. Human hematopoietic stem cells stimulated to proliferate in vitro lose engraftment potential during their S/G(2)/M transit and do not reenter G(0). Blood. 2000;96:4185-4193.

164. Carlesso N, Aster JC, Sklar J, Scadden DT. Notch1-induced delay of human hematopoietic progenitor cell differentiation is associated with altered cell cycle kinetics. Blood. 1999;93:838-848.

165. Yilmaz OH, Valdez R, Theisen BK, Guo W, Ferguson DO, Wu H, Morrison SJ. Pten dependence distinguishes haematopoietic stem cells from leukaemia-initiating cells. Nature. 2006;441:475-482.

166. Zhang J, Grindley JC, Yin T, Jayasinghe S, He XC, Ross JT, Haug JS, Rupp D, Porter-Westpfahl KS, Wiedemann LM, Wu H, Li L. PTEN maintains haematopoietic stem cells and acts in lineage choice and leukaemia prevention. Nature. 2006;441:518-522.

167. Harrison DE, Jordan CT, Zhong RK, Astle CM. Primitive hemopoietic stem cells: direct assay of most productive populations by competitive repopulation with simple binomial, correlation and covariance calculations. Experimental Hematology. 1993;21:206-219.

168. Methods in Bone Biology. London: Chapman and Hall; 1998.

169. Bakker A, Klein-Nulend J. Osteoblast isolation from murine calvariae and long bones. Methods Mol Med. 2003;80:19-28.

170. Cantley LC. The phosphoinositide 3-kinase pathway. Science. 2002;296:1655-1657.

171. Zhang X, Majerus PW. Phosphatidylinositol signalling reactions. Seminars in Cell & Developmental Biology. 1998;9:153-160.

172. Hazen AL, Smith MJ, Desponts C, Winter O, Moser K, Kerr WG. SHIP is required for a functional hematopoietic stem cell niche. Blood. 2008.

173. Wahle JA, Paraiso KH, Kendig RD, Lawrence HR, Chen L, Wu J, Kerr WG. Inappropriate Recruitment and Activity by the Src Homology Region 2 Domain-Containing Phosphatase 1 (SHP1) Is Responsible for Receptor Dominance in the SHIP-Deficient NK Cell. J Immunol. 2007;179:8009-8015.

174. Brauweiler AM, Tamir I, Cambier JC. Bilevel control of B-cell activation by the inositol 5-phosphatase SHIP. Immunol Rev. 2000;176:69-74.

175. Rauh MJ, Ho V, Pereira C, Sham A, Sly LM, Lam V, Huxham L, Minchinton AI, Mui A, Krystal G. SHIP represses the generation of alternatively activated macrophages. Immunity. 2005;23:361-374.

176. Collazo MM, Wood D, Paraiso KH, Lund E, Engelman RW, Le CT, Stauch D, Kotsch K, Kerr WG. SHIP limits immunoregulatory capacity in the T cell compartment. Blood. 2009.

177. Kiel MJ, Iwashita T, Yilmaz OH, Morrison SJ. Spatial differences in hematopoiesis but not in stem cells indicate a lack of regional patterning in definitive hematopoietic stem cells. Dev Biol. 2005;283:29-39.

178. Yilmaz OH, Kiel MJ, Morrison SJ. SLAM family markers are conserved among hematopoietic stem cells from old and reconstituted mice and markedly increase their purity. Blood. 2006;107:924-930.

179. Mizukami T, Hamaguchi I, Takizawa K, Kuramitsu M, Momose H, Naito S, Masumi A, Okada S, Yamaguchi K. Identification and Characterization of a Hematopoietic Stem Cell Niche in Spleen. ASH Annual Meeting Abstracts. 2008;112:1371-.

180. Perez LE, Desponts C, Parquet N, Kerr WG. SH2-inositol phosphatase 1 negatively influences early megakaryocyte progenitors. PLoS ONE. 2008;3:e3565.

181. Carninci P, Kasukawa T, Katayama S, Gough J, Frith MC, Maeda N, Oyama R, Ravasi T, Lenhard B, Wells C, Kodzius R, Shimokawa K, Bajic VB, Brenner SE, Batalov S, Forrest AR, Zavolan M, Davis MJ, Wilming LG, Aidinis V, Allen JE, Ambesi-Impiombato A, Apweiler R, Aturaliya RN, Bailey TL, Bansal M, Baxter L, Beisel KW, Bersano T, Bono H, Chalk AM, Chiu KP, Choudhary V, Christoffels A, Clutterbuck DR, Crowe ML, Dalla E, Dalrymple BP, de Bono B, Della Gatta G, di Bernardo D, Down T, Engstrom P, Fagiolini M, Faulkner G, Fletcher CF, Fukushima T, Furuno M, Futaki S, Gariboldi M, Georgii-Hemming P, Gingeras TR, Gojobori T, Green RE, Gustincich S, Harbers M, Hayashi Y, Hensch TK, Hirokawa N, Hill D, Huminiecki L, Iacono M, Ikeo K, Iwama A, Ishikawa T, Jakt M, Kanapin A, Katoh M, Kawasawa Y, Kelso J, Kitamura H, Kitano H, Kollias G, Krishnan SP, Kruger A, Kummerfeld SK, Kurochkin IV, Lareau LF, Lazarevic D, Lipovich L, Liu J, Liuni S, McWilliam S, Madan Babu M, Madera M, Marchionni L, Matsuda H, Matsuzawa S, Miki H, Mignone F, Miyake S, Morris K, Mottagui-Tabar S, Mulder N, Nakano N, Nakauchi H, Ng P, Nilsson R, Nishiguchi S, Nishikawa S, Nori F, Ohara O, Okazaki Y, Orlando V, Pang KC, Pavan WJ, Pavesi G, Pesole G, Petrovsky N, Piazza S, Reed J, Reid JF, Ring BZ, Ringwald M, Rost B, Ruan Y, Salzberg SL, Sandelin A, Schneider C, Schonbach C, Sekiguchi K, Semple CA, Seno S, Sessa L, Sheng Y, Shibata Y, Shimada H, Shimada K, Silva D, Sinclair B, Sperling S, Stupka E, Sugiura K, Sultana R, Takenaka Y, Taki K, Tammoja K, Tan SL, Tang S, Taylor MS, Tegner J, Teichmann SA, Ueda HR, van Nimwegen E, Verardo R, Wei CL, Yagi K, Yamanishi H, Zabarovsky E, Zhu S, Zimmer A, Hide W, Bult C, Grimmond SM, Teasdale RD, Liu ET, Brusic V, Quackenbush J, Wahlestedt C, Mattick JS, Hume DA, Kai C, Sasaki D, Tomaru Y, Fukuda S, Kanamori-Katayama M, Suzuki M, Aoki J, Arakawa T, Iida J, Imamura K, Itoh M, Kato T, Kawaji H, Kawagashira N, Kawashima T, Kojima M, Kondo S, Konno H, Nakano K, Ninomiya N, Nishio T, Okada M, Plessy C, Shibata K, Shiraki T, Suzuki S, Tagami M, Waki K, Watahiki A, Okamura-Oho Y, Suzuki H, Kawai J, Hayashizaki Y. The transcriptional landscape of the mammalian genome. Science. 2005;309:1559-1563.

182. Okazaki Y, Furuno M, Kasukawa T, Adachi J, Bono H, Kondo S, Nikaido I, Osato N, Saito R, Suzuki H, Yamanaka I, Kiyosawa H, Yagi K, Tomaru Y, Hasegawa Y, Nogami A, Schonbach C, Gojobori T, Baldarelli R, Hill DP, Bult C, Hume DA, Quackenbush J, Schriml LM, Kanapin A, Matsuda H, Batalov S, Beisel KW, Blake JA, Bradt D, Brusic V, Chothia C, Corbani LE, Cousins S, Dalla E, Dragani TA, Fletcher CF, Forrest A, Frazer KS, Gaasterland T, Gariboldi M, Gissi C, Godzik A, Gough J, Grimmond S, Gustincich S, Hirokawa N, Jackson IJ, Jarvis ED, Kanai A, Kawaji H, Kawasawa Y, Kedzierski RM, King BL, Konagaya A, Kurochkin IV, Lee Y, Lenhard B, Lyons PA, Maglott DR, Maltais L, Marchionni L, McKenzie L, Miki H, Nagashima T, Numata K, Okido T, Pavan WJ, Pertea G, Pesole G, Petrovsky N, Pillai R, Pontius JU, Qi D, Ramachandran S, Ravasi T, Reed JC, Reed DJ, Reid J, Ring BZ, Ringwald M, Sandelin A, Schneider C, Semple CA, Setou M, Shimada K, Sultana R, Takenaka Y, Taylor MS, Teasdale RD, Tomita M, Verardo R, Wagner L, Wahlestedt C, Wang Y, Watanabe Y, Wells C, Wilming LG, Wynshaw-Boris A, Yanagisawa M, Yang I, Yang L, Yuan Z, Zavolan M, Zhu Y, Zimmer A, Carninci P, Hayatsu N, Hirozane-Kishikawa T, Konno H, Nakamura M, Sakazume N, Sato K, Shiraki T, Waki K, Kawai J, Aizawa K, Arakawa T, Fukuda S, Hara A, Hashizume W, Imotani K, Ishii Y, Itoh M, Kagawa I, Miyazaki A, Sakai K, Sasaki D, Shibata K, Shinagawa A, Yasunishi A, Yoshino M, Waterston R, Lander ES, Rogers J, Birney E, Hayashizaki Y. Analysis of the mouse transcriptome based on functional annotation of 60,770 full-length cDNAs. Nature. 2002;420:563-573.

183. Ivanova NB, Dimos JT, Schaniel C, Hackney JA, Moore KA, Lemischka IR. A stem cell molecular signature. Science. 2002;298:601-604.

184. Ramalho-Santos M, Yoon S, Matsuzaki Y, Mulligan RC, Melton DA. "Stemness": transcriptional profiling of embryonic and adult stem cells. Science. 2002;298:597-600.

185. Fortunel NO, Otu HH, Ng HH, Chen J, Mu X, Chevassut T, Li X, Joseph M, Bailey C, Hatzfeld JA, Hatzfeld A, Usta F, Vega VB, Long PM, Libermann TA, Lim B. Comment on " 'Stemness': transcriptional profiling of embryonic and adult stem cells" and "a stem cell molecular signature". Science. 2003;302:393; author reply 393.

186. Venezia TA, Merchant AA, Ramos CA, Whitehouse NL, Young AS, Shaw CA, Goodell MA. Molecular signatures of proliferation and quiescence in hematopoietic stem cells. PLoS Biol. 2004;2:e301.

187. Lueking A, Horn M, Eickhoff H, Bussow K, Lehrach H, Walter G. Protein microarrays for gene expression and antibody screening. Anal Biochem. 1999;270:103-111.

188. MacBeath G, Schreiber SL. Printing proteins as microarrays for high-throughput function determination. Science. 2000;289:1760-1763.

189. Zhu H, Snyder M. Protein arrays and microarrays. Curr Opin Chem Biol. 2001;5:40-45.

190. Arenkov P, Kukhtin A, Gemmell A, Voloshchuk S, Chupeeva V, Mirzabekov A. Protein microchips: use for immunoassay and enzymatic reactions. Anal Biochem. 2000;278:123-131.

191. Diks SH, Kok K, O'Toole T, Hommes DW, van Dijken P, Joore J, Peppelenbosch MP. Kinome profiling for studying lipopolysaccharide signal transduction in human peripheral blood mononuclear cells. J Biol Chem. 2004;279:49206-49213.

192. Lemischka IR, Raulet DH, Mulligan RC. Developmental potential and dynamic behavior of hematopoietic stem cells. Cell. 1986;45:917-927.

193. Morrison SJ, Weissman IL. The long-term repopulating subset of hematopoietic stem cells is deterministic and isolatable by phenotype. Immunity. 1994;1:661-673.

194. Morrison SJ, Wandycz AM, Hemmati HD, Wright DE, Weissman IL. Identification of a lineage of multipotent hematopoietic progenitors. Development. 1997;124:1929-1939.

195. Christensen JL, Weissman IL. Flk-2 is a marker in hematopoietic stem cell differentiation: a simple method to isolate long-term stem cells. Proc Natl Acad Sci U S A. 2001;98:14541-14546.

196. Chambers SM, Boles NC, Lin KY, Tierney MP, Bowman TV, Bradfute SB, Chen AJ, Merchant AA, Sirin O, Weksberg DC, Merchant MG, Fisk CJ, Shaw CA, Goodell MA. Hematopoietic fingerprints: an expression database of stem cells and their progeny. Cell Stem Cell. 2007;1:578-591.

197. Caenepeel S, Charydczak G, Sudarsanam S, Hunter T, Manning G. The mouse kinome: discovery and comparative genomics of all mouse protein kinases. Proc Natl Acad Sci U S A. 2004;101:11707-11712.

198. Ficarro SB, McCleland ML, Stukenberg PT, Burke DJ, Ross MM, Shabanowitz J, Hunt DF, White FM. Phosphoproteome analysis by mass spectrometry and its application to Saccharomyces cerevisiae. Nat Biotechnol. 2002;20:301-305.

199. Nadon R, Shoemaker J. Statistical issues with microarrays: processing and analysis. Trends Genet. 2002;18:265-271.

200. Dumble M, Moore L, Chambers SM, Geiger H, Van Zant G, Goodell MA, Donehower LA. The impact of altered p53 dosage on hematopoietic stem cell dynamics during aging. Blood. 2007;109:1736-1742.

201. Chambers SM, Shaw CA, Gatza C, Fisk CJ, Donehower LA, Goodell MA. Aging hematopoietic stem cells decline in function and exhibit epigenetic dysregulation. PLoS Biol. 2007;5:e201.

202. Forsberg EC, Prohaska SS, Katzman S, Heffner GC, Stuart JM, Weissman IL. Differential expression of novel potential regulators in hematopoietic stem cells. PLoS Genet. 2005;1:e28.

203. Liu Y, Elf SE, Miyata Y, Sashida G, Liu Y, Huang G, Di Giandomenico S, Lee JM, Deblasio A, Menendez S, Antipin J, Reva B, Koff A, Nimer SD. p53 regulates hematopoietic stem cell quiescence. Cell Stem Cell. 2009;4:37-48.

204. Jin FY, Qiu LG, Li QC, Meng HX, Wang YF, Yu Z, Li Q, Han JL. [The effect of matrix metalloproteinase-9 in granulocyte colony stimulation factor-induced stem cell mobilization]. Zhonghua Yi Xue Za Zhi. 2006;86:2966-2970.

205. McQuibban GA, Butler GS, Gong JH, Bendall L, Power C, Clark-Lewis I, Overall CM. Matrix metalloproteinase activity inactivates the CXC chemokine stromal cell-derived factor-1. J Biol Chem. 2001;276:43503-43508.

206. Alsayed Y, Ngo H, Runnels J, Leleu X, Singha UK, Pitsillides CM, Spencer JA, Kimlinger T, Ghobrial JM, Jia X, Lu G, Timm M, Kumar A, Cote D, Veilleux I, Hedin KE, Roodman GD, Witzig TE, Kung AL, Hideshima T, Anderson KC, Lin CP, Ghobrial IM. Mechanisms of regulation of CXCR4/SDF-1 (CXCL12)-dependent migration and homing in multiple myeloma. Blood. 2007;109:2708-2717.

207. Kim CH, Hangoc G, Cooper S, Helgason CD, Yew S, Humphries RK, Krystal G, Broxmeyer HE. Altered responsiveness to chemokines due to targeted disruption of SHIP. J Clin Invest. 1999;104:1751-1759.

208. Zhou P, Kitaura H, Teitelbaum SL, Krystal G, Ross FP, Takeshita S. SHIP1 negatively regulates proliferation of osteoclast precursors via Akt-dependent alterations in D-type cyclins and p27. J Immunol. 2006;177:8777-8784.

209. Zhu QS, Xia L, Mills GB, Lowell CA, Touw IP, Corey SJ. G-CSF induced reactive oxygen species involves Lyn-PI3-kinase-Akt and contributes to myeloid cell growth. Blood. 2006;107:1847-1856.

210. Jang YY, Sharkis SJ. A low level of reactive oxygen species selects for primitive hematopoietic stem cells that may reside in the low-oxygenic niche. Blood. 2007;110:3056-3063.

211. Platzbecker U, Prange-Krex G, Bornhauser M, Koch R, Soucek S, Aikele P, Haack A, Haag C, Schuler U, Berndt A, Rutt C, Ehninger G, Holig K. Spleen enlargement in healthy donors during G-CSF mobilization of PBPCs. Transfusion. 2001;41:184-189.

212. Visnjic D, Kalajzic Z, Rowe DW, Katavic V, Lorenzo J, Aguila HL. Hematopoiesis is severely altered in mice with an induced osteoblast deficiency. Blood. 2004;103:3258-3264.

213. Gardai S, Whitlock BB, Helgason C, Ambruso D, Fadok V, Bratton D, Henson PM. Activation of SHIP by NADPH oxidase-stimulated Lyn leads to enhanced apoptosis in neutrophils. J Biol Chem. 2002;277:5236-5246.

214. Stephens L, Anderson K, Stokoe D, Erdjument-Bromage H, Painter GF, Holmes AB, Gaffney PR, Reese CB, McCormick F, Tempst P, Coadwell J, Hawkins PT. Protein kinase B kinases that mediate phosphatidylinositol 3,4,5-trisphosphate-dependent activation of protein kinase B. Science. 1998;279:710-714.

215. Ma K, Cheung SM, Marshall AJ, Duronio V. PI(3,4,5)P3 and PI(3,4)P2 levels correlate with PKB/akt phosphorylation at Thr308 and Ser473, respectively; PI(3,4)P2 levels determine PKB activity. Cell Signal. 2008;20:684-694.

216. Harrison DE, Zsebo KM, Astle CM. Splenic primitive hematopoietic stem cell (PHSC) activity is enhanced by steel factor because of PHSC proliferation. Blood. 1994;83:3146-3151.

217. Chan CK, Chen CC, Luppen CA, Kim JB, DeBoer AT, Wei K, Helms JA, Kuo CJ, Kraft DL, Weissman IL. Endochondral ossification is required for haematopoietic stem-cell niche formation. Nature. 2009;457:490-494.

218. Hanahan D, Weinberg RA. The hallmarks of cancer. Cell. 2000;100:57-70.

219. Gloire G, Charlier E, Rahmouni S, Volanti C, Chariot A, Erneux C, Piette J. Restoration of SHIP-1 activity in human leukemic cells modifies NF-kappaB activation pathway and cellular survival upon oxidative stress. Oncogene. 2006;25:5485-5494.

220. Luo JM, Yoshida H, Komura S, Ohishi N, Pan L, Shigeno K, Hanamura I, Miura K, Iida S, Ueda R, Naoe T, Akao Y, Ohno R, Ohnishi K. Possible dominant-negative mutation of the SHIP gene in acute myeloid leukemia. Leukemia. 2003;17:1-8.

221. Lapidot T, Sirard C, Vormoor J, Murdoch B, Hoang T, Caceres-Cortes J, Minden M, Paterson B, Caligiuri MA, Dick JE. A cell initiating human acute myeloid leukaemia after transplantation into SCID mice. Nature. 1994;367:645-648.

222. Bonnet D, Dick JE. Human acute myeloid leukemia is organized as a hierarchy that originates from a primitive hematopoietic cell. Nat Med. 1997;3:730-737.

223. Al-Hajj M, Wicha MS, Benito-Hernandez A, Morrison SJ, Clarke MF. Prospective identification of tumorigenic breast cancer cells. Proc Natl Acad Sci U S A. 2003;100:3983-3988.

224. Hemmati HD, Nakano I, Lazareff JA, Masterman-Smith M, Geschwind DH, Bronner-Fraser M, Kornblum HI. Cancerous stem cells can arise from pediatric brain tumors. Proc Natl Acad Sci U S A. 2003;100:15178-15183.

225. Singh SK, Clarke ID, Terasaki M, Bonn VE, Hawkins C, Squire J, Dirks PB. Identification of a cancer stem cell in human brain tumors. Cancer Res. 2003;63:5821-5828.

226. Tan BT, Park CY, Ailles LE, Weissman IL. The cancer stem cell hypothesis: a work in progress. Lab Invest. 2006;86:1203-1207.

227. Quintana E, Shackleton M, Sabel MS, Fullen DR, Johnson TM, Morrison SJ. Efficient tumour formation by single human melanoma cells. Nature. 2008;456:593-598.

About the Author

Amy Hazen graduated from the University of Florida in 2003 with a Bachelors of Science in Biological Engineering. During this time she worked in the laboratory of David P. Chynoweth Ph.D. developing a sustainability subsystem as part of the Advanced Life Support systems needed by NASA in long duration space missions. During her final year of college, she began an independent study under the leadership of Daniel L. Purich Ph.D., examining the actin-based motility of intracellular pathogens. This experience developed her interest in basic science research. In 2003, Amy joined the Cancer Biology Ph.D. program at H. Lee Moffitt Cancer Center and Research Institute at the University of South Florida. Here she joined the laboratory of William G. Kerr Ph.D. and began her work exploring the role of Src homology 2 domain containing 5' inositol phosphatase 1 in hematopoietic stem cell biology.